

Kumulative Dissertation  
zur  
Erlangung des Doktorgrades

Dr. rer. nat.

der Fakultät für  
Biologie

an der  
Universität Duisburg-Essen

**Targeting transcriptional regulators for the treatment  
of therapy resistant carcinomas**

vorgelegt von

Tim Zegar  
aus Witten

Essen, August 2020

Die der vorliegenden Arbeit zugrunde liegenden Experimente wurden im Brückeninstitut für Experimentelle Tumorthherapie, Westdeutsches Tumorzentrum, Universitätsklinikum Essen und in der DKTK Abteilung für Translationale Onkologie Solider Tumore am Partnerstandort Essen (Direktor: Prof. Dr. Jens Siveke) durchgeführt.

1. Gutachter: Prof. Dr. Jens Siveke

2. Gutachter: Prof. Dr. Andrea Vortkamp

Vorsitzender des Prüfungsausschusses: Prof. Dr. Frank Kaiser

Tag der mündlichen Prüfung: 08.01.2021



**DuEPublico**  
Duisburg-Essen Publications online

UNIVERSITÄT  
DUISBURG  
ESSEN  
*Offen im Denken*

ub | universitäts  
bibliothek

Diese Dissertation wird über DuEPublico, dem Dokumenten- und Publikationsserver der Universität Duisburg-Essen, zur Verfügung gestellt und liegt auch als Print-Version vor.

**DOI:** 10.17185/duepublico/74002  
**URN:** urn:nbn:de:hbz:464-20210225-093827-9

Alle Rechte vorbehalten.

## List of contents

<b>List of abbreviations</b> .....	<b>4</b>
<b>List of figures</b> .....	<b>5</b>
<b>1. Introduction</b> .....	<b>6</b>
<b>1.1 Therapy resistance in cancer</b> .....	<b>6</b>
1.1.1 Therapy resistance in pancreatic ductal adenocarcinoma .....	8
1.1.2 Therapy resistance in nut midline carcinoma .....	8
<b>1.2 Cell plasticity</b> .....	<b>9</b>
1.2.1 Tumor cell plasticity in resistance to targeted therapy .....	11
1.2.2 Epithelial–mesenchymal-transition.....	11
<b>1.3 Transcriptional addiction</b> .....	<b>15</b>
1.3.1 Transcriptional dysregulation in cancer .....	17
1.3.2 Targeting transcriptional dependencies .....	19
<b>1.4 Challenges in epigenetic drug discovery</b> .....	<b>21</b>
1.4.1 Structural Genomics Consortium (SGC).....	23
1.4.2 Drug discovery in targeting bromodomains .....	23
<b>2. Characterization of a dual BET/HDAC inhibitor for treatment of pancreatic ductal adenocarcinoma</b> .....	<b>25</b>
<b>3. Therapeutic targeting of p300/CBP HAT domain for the treatment of NUT midline carcinoma</b> .....	<b>44</b>
<b>4. Discussion</b> .....	<b>58</b>
<b>4.1 Combinational and low dose therapies</b> .....	<b>58</b>
<b>4.2 Future directions</b> .....	<b>60</b>
<b>5. List of literature</b> .....	<b>63</b>
<b>6. Acknowledgements</b> .....	<b>71</b>
<b>7. Statutory declaration</b> .....	<b>72</b>

## List of abbreviations

ABC	ATP-binding-protein
AML	acute myeloid leukemia
APML	acute promyelocytic leukemia
ASTRA	all-trans retinoic acid
BCRP	breast cancer resistant protein
BET	bromodomain and extra-terminal motif
CBP	CREB-binding-protein
ChIP	chromatin immunoprecipitation
CSC	cancer stem cell
ECM	extracellular matrix
EMT	epithelial-mesenchymal-transition
FDA	food and drug administration
GSE	genes set enrichment
HAT	histone-acetyltransferase
HDAC	histone-deacetylase
HTS	high-throughput screening
IL-6	interleukin-6
LIF	leukemia inhibitory factor
MET	mesenchymal-epithelial-transition
NMC	NUT-midline-carcinoma
NSCLC	non-small-cell lung carcinoma
NUT	nuclear protein in testis
OS	overall survival
PDAC	pancreatic ductal adenocarcinoma
PROTAC	protein-targeting chimeric molecule
RNAPII	RNA-polymerase II
RT-PCR	real-time-polymerase-chain-reaction
SAR	structure-activity-relationship
SGC	Structural Genomics Consortium
TAD	topologically associating domains
TF	transcription factor
TGF- $\beta$	transforming growth factor- $\beta$
ZEB	zinc finger E-box-binding homeobox

## List of figures

<b>Fig. 1</b> Darwinian and dynamic fluctuation models of cell resistance.....	7
<b>Fig. 2</b> Process of cell differentiation.....	10
<b>Fig. 3</b> Physiological changes associated with the epithelial-mesenchymal transition.....	12
<b>Fig. 4</b> EMT-associated contribution to general drug resistance in tumor cells.....	13
<b>Fig. 5</b> From drug tolerance to drug resistance.....	15
<b>Fig. 6</b> Master transcription factors and super enhancers.....	17
<b>Fig. 7</b> Typical workflow of preclinical drug discovery.....	22

## 1. Introduction

### 1.1 Therapy resistance in cancer

Cancer is by far one of the deadliest diseases in our modern world, even the evolving field of personalized medicine, including cancer prevention, new diagnosis and targeted therapies revolutionized the treatment of cancer and the patient outcomes during the last decades. Especially the identification of oncogenic driver mutations and the resulting molecular targeted therapy demonstrated notable clinical success in many cancer types like breast, leukemia, colorectal, lung or ovarian cancers<sup>1</sup>. Despite this mostly very effective and less toxic treatments, tumor cells often return after an initial response to therapy. The success of precision medicine is defeated by evolution of resistance, making therapy resistance the central cause of death in most cancers<sup>2</sup>. Thus, understanding the dynamics and mechanisms that control the response and resistance to therapeutics is just as important as the initial identification of biomarkers and effective treatments itself.

In part, difficulties in treating cancer are caused by cancer stem cells (CSC), a small subpopulation of cells within tumors with capabilities of repeated processes of self-renewal and differentiation into diverse cell types<sup>3, 4</sup>. CSCs demonstrated to be resistant to conventional chemotherapy and radiation treatment and they are under suspicion to play important roles in cancer relapse and metastasis<sup>3</sup>. They have been identified in a variety of tumors, including breast and brain cancer and human acute myeloid Leukemia (AML)<sup>5-7</sup>. It is most likely, that they are partially responsible for therapy resistance. ATP-binding cassette (ABC) transporter proteins are used for the drug efflux and are highly expressed in stem cells<sup>2, 4</sup>. It has been shown that the breast cancer resistance protein (BCRP), an ABC transporter, is expressed in high levels and responsible for drug resistance in CD34+/CD38- cells in AML, considering them as stem cell subpopulation<sup>8</sup>.

Another factor, which is affecting the therapy response is spatial heterogeneity in the tumor environment. Angiogenesis and complex interactions with adjacent host cells deliver local concentrations of factors, which mediate proliferation, cell survival or phenotype<sup>2</sup>. This effect goes hand in hand with cellular diversity and spatial heterogeneity in the genotypic and phenotypic properties of tumor cells<sup>2</sup>. Nowadays, cellular heterogeneity within tumor cells may be considered as a major driver of the development of therapy resistance.

Historically the focus in understanding cell resistance has been on genetic driver mutations<sup>9</sup>. A small subpopulation or even a single cell acquires a drug-tolerant state through genetic key alterations and will survive the treatment based on Darwinian selection (Fig. 1A). These mechanisms of resistance can be a result of rare pre-existing cells or randomly acquired during

treatment<sup>10, 11</sup>. In both ways, cells are driven by Darwinian dynamics, independent of therapeutics and treatment. But there has been emerging evidence, that non-mutational mechanisms also play an important role in therapy resistance<sup>9, 12-14</sup>. It has been shown, that tumor cells may dynamically express fluctuating levels of resistance genes<sup>15, 16</sup>. Cells with high levels of these genes survive a certain treatment and are further reprogrammed, forming a drug-tolerant subpopulation (Fig. 1B)<sup>15, 16</sup>. In contrast to Darwinian selection model, the surviving cells are a direct response to therapy and drug induced. These two models are not mutually exclusive and may complement each other.<sup>15</sup>

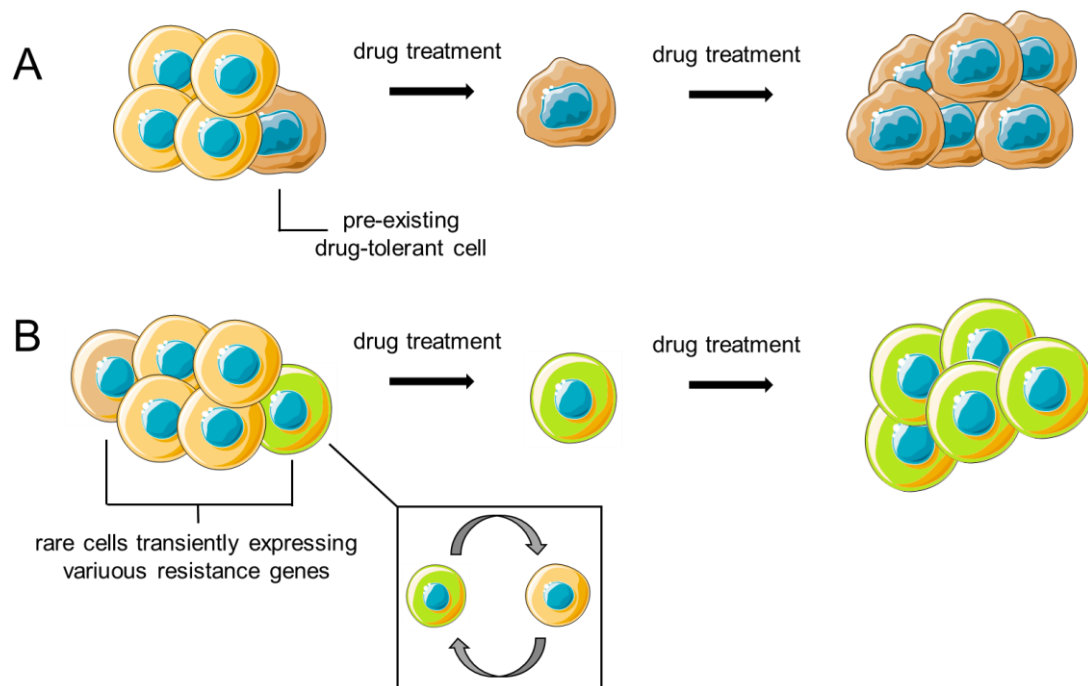


**Fig. 1:** **A:** Darwinian selection model proposes pre-existing drug-tolerant cells, which are surviving the treatment. **B:** Dynamic fluctuation model suggests rare cells, transiently expressing various resistance genes, which are surviving and reprogrammed to stably express resistance genes. Both models are not mutually exclusive. Adapted from Boumahdi et al, Nat Rev Drug Discov, 2020.

This dynamic and fluctuating drug-tolerant state thus rely on the process of phenotype switching, allowing one given genotype to switch between various phenotypes in response to external signals<sup>9</sup>. A process, also known as cell plasticity, which is usually observed during development, but also injuries to adapt to their environment<sup>17, 18</sup>. Thus, cell plasticity and the epigenetic mechanisms behind phenotype switching and reprogramming opening new opportunities to target therapy resistance in cancer.

### **1.1.1 Therapy resistance in pancreatic ductal adenocarcinoma**

Pancreatic ductal adenocarcinoma (PDAC) is the most common form of pancreatic cancer, one of the most difficult to treat tumors and a remarkable example for therapy resistance. Due to late diagnosis, metastasis and treatment resistance, the 5-year overall survival (OS) is around 8%<sup>19</sup>. It is estimated that pancreatic cancer will be the second leading cause of cancer death in the United States by the year 2030<sup>20</sup>.

PDAC is associated with poor prognosis for several reasons. Because of the absence of symptoms in most cases and the lack of specific biomarkers, it is diagnosed most often in an advanced stage<sup>21</sup>. In addition, multiple different genetic and epigenetic alterations occur in pancreatic cancer, creating a complex cell heterogeneity, which is completed by a dense and considerable immunosuppressive and hypoxic microenvironment<sup>21</sup>. Finally, PDAC is characterized by a remarkable resistance to virtually all chemo- and targeted therapeutic approaches<sup>21</sup>. Thus, surgery remains the only potentially option, but for many patients the tumor is too far progressed for curative approaches or shows fast recurrence after resection.

Most therapy approaches are based on multi-chemotherapy regimen such as FOLFIRINOX<sup>22</sup> or gemcitabine, a nucleoside analogue, which was already approved by the US Food and Drug Administration (FDA) in 1997<sup>23</sup> and albumin-bound Paclitaxel, which showed median overall survival of around 8.5 month<sup>24</sup>. However, these therapies show significant toxicities and are only effective in a subset of patients for limited duration of time<sup>21</sup>. Given the limited efficacy and side effects, there is an urgent need for novel therapeutic strategies for pancreatic cancer. In addition, growing evidence demonstrates that different molecular subtypes in PDAC impact the clinical response. Several transcriptomic subtypes have been described, underlining the complex heterogeneity in pancreatic cancer cells<sup>25</sup>. Two major subtypes are well accepted, Classical and Basal-like<sup>25, 26</sup>. Classical tumors respond better to first-line chemotherapy compared to Basal-like tumors<sup>27</sup>. Basal-like cells, alternatively named Quasi-mesenchymal (QM), are also associated with a poor clinical outcome<sup>25</sup>. These findings suggest, that this more aggressive subtype needs novel, non-standard chemotherapy approaches to improve the overall outcome for pancreatic cancer.

### **1.1.2 Therapy resistance in nut midline carcinoma**

Nuclear protein of the testis (NUT) midline carcinoma (NMC) is a rare but highly aggressive subtype of undifferentiated squamous cell carcinoma. It is defined by chromosomal rearrangement of the NUT gene to another gene<sup>28</sup>. The most common rearrangement is a translocation between NUT and the bromodomain and extraterminal domain (BET) gene BRD4, forming a NUT-BRD4 fusion oncogene.<sup>28</sup> It mostly arises from the head and neck

region and is characterized by the oncogenic function of blocking differentiation and maintaining proliferation<sup>29</sup>. NMC is very aggressive and therapy resistant cancer with an overall survival rate around 20 % one year after diagnosis<sup>29</sup>. Since all fusion partners of NUT are functionally BRD4-related, BET-inhibitors hold great promise for treating this disease<sup>29</sup>. Combinational approaches with histone deacetylase inhibitors (HDACi) demonstrated promising clinical activity and confirmed the importance of bromodomain inhibitors in targeting NUT-BRD4<sup>29, 30</sup>. However, the clinical response rate in NMC is still low and even after a rapid initial response, patient relapses were observed, indicating an occurring resistance mechanism<sup>30</sup>. Furthermore, toxicity of BET-inhibitors is another concern, which is additionally limiting the therapy<sup>30, 31</sup>. Since BET-inhibition in NMC provided a proof of concept and partially high efficacy, future investigations on combinational treatments to overcome adaptive resistance mechanisms remain crucial.

## 1.2 Cell plasticity

The effect of cellular plasticity represents the ability of cells to change their phenotype in response to environmental signals and external cues, without changing their genotype. Given the fact, that only 2 % of the genome encodes proteins and the remaining DNA is replete with regulatory elements, a single human cell gives rise to innumerable different cell types<sup>32</sup>. Cell plasticity is most notably relevant in developmental and regenerative processes<sup>17, 33</sup>. The cellular identity is mainly mediated by chromatin structure, its regulators and transcription factors (TFs) and originally the developmental specification was conceptualized by Conrad Waddington as epigenetic landscape, in which cells move downhill along canals, separated by walls<sup>34</sup>. After passing these walls, cells irreversibly lose the ability to give rise to progeny outside of their given lineage (Fig 2A)<sup>9, 34</sup>. However, there is emerging evidence since Waddington's description, that the cell state is highly dynamic and chromatin structure and its regulators are responsible for the height of the walls, that separate cell identities<sup>35, 36</sup>. For example, it has been shown, that bulge stem cells, normally restricted to hair follicles, are recruited into the epidermis after epidermal injury, contributing to the wound repair<sup>37</sup>. The mechanisms behind this phenotype switching are called transdetermination or trans-differentiation (Fig. 2B, C). Transdetermination, describes a process, in which mature cells dedifferentiate to their progenitor state in order to differentiate to another, closely related cell identity<sup>38</sup>. In contrast to this, during transdifferentiation, differentiated cells switch their phenotype without dedifferentiate to an intermediate state first<sup>9, 38</sup>. It is known that pancreas and liver arise from the same area of the endoderm. In animal experiments, it was possible to develop hepatocytes, which are liver cells, in the pancreas of adult rats on a copper-deficient

diet<sup>39</sup>. A process that requires transdifferentiation. Chromatin regulation is given a central role in maintaining the height of the walls, which are preventing cells from switching their phenotypes<sup>32</sup>. Its structure is characterized by active and repressive areas. The active state, also known as euchromatin, is usually highly acetylated and accessible to TFs. While the repressive state, also called heterochromatin, is densely packed and slightly acetylated, allowing no transcription to take place.

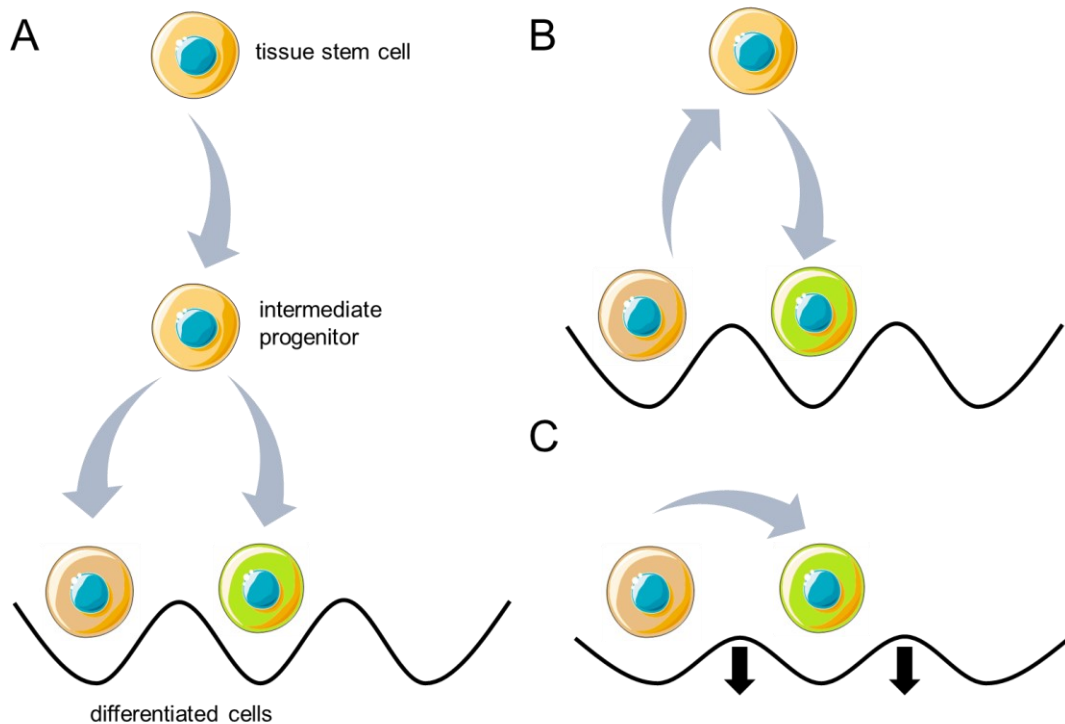


**Fig. 2:** **A:** Directed process of a stem cell giving rise to differentiated states. The epigenetic landscape is separating cell identities. **B:** Transdetermination, mature cells return to progenitor or stem cell-like state to differentiate to a closely related cell type. **C:** Transdifferentiation, cells acquire different cell identity without reversion to immature states. Adapted from Mills et al, The EMBO Journal, 2019.

Chromatin networks mediate the cell identity and the responsiveness to intrinsic and extrinsic cues by regulating these active and repressive regions<sup>32</sup>. Thus, cells are highly flexible in different stages of development or able to adapt to environmental changes. If the chromatin homeostasis is disrupted, cells may fail to respond appropriately to external cues<sup>32</sup>. Overly restrictive areas prevent cells to differentiate, forcing them to stay in a proliferative state.<sup>32</sup> Too much active chromatin lowers epigenetic barriers, allowing cells to switch phenotypes and receive alternate identities, which may result in drug-tolerant subtypes<sup>32</sup>.

### **1.2.1 Tumor cell plasticity in resistance to targeted therapy**

Although cancer is considered to be a genetic disease, it is well accepted, that epigenetic alterations also play an important role in tumorigenesis. Dysregulations of the chromatin structure, which lead to accumulation of active chromatin, give rise to cellular plasticity, that allows stochastic activation of alternate gene programs. These epigenetic changes may result in the activation of oncogenic drivers or bring cells in phenotypic states, that no longer depend on a drug-targeted pathway<sup>32</sup>. It has been shown before, that a rare subpopulation of tumor cells is dynamically expressing fluctuating levels of genes, which could result in a drug-tolerant state (Fig. 1B)<sup>15, 16</sup>. Clinical cases, in which patients regained drug sensitivity after drug holidays, underline the role of cell plasticity as resistance mechanism<sup>40,41</sup>. Only non-mutational processes could explain this reversibility of drug sensitivity<sup>9</sup>.

### **1.2.2 Epithelial–mesenchymal-transition**

Epithelial–mesenchymal-transition (EMT) is remarkable example for phenotype switching and highly involved in resistance to targeted therapy<sup>9,42</sup>. The EMT program describes the process, in which tumor cells partially lose epithelial features, like cell junctions or the expression of E-cadherin, and gain mesenchymal abilities, including a fibroblast-like morphology as well as an increased capacity for migratory and invasive properties<sup>42, 43</sup>. The exact molecular processes behind this cellular change is still poorly understood, but it is clearly linked to cellular plasticity of tumor cells. Intermediate EMT states and the reversibility of the process, also know an mesenchymal-epithelial-transition (MET), pointing towards phenotype switching as major driver for this program<sup>9, 42</sup>. Just like cell plasticity, EMT was studied in the context of development and embryonic morphogenesis, as well as pathological processes, including wound healing<sup>44, 45</sup>. For example, cells from the primitive ectoderm, the first embryonic epithelial tissue, induce the EMT program to differentiate into primary mesenchymal cells and giving rise to mesodermal and endodermal cell layers<sup>46</sup>. In general, activation of the EMT program induces fundamental changes in the cellular physiology and morphology and is a crucial building block of the early development of healthy cells.

A small group of transcription factors, often condensed as EMT-inducing transcription factors (EMT-TFs), was identified to maintain gene expression associated with EMT<sup>47</sup>. EMT-TFs, mainly containing transcription factors of the Snail and ZEB (Zinc finger E-box-binding homeobox) protein families, are known to suppress genes, related to an epithelial phenotype like cytokeratin or E-cadherin and to induce expression of N-cadherin or vimentin, associated with a mesenchymal phenotype<sup>47</sup>. In addition, they tend to regulate the expression of each other, resulting in a cooperatively activation of the full EMT program after overexpression of one

EMT-TF<sup>42</sup>. Interestingly, there is a partial overlap of genes, related to EMT and genes mediating transdifferentiation in various tumors like lung or prostate adenocarcinomas<sup>48,49</sup>. In the context of tumorigenesis, the role of EMT is still a highly discussed topic. While there is a general agreement on the contribution of EMT to embryonic development, the impact on carcinoma progression is a matter of debate<sup>42</sup>. This is based on the fact, that the EMT program is only partially activated in most tumors, impeding the detection of relevant markers<sup>42</sup>. However, there is growing evidence underlining the contribution of activated EMT program to invasiveness, progression and drug resistance in cancer (Fig. 3). It is well accepted, that the loss of E-cadherin, a hallmark of invasiveness in carcinomas, is associated with poor prognosis<sup>50,51</sup>. Additionally, the expression of EMT-TFs was linked to tumor progression, giving Snail or Twist1 an critical role in metastasis<sup>52, 53</sup>. The incomplete form of the EMT program and its reversibility, leads to a spatial phenotypic diversity within one tumor and it has been shown, that tumor-initiating abilities in cells are increased at intermediate levels of EMT<sup>54</sup>. Thus, the partial activation of EMT, triggered by increased expression of EMT-TFs may represent a key step in enabling drug induced cell plasticity, in contrast to a fully transformation to a mesenchymal phenotype<sup>9</sup>.

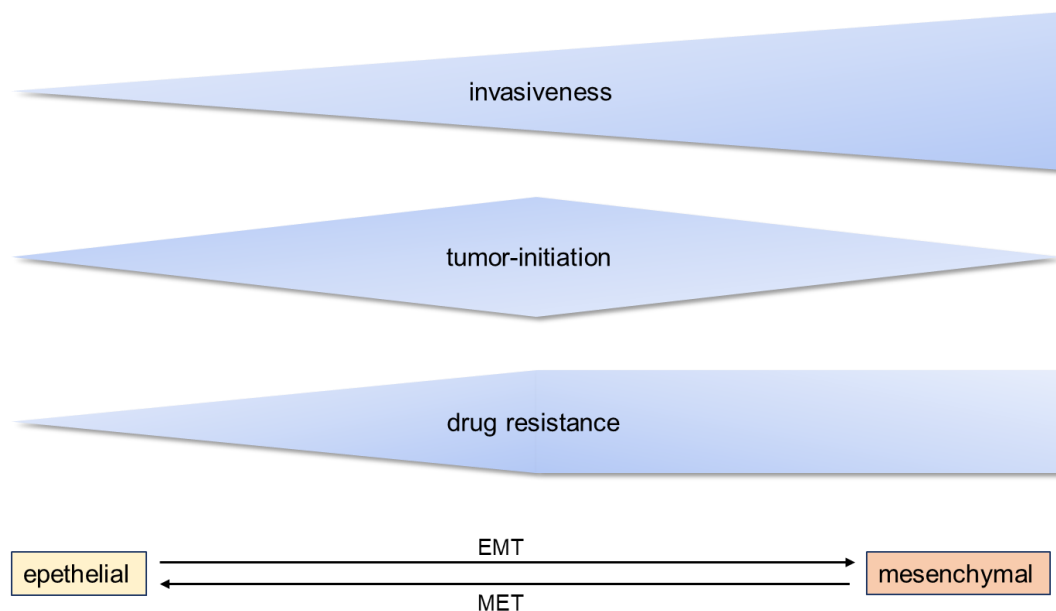


**Fig.3:** Physiological changes associated with the epithelial-mesenchymal transition (EMT) in tumor cells. Illustration how invasiveness, the tumor-initiating ability and degree of drug resistance change across the spectrum of EMT program activation. Adapted from Shibue and Weinberg, Nat Rev Clin Oncol, 2017.

Observations in mouse models even indicate, that for the formation of metastases, cells have to undergo the EMT program first, to leave the primary tumor and invade the surrounding tissue and regain epithelial characteristics later, to form metastases<sup>55, 56</sup>. The findings suggest that the activation of the EMT program is highly dynamic over time and the MET program may be as important as the initial loss of epithelial abilities. Furthermore, genetically-engineered mouse models could demonstrate high expression levels of EMT-TFs like Snail, Zeb1 or Twist1 in epithelial cells in early or pre-malignant stages of carcinoma development<sup>57-59</sup>. However, the mechanisms, which lead to activation of the previously silent EMT program in early stages of tumorigenesis remain unclear.

The incomplete and reversible epithelial–mesenchymal-transition in tumor cells results in a spatial and temporal diversity, which is increasing the capacity for cell plasticity. In this way, the EMT program is both, driving the tumor progression and increasing chances to develop drug-tolerant subpopulations. Further, EMT has been associated with highly treatment resistant cancer stem cells (CSC)<sup>42</sup>. Analysis of surface-markers and expression patterns suggest, that the activation of the EMT program in tumor cells is closely linked to entrance into the CSC state<sup>42, 60</sup>. Mesenchymal phenotype-like cells demonstrate many characteristics like slow proliferation, increased expression of anti-apoptotic proteins or enhanced levels of ABC transporters, which are usually related with CSCs (Fig. 4)<sup>8, 9, 42</sup>.

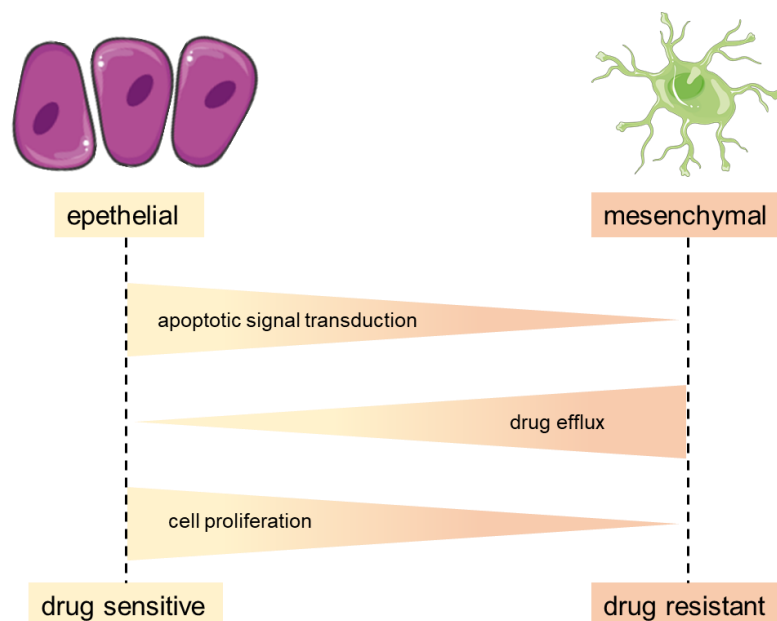


**Fig. 4:** EMT-associated contribution to general drug resistance in tumor cells. Decreased cell proliferation or transduction of apoptotic signals and enhanced drug efflux are also linked to CSCs. Adapted from Shibue and Weinberg, Nat Rev Clin Oncol, 2017.

The findings suggest that EMT and MET enabling cells to transit back and forth between the CSC and non-CSC states and especially the EMT program may serve as founder of metastatic colonies.

The observation of slow cycling subpopulations, which survive lethal drug exposures, has been described in various tumor types and underlines the connection between entering low proliferative CSC states and therapy resistance<sup>11, 61, 62</sup>. Relapses after treatment, but also the previously described resensitization after drug holidays indicating, that drug tolerant tumor cells can undergo reprogramming steps in several directions (Fig. 5). It is assumed, that drug tolerant, persistent tumor cells randomly acquire genetic mutations or are further reprogrammed and activate alternative pathways to become re-proliferative and permanently drug resistant<sup>9</sup>. Notably, drug tolerant cells can also become proliferative and drug sensitive again, after therapeutic withdrawal<sup>63</sup>. It was shown, that this process is re-inducible upon new cycles of treatment, indicating that cells may need to exit cell cycle to become resistant<sup>63</sup>. These findings give rise to the theory that therapy resistance always comes with a price. Maintenance of alternative pathways and unusual expression patterns requires resources, which must be diverted from proliferation. This leads to decreased fitness of resistant cells compared to the sensitive subtype in an environment of limited substrate<sup>2</sup>. In addition, cancer cells become highly dependent on certain pathways and transcriptional regulators, since the only alternative is to become sensitive to the current treatment again. These dependencies, also known as transcriptional addiction, provide new opportunities for novel therapeutics and targeting therapy resistance.

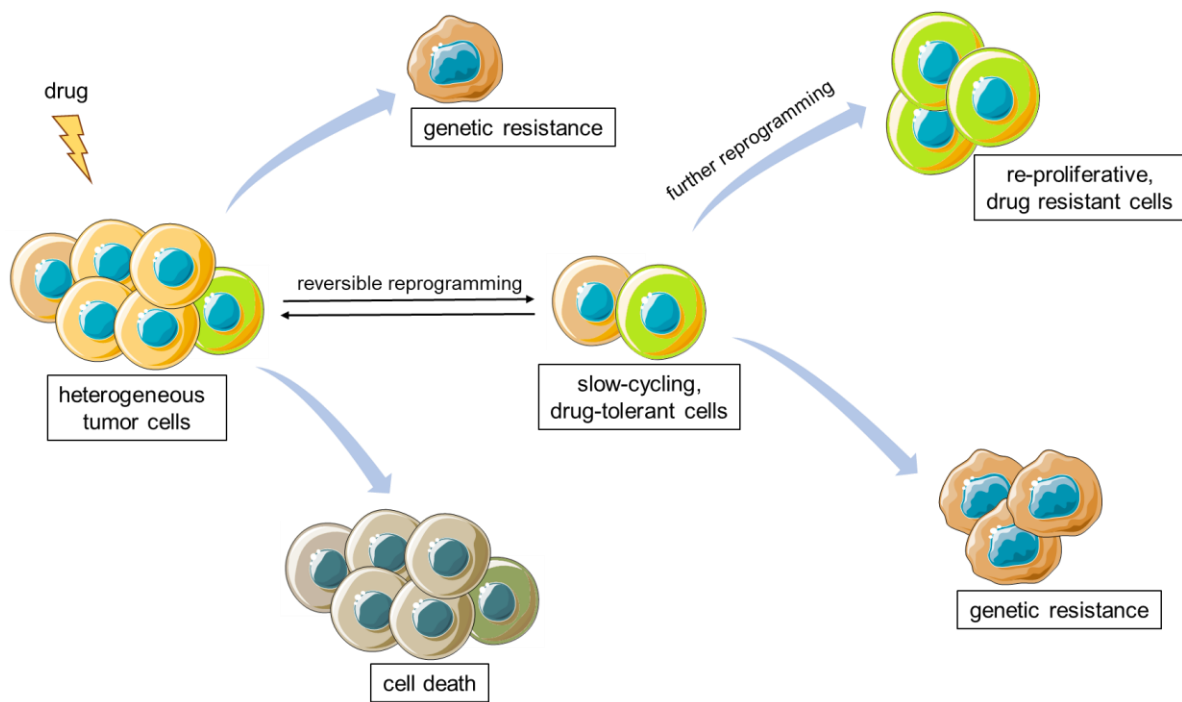


**Fig.5:** From drug tolerance to drug resistance. After drug exposure only fluctuating, slow cycling, drug-tolerant cells remain. Persistent cells can either resume proliferation through further reprogramming or through de novo acquisition of genetic mutation and become permanently resistant. If the treatment is discontinued, drug tolerant cells can also reactivate previous oncogenic pathways and resume proliferation and drug sensitivity again. Adapted from Boumahdi et al, Nat Rev Drug Discov, 2020.

### 1.3 Transcriptional addiction

The dysregulation of transcriptional programs is one of the hallmarks of cancer. Genetic alterations or cellular plasticity establish phenotypes, which drive tumorigenesis or do not longer depend on a drug-targeted pathway. Especially persistent, drug tolerant cells, which are mainly affecting clinical responsiveness, rely on the transcription of key genes, a process termed transcriptional addiction<sup>64</sup>. Epigenetic regulators, involved in maintenance of cell identity and transcriptional control, thus represent novel attractive targets of a new generation of inhibitors. Cancer genome sequencing and identification of oncogenic driver mutations enabled molecular targeted therapy but gave no insights on which dysregulated pathway the cell survival relies on. A deeper understanding of mechanisms of gene control in normal cells is required to identify alterations in transcriptional programs of tumor cells<sup>64</sup>.

It was previously described, that cell identity is predominantly controlled by transcription factors (TFs), while the chromatin structure is stabilizing the cell fate and adjusting cellular plasticity<sup>32</sup>. Since nearly half of all of the TFs encoded in the human genome are expressed in

every cell type, only a small group of regulators, also known as master transcription factors, is responsible for defining cell identity<sup>65-67</sup>. Thus, master TFs are highly expressed in a particular cell type and tend to regulate their own gene expression in an autoregulatory loop (Fig. 6A)<sup>67</sup>. It has been shown, that they co-occupy most enhancers together with other master TFs at genes, which are mediating the specific cell type<sup>67</sup>. Binding to enhancer elements leads to recruitment of coactivators and RNA polymerase II (RNAPII) to target genes<sup>68</sup>. Additionally, master TFs also activate transcription from the enhancer sequence itself to express enhancer RNA (eRNA), which binds other TFs to maintain the enhancer activity<sup>69</sup>. Combined to large regulatory elements, so called super-enhancers (SEs), these transcription-regulating complexes determine cellular identity and function (Fig 6B)<sup>64, 70</sup>. Within one SE element, single enhancers can interact with each other and high levels of TFs, cofactors, eRNA and RNAPII are present at each constituent enhancer<sup>64</sup>.

Enhancers and SEs can activate any gene, they are physically connected to. Their target genes generally occur within so called insulated neighborhoods, chromosomal loop structures formed by the interaction of two DNA sites bound by the CTCF protein and occupied by a cohesin complex (Fig. 6C)<sup>71</sup>. This allows enhancer-gene interaction, even if they are separated by thousands of bases. Around 13.000 of these insulated neighborhoods with an average size of 190 kb are known, forming the mechanistic basis of higher-order chromosome structures such as Topologically Associating Domains (TADs)<sup>71</sup>.

The cell state relies on an intricate network and balance of cell-autonomous and non-cell-autonomous mechanisms including signals delivered from the tissue environment. SEs are very responsive to most signal pathways and it has been shown, that especially the transcription factor targets of Wnt, leukemia inhibitory factor (LIF) and transforming growth factor- $\beta$  (TGF- $\beta$ ), a well-known EMT-inducer, are enriched in super-enhancers in embryonic stem cells (ESC)<sup>72</sup>. Finally, chromatin regulators control the accessibility of chromatin for TFs by modulating histone proteins. Their role is to maintain the current expression state, which is additionally supported by DNA methylation<sup>64</sup>. Depending on the methylation site, transcription is enhanced, decreased or the structure of insulated neighborhoods can be altered<sup>64</sup>.

In summary, transcriptional programs that define cell identity are maintained by master TFs, which bind to specific enhancer elements. Combined to large, regulatory complexes, SEs control the expression state of genes within their insulated neighborhood. The tissue environment is mainly responsible for the cell state and delivers information by signal pathways directly to SEs. Chromatin regulators, like histone readers, writers, and erasers as well as DNA methylation, consolidate the current cell state, but also ensure high flexibility in order to adapt to external cues.

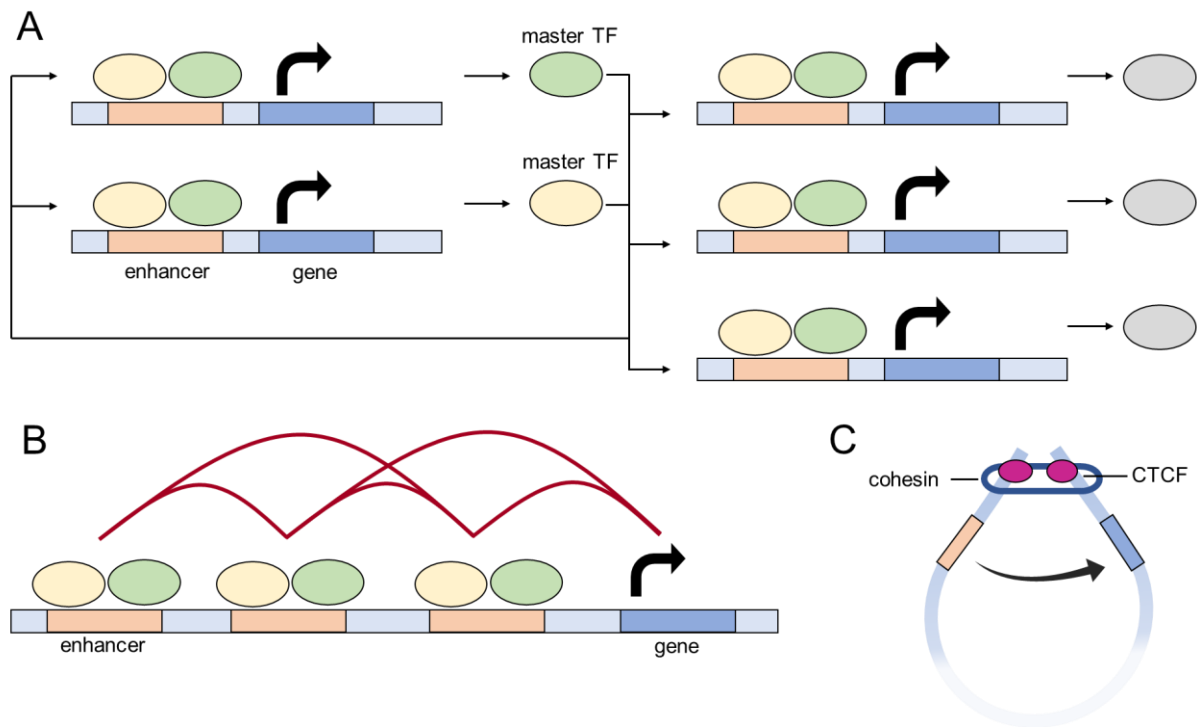


**Fig. 6:** **A:** Core regulatory circuitry. Master TFs co-regulate their own expression as well as the expression of cell type specific genes. **B:** Enhancers within SE complexes are physically connected and interact with each other and the target gene. **C:** Insulated neighborhoods are produced by multimerization of CTCFs and reinforced by cohesion, enabling most of the enhancer-gene interactions. Adapted from Bradner et al, Cell, 2017.

### 1.3.1 Transcriptional dysregulation in cancer

Transcriptional dysregulation in cancer can be a result of alterations directly in gene regulators or indirectly an outcome of mutations in signal pathway proteins. In both ways, the dysregulated transcriptional program can drive tumorigenesis or offer alternate pathways to escape drug treatment. Tumor cells develop a dependency on SE-driven transcription for proliferation and survival, which offers an Achilles' heel for the therapeutic targeting of cancer.<sup>64</sup>

Alterations may occur in all parts of the transcriptional control, including trans-factors (TFs, cofactors, signal pathways and chromatin regulators) and cis factors (enhancer, promoter and insulated neighborhoods). Dysregulated TFs can induce distinctly changes in the gene expression program and can be separated into three groups: master TFs, TFs involved in proliferation and signaling<sup>64</sup>. Activation of master TFs, that are normally expressed in early development, can activate previously silenced genes, which may result in phenotype switching. Alterations in proliferation control TFs like Myc, can have a profound effect, since they amplify the entire gene expression program<sup>73</sup>. Myc is frequently mutated or overexpressed in a various

types of cancer<sup>64</sup>. Further, a dysregulated signaling TF can bind enhancers occupied by master TFs and increase the expression of a specific gene or even stimulate the formation of SEs<sup>74</sup>. In addition, genetic alterations in cofactors, which are part of a large mediator complexes recruited by TFs to the transcription site, are frequently observed in different tumors<sup>75,76</sup>. The interaction between enhancers and promoters as well as the accessibility for TFs is mediated by chromatin structure and its regulators. Thus, alterations in chromatin regulators can have a profound effect on global gene expression. More than 50% of human cancers carry mutations in enzymes that are involved in chromatin organization, underlining the significance of chromatin regulators for tumor progression<sup>77</sup>.

The contribution to cancer pathogenesis by regulatory cis factors is mainly characterized by alterations in SE structure and insulators. Different mechanisms lead to acquisition of SEs at oncogenic driver genes, making tumor cells highly addicted to certain transcriptional programs. For example DNA translocation or focal amplification as well as dysregulated signaling can result in formation of SE at oncogenic key genes<sup>64,78</sup>. A high density of cofactors and chromatin regulators can be found around those regulatory areas compared to typical enhancers<sup>78</sup>. Enriched levels of RNAPII, histone acetyltransferase (HAT) p300, BRD4, a member of the bromodomain protein family and chromatin reader, as well as Nipbl, which is required for the association of cohesin with DNA, are often found at SEs<sup>78</sup>. All of these proteins increase the transcriptional activity and maintain enhancer activity. Further, SEs are often observed to be hyperacetylated and increased levels of Chd7, a chromatin remodeler that also interacts with p300, are found around these areas<sup>78</sup>. ChIP-seq data revealed, that a remarkable number of known oncogenic drivers are associated with super-enhancers in cancer cells, which are not present in their healthy counterparts<sup>78</sup>. These findings may even support the identification of key oncogenes in specific cancers and expose the dependencies on transcriptional programs.

Alterations in sequences of insulated neighborhoods can also contribute to dysregulations of gene expression. Mutations in loop anchors of oncogene-containing insulated neighborhoods are often observed in tumor cells, altering the CTCF DNA-binding motif<sup>79</sup>. DNA-hypermethylation was associated with disrupting CTCF-binding in some cancers as well<sup>80</sup>. These chromosomal rearrangements and disruptions in insulated neighborhoods can relocate enhancers and bring them in physical connection to previously silenced proto-oncogenes. In this way the oncogene is activated and driving tumor progression without harboring an alteration in its own sequence.

The identification of these mechanisms is the key step in understanding dependencies on certain transcriptional programs, which offers vulnerabilities for specific cancer cells. For instance, the previously mentioned subtypes of pancreatic cancer, Classical and Basal-like, significantly

affect the therapy response and prognosis. It was shown that most pancreatic tumors develop through the same mutations, suggesting that non-genetic mechanisms are responsible for the complex heterogeneity and different subtypes in PDAC<sup>26</sup>. In addition, the more aggressive Basal-like expression program is associated with enriched TGF- $\beta$  signaling, the EMT program<sup>26</sup> and mutations in genes involved in chromatin modification<sup>81</sup>. These findings suggest an epigenetic driven transition from a Classical- to a Basal-like subtype and may offer transcriptional dependencies, which can be exploited. This is supported by observations, that Basal-like cells are more often sensitive to BET inhibition compared to Classical cells.

Another example is the therapy resistant nut midline carcinoma. It is well accepted, that the chromosomal rearrangement of the NUT gene to BRD4 leads to the oncogenic function of blocking differentiation and maintaining proliferation, making NMC cells highly addicted to transcriptional regulation by the BRD4-NUT fusion protein and offers vulnerabilities by targeting BRD4-mediated functions and restoring differentiation.

### **1.3.2 Targeting transcriptional dependencies**

Given its role in the context of cellular plasticity, a reversible process that enables drug tolerance, transcriptional addiction offers three main approaches to target therapy resistance.<sup>9</sup> Exploiting cell vulnerabilities and selectively targeting the new cell identity. Using the epigenetic mechanisms that control cell plasticity to revert and resensitize cells to therapy. And preventing cell plasticity by blocking crucial epigenetic mechanisms required for phenotype switching.

The emerging drug tolerant cells may deliver specific vulnerabilities that can be exploited. For instance, in the case of epithelial–mesenchymal-transition (EMT), which is highly associated with cell plasticity. EMT-TF Snail induces the expression of the AXL receptor tyrosine kinase in carcinoma cells, offering a compensatory signaling to EGFR<sup>42</sup>. EMT-triggered AXL signaling confers Erlotinib resistance in non-small-cell lung carcinoma (NSCLC)<sup>42</sup>. It was shown, that exploiting this mesenchymal feature and combine treatment with AXL and EGFR inhibitors overcame EGFR inhibitor resistance associated with the mesenchymal phenotype in mouse xenograft models<sup>82</sup>.

Another approach is targeting the reversibility of the process of cell plasticity and resensitize cells to drug treatment. Since the cell identity is tightly controlled by the chromatin landscape, chromatin modifying enzymes are a promising target<sup>9</sup>. Additionally, reverting EMT has the potential to significantly decrease therapy resistance, because the mesenchymal phenotype contains CSC-comparable resistance mechanisms and the activation of the EMT program itself increases the capacity of cell plasticity. By doing so, it would be required to induce MET

program and force cancer cells to differentiate into a non-CSC state again and regain epithelial abilities. Blocking TGF- $\beta$  signaling, which is among the best characterized pathways involved in EMT induction, would be a promising approach<sup>42</sup>. However, given its complex roles and also antiproliferative effects on tumor progression, targeting TGF- $\beta$  signaling requires caution and remains a challenge<sup>9, 54</sup>.

Preventing cell plasticity may hold most promise, since several strategies could avoid phenotype switching from the very beginning. As previously mentioned, slow-cycling persistent subtypes are a key step in the process of induces drug resistance. Since epigenetic alterations are highly related with drug tolerant persister (DTP) cells, transcriptional regulators and specific pathways offer a wide range of potential targets. The most direct and encouraging way would be to target TFs and Cofactors, which are predominantly regulating transcription and cell identity. Especially dysregulations in master TFs such as Myc are driving proliferative programs in the majority of human cancers<sup>64</sup>. Transcriptional addiction of tumor cells to Myc has been shown in different model systems<sup>83, 84</sup> Unfortunately, as for many TF, direct inhibition of Myc remains challenging<sup>64</sup>. Such challenges include its crucial physiological function for healthy cells, the lack of binding pockets and the nuclear localization additionally impede the progress in drug discovery<sup>85</sup>. Nevertheless, a remarkable example for direct inhibition of oncogenic TFs is the development of all-trans retinoic acid (ATRA) as therapy for acute promyelocytic leukemia (APML)<sup>64</sup>. In combination with chemotherapy, ASTRA is the standard of care for APML and exemplifies transcriptional addiction in cancer cells<sup>86</sup>.

If inhibition of oncogenic TFs is not possible, targeting transcriptional cofactors and chromatin regulators is another promising approach, since they are connecting the transcriptional machinery and regulate chromatin accessibility. Inhibition of the bromodomain of BET proteins is a successful example of targeting oncogenic coactivators. In 2010 the first inhibitor targeting BET proteins (BRDT, BRD2, BRD3 and BRD4) JQ1 was reported<sup>87</sup>. Preclinical mouse models with NUT-midline carcinoma (NMC) xenografts underlined the potential of inhibiting this coactivator and various derivatives went into clinical trials based on the structure of JQ1<sup>64</sup>. Interestingly, BRD4 was shown to be highly associated with transcription of oncogenic Myc<sup>70</sup>. In its function of recognizing acetylated histones, super-enhancers (SEs) and promoters of Myc and other oncogenes were highly occupied by BRD4<sup>70</sup>. Thus, BRD4 was shown to be an important co-activator of MYC mediated transcription in tumor cells and a novel therapeutic strategy to indirectly target oncogenic TFs.<sup>64</sup> Further, SEs-driven transcription is exceptional vulnerable to BRD4 inhibition, since decreased levels of TFs impair the auto-regulation mechanism, which is required to maintain large SE-complexes of master TFs<sup>64</sup>.

The Inhibition of chromatin modulators like histone acetyltransferases (HATs) and histone deacetylases (HDACs) is another approach to alter the epigenetic landscape of cancer cells. Hyperacetylation of SEs and oncogenes or a shutdown of tumor suppressor genes, induced by cell plasticity or genetic alterations result in transcriptional adaptation but also dependency on key regulators. Combinational therapy approaches got in the center of attention, using chromatin regulator inhibition to overcome resistance to certain treatments<sup>9, 12</sup>. Especially, HDAC inhibition seems to be a promising approach to sensitize tumor cells to a specific treatment and decrease the emergence of resistance<sup>88</sup>. HDAC inhibitors have been shown to have a limited therapeutic efficacy as a single therapeutic agent, but demonstrated preclinical and clinical success in combinational therapies since the first HDACi SAHA (Vorinostat) was approved by the FDA in 2006<sup>88</sup>. However, as for most epigenetic inhibitors, HDACi are not selective for tumor cells and effect additionally a complex network of non-histone proteins<sup>88</sup>. Thus, off-target toxicity associated with HDACi and other epigenetic inhibitors remains as crucial challenge for future drug development.

#### **1.4 Challenges in epigenetic drug discovery**

Epigenetic drugs have undergone a rapid clinical development in recent years. They have primarily been studied for their use in treating cancer, but also demonstrate progress in the fields of neurological disorders, inflammatory or immune diseases<sup>89</sup>. Especially HDACi and bromodomain inhibitors showed promising preclinical in vitro and in vivo antitumor activity in hematological malignancies and solid tumors and many inhibitors have entered phase I-III clinical trials<sup>90, 91</sup>. In most cases, epigenetic inhibitors show limited single agent activity, but synergistic effects are observed in many different tumor types that have been investigated after combinational treatment with other epigenetic and non-epigenetic drugs<sup>90, 91</sup>. However, current epigenetic compounds lack isoform selectivity and also affect the global epigenome of healthy cells, thus on- and off-target toxicity is not uncommon in most therapies<sup>89</sup>. Although many epigenetic targets have been identified, substantial challenges remain in drug discovery. For instance, substrates of HDACs and HATs are not exclusively limited to chromatin proteins. It has been shown that HAT P300/CBP effects histones as well as the oncogene p53<sup>92</sup>.

The lack of knowledge about chromatin networks impedes the development of accurate in vitro assay systems, which may not fully represent the drug activity in a cellular system<sup>93</sup>. Most epigenetic modulators work in complexes with other chromatin-related proteins. Thus, inhibiting one protein may induce unexpected cross-talk between chromatin regulators<sup>93</sup>. New generations of more selective epigenetic compounds would help to understand the specific role of each isoform and open new possibilities for future clinical development of anti-cancer

inhibitors. In addition to the epigenetic-specific challenges, the development of new epigenetic compounds has to deal with the typical problems of preclinical drug discovery (Fig. 7). After proof of activity and identification of structure-activity-relationship (SAR), many compounds still struggle with organic solubility, metabolic stability, target potency and molecular weight, also known as druglikeness. The majority of compounds already fails before entering clinical trials. High-throughput screening (HTS) will increase chances to identify novel epigenetic candidates. Phenotypic screening has shown to be important for the discovery of certain epigenetic drugs like the BETi RVX-208 or the HDACi SAHA (Vorinostat)<sup>93</sup>. Further, the focus on chemical libraries designed for the epigenetic enzyme pockets and structural features that are unique to the targeted sites will increase the efficiency of lead discovery<sup>93, 94</sup>.

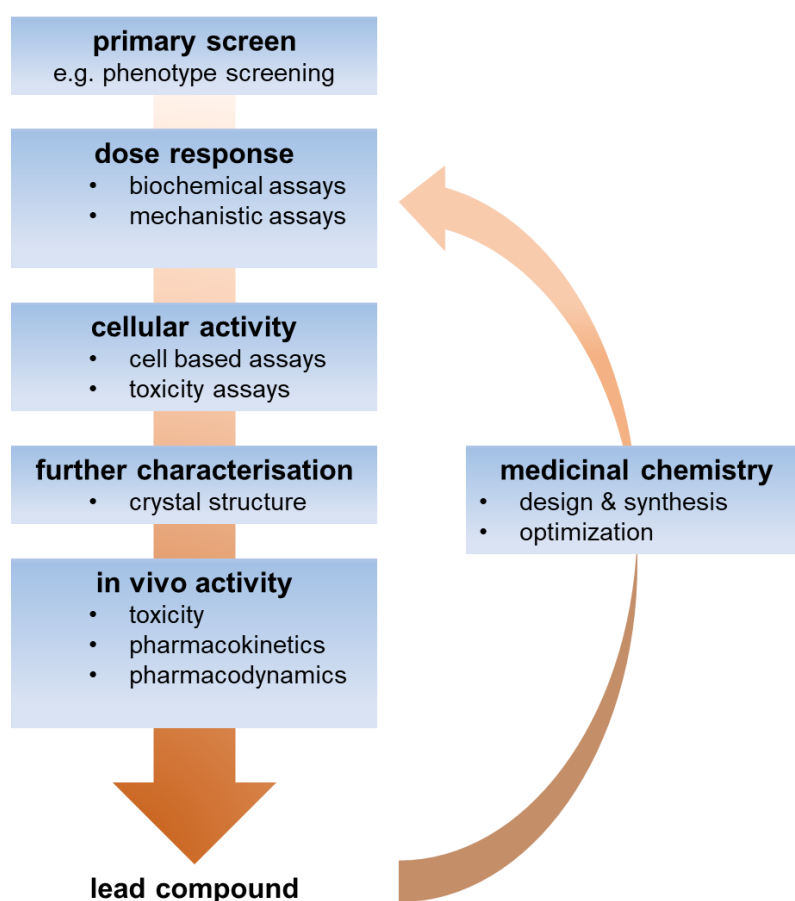


**Fig. 7:** Typical workflow of preclinical drug discovery, characterization and compound optimization. Multiple repeatable steps are required to obtain a promising compound, which fulfills all criteria before entering clinical trials. Adapted from Müller et al, eLife, 2018.

### **1.4.1 Structural Genomics Consortium (SGC)**

The Structural Genomics Consortium is a public-private partnership with scientists in many geographical sites like Frankfurt, Oxford or Toronto and funded by members from pharmaceutical industry. The SGC focuses on the development and rational design of selective inhibitors, that help to reach a deeper understanding of molecular mechanisms in different diseases<sup>95</sup>. Their libraries contain a wide spectrum of compounds such as kinase, receptor or epigenetic inhibitors. The compounds are either developed by academic research groups associated with Structural Genomics Consortium or donated as chemical probes (DCP) by industry. High-quality chemical probes developed by pharmaceutical industry and compound-associated data are usually not accessible, which makes it difficult for academia to choose the right chemical tools. The highly specific inhibitors developed for diverse therapeutic areas are no longer pursued as drug candidates for several reasons, thus they offer resources for basic research, structure-activity-relationships and target validation<sup>95</sup>. Potency, selectivity and cellular activity are well characterized for every inhibitor and the compound related data base is constantly updated. Additionally, most compounds contain an inactive, structurally highly related analogues, which facilitate validation of on-target effects. Especially the release of previously hidden epigenetic compounds to the SGC epigenetics probes project can accelerate drug discovery in this research field. The SGC Frankfurt has additionally high capacities for protein expression, in vitro screening, NMR and X-ray crystallography to further develop and optimize lead structures<sup>95</sup>. Based on the open science probe project, a large number of these high-quality probes are available to the research community and will provide value to science and to the companies.

### **1.4.2 Drug discovery in targeting bromodomains**

With the cell-permeable small molecule JQ1 the first bromodomain targeting inhibitor was reported in 2010<sup>87</sup>. Until then, chromatin-acting efforts have been limited to chromatin modifying enzymes like HDACs, HATs, DNMTs and KMTs. The first inhibition of an epigenetic reader molecule had significant impact on cancer therapy and drug discovery. The development was based on an observation by Mitsubishi Pharmaceuticals that thienodiazepines have antitumor activity and the ability to inhibit binding between acetylated histone and bromodomain-containing proteins<sup>87, 91</sup>. Co-crystal structures of protein and inhibitor revealed, that only the (+)-JQ1 enantiomer competitively binds in acetyl-lysine binding sites in both bromodomains (BD1 and BD2) of BET-family proteins<sup>87</sup>. Binding to all members of the protein family (BRDT, BRD2, BRD3 and BRD4) was observed, whereas the binding affinity ( $K_d$ ) to both subdomains BD1 and BD2 differs in every protein<sup>87</sup>. While there are 61 different

bromodomains expressed in the human genome, JQ1 seems to be selective for bromodomains of the BET-family, but unselective for both BD1 and BD2<sup>96</sup>.

Further, xenograft models of NUT midline carcinoma (NMC) demonstrated profound anti-tumor activity in BRD4-dependent carcinomas by JQ1 and revealed that the BETi is able to induce differentiation, cell cycle arrest and apoptosis in tumor cells<sup>87</sup>. Targeting of BRD4, which is by far the best studied member of the bromodomain family, was also a successful in downregulating proinflammatory pathways<sup>96</sup>.

Based on JQ1, several BET inhibitors have entered clinical evaluation or are in preclinical development<sup>91,96</sup>. Many of the BETi as well as JQ1 have been developed by academic groups, underlining the important role of academia in drug discovery and novel target identification<sup>96</sup>. However, until now no BRD inhibitor has been FDA approved, since most compounds struggle with therapeutic benefit or toxicity<sup>91,96</sup>. Additionally, mechanisms of resistance have been reported from preclinical and clinical models<sup>30,91</sup>. Certainly, a better understanding of molecular mechanisms will lead to more effective drugs in the future. Selectivity for single members of the BET-family proteins may decrease toxicity and offer new insights into roles of specific isoforms. A recent study from 2020 reports about BD1- and BD2-selective inhibitors with unprecedented selectivity and that specific inhibition of each domain alters gene expression in different ways<sup>97</sup>. Domain-selective inhibitors will provide exciting research on the role of both subdomains in the future.

Since synergistic effects have been frequently observed for BETi in combination with other drugs, combinational approaches as well as the development of novel dual inhibitors are a promising strategy for next generation of anticancer agents<sup>91</sup>. It is assumed, that synergism appears due to blocking of a BRD4-mediated feedback mechanism by BETi, that would usually activate additional kinases<sup>98</sup>. Thus, combination therapies with kinase inhibitors are under preclinical investigation<sup>91</sup>. Another strategy is the development of protein-targeting chimeric molecules (PROTACs), which binds BET proteins with one part and mediates the binding to an E3 ubiquitin with another part, thus degrading the BET protein via the proteasome<sup>91,96</sup>. In this way not only the bromodomain is inhibited, but the loss of BET protein as part of the chromatin complex would significantly impact the core transcriptional machinery<sup>91</sup>.

## **2. Characterization of a dual BET/HDAC inhibitor for treatment of pancreatic ductal adenocarcinoma**

### **Summary**

Pancreatic ductal adenocarcinoma (PDAC) is one of the most therapy resistant tumors. Previous studies showed that combined BET and HDAC inhibition is synergistic in tumor models of various malignancies including PDAC<sup>99</sup>. However, toxicity, drug-drug interactions or pharmacokinetics can limit the application of combination therapies. The aim of this study was to design and analyze the efficacy of a novel dual BET/HDAC inhibitor to combine the benefits of a combinational approach in one single molecule.

In cooperation with the group of Prof. Dr. Stefan Knapp (Goethe Universität, Frankfurt), three small molecules, containing the backbone of JQ1 as BET inhibitor and SAHA, Panobinostat or CI994 as HDAC inhibitor, were synthesized and tested. Based on cellular activity assays, TW9, the combination of JQ1 and CI994, was chosen as most potent BET/HDAC inhibitor for further characterizations. TW9 preserves both BETi and HDACi activities in cancer cells, comparable to single drug treatment. Additionally, washout experiments could demonstrate an enhanced histone acetylation for TW9-treated samples, in contrast to CI994 alone. In NUT midline carcinoma (NMC), a poorly differentiated squamous cell carcinoma, previous study showed that inhibition by JQ1 was able to induce squamous differentiation. Treatment with TW9 was significantly more efficient than JQ1 in inducing canonical squamous tissue genes like KRT10, KRT14 or TGM1 and induced morphological changes. Cell viability assays in different PDAC cell lines showed more pronounced anti-proliferative effects for TW9 compared to JQ1, CI994 or the combination of both inhibitors. Immunoblot analysis also indicated a stronger induction of apoptosis by TW9. Notably, a prolonged suppression of proliferation by TW9 compared to single inhibitor or combinational treatment was observed, using short-time treatment. The combinational efficacy of TW9 and gemcitabine, the standard-of-care chemotherapeutic agent in the treatment of PDAC, was also evaluated. Sequential administration of gemcitabine and TW9 showed synergistic antitumor effects and strong induction of apoptosis compared to gemcitabine alone. Further, phospho-CHEK1, an indicator for replicative stress induced by gemcitabine, was enhanced after sequential treatment. Simultaneous treatment largely prevented cells from replicative stress. TW9 was shown, just like JQ1, to induced accumulation of the cell-cycle regulator p21, which led to G1 arrest and to decrease the incorporation into DNA by gemcitabine. To explore more about the molecular mechanisms of TW9, transcriptomic profiling was performed. TW9 largely recapitulated the activity of JQ1 and CI994 and was mainly associated with metabolic processes, cellular component organization

and cell cycle-related processes. The aim was to identify TW9-downregulated master transcriptional regulators that control cell cycle progression and are driven by super-enhancers. 453 super-enhancers were identified by ChIP-seq and 12 super-enhancers-associated genes were identified to be TW9-specific. The analysis revealed that downregulation of transcription factor FOSL1 may contribute to the antitumor effects of TW9, since FOSL1 is a prognostic marker and high expression levels are unfavorable for patient survival.

In summary, we reported on the generation and characterization of a novel dual BET/HDAC inhibitor with promising anti-tumor properties in PDAC and revealed insights regarding molecular mechanisms.

### **Zusammenfassung**

Das duktales Adenokarzinom des Pankreas (engl. PDAC) ist eines der therapieresistentesten Karzinome. Frühere Studien zeigten, dass die kombinierte Behandlung mit BET und HDAC Inhibitoren zu Synergien in verschiedenen Tumorarten, inklusive PDAC, führt<sup>99</sup>. Toxizität, Inhibitor-Interaktionen oder Probleme mit der Pharmakokinetik limitieren den Einsatz von Kombinationstherapien für gewöhnlich. Das Ziel dieser Arbeit war es, einen neuartigen dualen BET/HDAC Inhibitor zu designen und seine Wirksamkeit zu testen um die Vorteile einer Kombinationstherapie in einem Molekül zu vereinen.

In Kooperation mit der Arbeitsgruppe von Herrn Prof. Dr. Stefan Knapp (Goethe Universität, Frankfurt), wurden drei Inhibitoren, bestehend aus den Grundgerüsten von JQ1 als BET Inhibitor und SAHA, Panobinostat und CI994 als HDAC Inhibitoren, synthetisiert und getestet. Basierend auf Ergebnissen aus zellularen Assay-Systemen, wurde TW9, die Kombination aus JQ1 und CI994, als potentester Dual-inhibitor ausgewählt und weiter charakterisiert. Es zeigte sich, dass TW9 sowohl BETi- als auch HDACi-Aktivitäten in sich vereint, vergleichbar zu den einzelnen Substanzen. Zusätzlich konnten *washout*-Experimente zeigen, dass TW9 im direkten Vergleich zu CI994 eine verstärkte Acetylierung von Histonen bewirkt. Es wurde bereits vorher veranschaulicht, dass eine Behandlung mit JQ1 im NUT *midline carcinoma* (NMC), einem undifferenzierten Plattenepithelkarzinom, Differenzierung induzieren kann. Behandlungen mit TW9 wiesen eine wesentlich effizientere differentielle Induktion von Plattenepithelgewebegenen wie KRT10, KRT14 oder TGM1 auf. *Cell viability assays* in verschiedenen PDAC Zelllinien verdeutlichten einen ausgeprägteren anti-proliferativen Effekt von TW9 im Vergleich zu den Einzelinhibitoren oder deren Kombination. Immunoblot-Analysen deuten zusätzlich eine starke Induktion von Apoptose in TW9-behandelten Zellen an. Bemerkenswerterweise wies TW9 in Kurzzeitexperimenten ebenfalls eine verlängerte und ausgeprägte anti-proliferative Wirkung auf. Zusätzlich wurde eine Kombinationstherapie mit

Gemcitabine, dem Standard-Chemotherapeutikum für PDAC, getestet. Dabei zeigte sich, dass eine sequentielle Verabreichung von TW9 und Gemcitabine synergistische Effekte aufwies und Apoptose deutlich stärker induzierte als Gemcitabine alleine. Des Weiteren wurde verdeutlicht, dass phospho-CHK1, ein Indikator für durch Gemcitabine induzierten replikativen Stress, nach sequentieller Verabreichung verstärkt nachweisbar war. Simultane Verabreichung hingegen schützte die Zellen weitestgehend vor replikativem Stress. TW9, wie auch JQ1, sorgt für eine Anreicherung von Zellzyklusregulator p21, was die Zellen in der G1 Phase festsetzt und verhindert, dass Gemcitabine in die DNA eingebaut wird. Um mehr über den molekularen Mechanismus hinter TW9 zu erfahren, wurde ein Transkriptom-Profil erstellt. Es zeigte sich, dass TW9 zum großen Teil Effekte von JQ1 und CI994 in sich vereint und hauptsächlich mit metabolischen und Zellzyklus-Prozessen in Verbindung gebracht werden kann. Das Ziel war es TW9-spezifische *master*-Transkriptionsfaktoren zu identifizieren, die den Zellzyklus regulieren und zusätzlich durch *super-enhancers* (SEs) angetrieben werden. Insgesamt wurden 453 SEs ermittelt, von denen 12 exklusiv von TW9 beeinflusst werden. Die Auswertung ergab, dass die Runterregulierung von Transkriptionsfaktor FOSL1 durch TW9 möglicherweise für die starke anti-proliferative Wirkung mitverantwortlich ist. FOSL1 dient zusätzlich als prognostischer Marker und hohe Expressionslevel werden mit einer geringeren Überlebensrate von Patienten in Verbindung gebracht.

Zusammenfassend wurde die Synthese und Charakterisierung eines neuartigen dualen BET/HDAC-Inhibitors beschrieben, der eine vielversprechende anti-Tumorwirkung aufweist und dessen molekulare Mechanismen genauer beleuchtet wurden.

## Cumulative dissertation of Tim Zegar - author contributions

### Characterization of a dual BET/HDAC inhibitor for treatment of pancreatic ductal adenocarcinoma

Xin Zhang, Tim Zegar, Tim Weiser, Feda H. Hamdan, Benedict-Tilman Berger, Romain Lucas, Dimitrios-Ilias Balourdas, Swetlana Ladigan, Phyllis F. Cheung, Sven-Thorsten Liffers, Marija Trajkovic-Arsic, Björn Scheffler, Andreas C. Joerger, Stephan A. Hahn, Steven A. Johnsen, Stefan Knapp and Jens T. Siveke

Xin Zhang, Tim Zegar and Tim Weiser are co-first authors of this article.

**conception** - 0 %: The conception was done by Prof. Dr. Jens T. Siveke, Prof. Dr. Stefan Knapp and Dr. Xin Zhang.

**experimental work** - 40 %: Tim Zegar was involved in biological and biochemical experiments (immunoblot analysis, RT-qPCR, colony formation assay, cell morphology analysis).

**data analysis** - 50 %: Tim Zegar was involved in data analysis from biological and biochemical experiments.

**data collection and statistical analysis** - 30 %: Tim Zegar was collecting and combining results. The final statistical analysis was done by Dr. Xin Zhang.

**writing the manuscript** - 5 %: Tim Zegar was partially writing the experimental part.

**revision process of the manuscript** - 40 %: Tim Zegar was involved in experimental work and revising and editing of figures.

---

Signature PhD student

---

Signature supervisor

## CANCER THERAPY AND PREVENTION

# Characterization of a dual BET/HDAC inhibitor for treatment of pancreatic ductal adenocarcinoma

Xin Zhang<sup>1,2</sup> | Tim Zegar<sup>1,2</sup> | Tim Weiser<sup>3,4,5</sup> | Feda H. Hamdan<sup>6,7</sup> |  
 Benedict-Tilman Berger<sup>3,4</sup> | Romain Lucas<sup>3,4,5</sup> | Dimitrios-Ilias Balourdas<sup>3,4</sup> |  
 Svetlana Ladigan<sup>8,9</sup>  | Phyllis F. Cheung<sup>1,2</sup> | Sven-Thorsten Liffers<sup>1,2</sup> |  
 Marija Trajkovic-Arsic<sup>1,2</sup> | Bjoern Scheffler<sup>10</sup> | Andreas C. Joerger<sup>3,4,5</sup> |  
 Stephan A. Hahn<sup>8</sup> | Steven A. Johnsen<sup>6,7</sup> | Stefan Knapp<sup>3,4,5</sup> | Jens T. Siveke<sup>1,2</sup> 

<sup>1</sup>Institute for Developmental Cancer Therapeutics, West German Cancer Center, University Medicine Essen, Essen, Germany

<sup>2</sup>Division of Solid Tumor Translational Oncology, German Cancer Consortium (DKTK, partner site University Hospital Essen) and German Cancer Research Center, DKFZ, Heidelberg, Germany

<sup>3</sup>Structural Genomics Consortium, Buchmann Institute for Life Sciences, Goethe University Frankfurt, Frankfurt, Germany

<sup>4</sup>Institute of Pharmaceutical Chemistry, Goethe University Frankfurt, Frankfurt, Germany

<sup>5</sup>German Cancer Network (DKTK), Frankfurt, Germany

<sup>6</sup>Department of General, Visceral and Pediatric Surgery, University Medical Center Göttingen, Göttingen, Germany

<sup>7</sup>Gene Regulatory Mechanisms and Molecular Epigenetics Lab, Division of Gastroenterology and Hepatology, Mayo Clinic, Rochester, Minnesota

<sup>8</sup>Department of Molecular Gastrointestinal Oncology, Ruhr-University Bochum, Bochum, Germany

<sup>9</sup>Department of Internal Medicine, Knappschaftskrankenhaus Bochum, Ruhr-University of Bochum, Bochum, Germany

<sup>10</sup>DKFZ Division of Translational Neurooncology, West German Cancer Center, DKTK partner site University Hospital Essen, Essen, Germany

### Correspondence

Stefan Knapp, Buchmann Institute for Molecular Life Sciences and Institute of Pharmaceutical Chemistry, Goethe University Frankfurt, Max-von-Laue-Str. 9, 60438 Frankfurt am Main, Germany.  
 Email: knapp@pharmchem.uni-frankfurt.de

Jens T. Siveke, Institute for Developmental Cancer Therapeutics and Division of Solid Tumor Translational Oncology (German Cancer Consortium (DKTK), partner site Essen), West German Cancer Center, University Hospital Essen, Hufelandstraße 55, Essen D-45147, Germany.  
 Email: jens.siveke@uk-essen.de

### Funding information

Deutsche Forschungsgemeinschaft, Grant/Award Numbers: Clinical Research Unit KFO337 / S11549/3-1, SFB824 (project C4)

### Abstract

Pancreatic ductal adenocarcinoma (PDAC) is resistant to virtually all chemo- and targeted therapeutic approaches. Epigenetic regulators represent a novel class of drug targets. Among them, BET and HDAC proteins are central regulators of chromatin structure and transcription, and preclinical evidence suggests effectiveness of combined BET and HDAC inhibition in PDAC. Here, we describe that TW9, a newly generated adduct of the BET inhibitor (+)-JQ1 and class I HDAC inhibitor CI994, is a potent dual inhibitor simultaneously targeting BET and HDAC proteins. TW9 has a similar affinity to BRD4 bromodomains as (+)-JQ1 and shares a conserved binding mode, but is significantly more active in inhibiting HDAC1 compared to the parental HDAC inhibitor CI994. TW9 was more potent in inhibiting tumor cell proliferation compared to (+)-JQ1, CI994 alone or combined treatment of both inhibitors. Sequential administration of gemcitabine and TW9 showed additional synergistic antitumor effects. Microarray analysis revealed that dysregulation of a FOSL1-directed transcriptional program contributed to the antitumor effects of TW9. Our

**Abbreviations:** BET, bromodomain and extra-terminal; DNMT, DNA methyltransferase; HDAC, histone deacetylase; NMC, NUT midline carcinoma; PDAC, pancreatic ductal adenocarcinoma; SE, super-enhancer.

Xin Zhang, Tim Zegar and Tim Weiser shared equally to the first authorship.

This is an open access article under the terms of the Creative Commons Attribution License, which permits use, distribution and reproduction in any medium, provided the original work is properly cited.

© 2020 The Authors. *International Journal of Cancer* published by John Wiley & Sons Ltd on behalf of UICC

and JO1473/1-1; Deutsche Krebshilfe, Grant/Award Number: PIPAC consortium/grant no. 70112505; Deutsches Konsortium für Translationale Krebsforschung, Grant/Award Numbers: JF MYC, SGC/ charity no. 1097737

results demonstrate the potential of a dual chromatin-targeting strategy in the treatment of PDAC and provide a rationale for further development of multitarget inhibitors.

#### KEYWORDS

BET inhibitor, combined therapy, dual BET/HDAC inhibitor, HDAC inhibitor, pancreatic ductal adenocarcinoma

## 1 | INTRODUCTION

Tumorigenesis is often considered a consequence of the accumulation of driver mutations. However, the extensive intratumor and intertumor heterogeneity in established tumors involves additional regulatory layers controlling transcriptomic activity. The epigenome, a key determinant of the transcriptional output, controls cell identity and disease status. In contrast to the irreversibility of genomic mutations, aberrant epigenomic changes can potentially be reversed by small molecules targeting chromatin modulators. Epigenome-targeting drugs that are approved or in clinical trials include DNA methyltransferase inhibitors (DNMTi), histone methyltransferase inhibitors, histone deacetylase (HDAC) inhibitors (HDACi) and bromodomain and extra-terminal (BET) inhibitors (BETi) among others.<sup>1</sup> Despite the clinical efficacy of epigenetic drugs in hematological malignancies, chromatin-acting therapeutic strategies such as HDAC inhibition in solid tumors have so far been challenging.<sup>2</sup>

Pancreatic ductal adenocarcinoma (PDAC) is the most common and lethal form of pancreatic cancer. It is now the fourth leading cause of cancer death in men and women. Due to late diagnosis and metastasis, most patients with PDAC undergo conventional chemotherapy and obtain improved albeit limited benefits from intensified and toxic chemotherapy regimens, inevitably leading to secondary resistance.<sup>3</sup> In 2015, we reported a promising epigenetic-based therapeutic strategy for PDAC that combined BET and HDAC inhibitors.<sup>4</sup> We have now generated a dual inhibitor simultaneously targeting BET and HDAC proteins. Compared to combination therapies of two or more drugs, multitarget drugs may achieve the same goal but utilize a single compound. The potential advantages of dual targeting are a linked pharmacokinetic profile, reduced risk of drug-drug interactions and simplified dosing scheduling. Here, we present the design and synthesis of dual BET/HDAC inhibitors, resulting in the identification of the potent dual inhibitor TW9. Importantly, we examined its biological effects in PDAC tumor cell lines, showing its potency as a novel chromatin-targeting approach for future clinical development for treatment of PDAC.

## 2 | MATERIALS AND METHODS

### 2.1 | Synthetic procedures

Synthetic routes for inhibitors 1 (TW9), 2 (TW12) and 3 (TW22) are described in detail in the Supporting Information.

### What's new?

Preclinical evidence suggests effectiveness of the combined inhibition of bromodomain and extra-terminal (BET) and histone deacetylase (HDAC) proteins in pancreatic ductal adenocarcinoma (PDAC). However, toxicity, scheduling, and drug-drug interactions are common challenges in combined therapy. Here, the authors developed a novel dual inhibitor, TW9, simultaneously targeting BET and HDAC proteins. TW9 showed high potency in suppressing tumor growth in PDAC. Furthermore, optimized scheduling of TW9 improved the efficacy of the chemotherapeutic agent gemcitabine. The results demonstrate the potential of a dual chromatin-targeting strategy in the treatment of PDAC and provide a rationale for further development of multi-target inhibitors.

### 2.2 | Cell culture and reagents

Pancreatic ductal adenocarcinoma cell lines (MIA PaCa-2 [RRID: CVCL\_0428], PaTu 8988t [RRID:CVCL\_1847], HPAC [RRID:CVCL\_3517], DAN-G [RRID:CVCL\_0243], PANC-1 [RRID:CVCL\_0480]) and HEK293T [RRID:CVCL\_0045] were obtained from ATCC and cultured in Dulbecco's Modified Eagle Medium (DMEM) containing 10% FBS, 25 mM glucose, 4 mM L-glutamine, 1 mM sodium pyruvate and 1% penicillin-streptomycin. Nut midline carcinoma cell line HCC2429 (RRID: CVCL\_5132) was a gift from Lead Discovery Center GmbH (Dortmund, Germany) and was cultured in RPMI1640 medium containing 10% FBS, 2 mM L-glutamine and 1% penicillin-streptomycin. All cell lines were free of mycoplasma contamination. Cell lines (MIA PaCa-2, PaTu 8988t, HPAC, DAN-G, PANC-1) were authenticated using Multiplex human Cell line Authentication Test (MCA) by Multiplexion GmbH and cell lines HCC2429 were authenticated using short tandem repeat (STR) profiling within the last 3 years. HEK293T was only used for overexpressing nanoLUC fusion constructs. (+)-JQ1, CI994 and gemcitabine were purchased from Biomol, Selleck Chemicals and Biozol Diagnostica Vertrieb, respectively. (+)-JQ1, CI994 and gemcitabine were dissolved in DMSO as 10 mM stocks.

### 2.3 | Protein expression, purification and crystallography

The first two bromodomains of BRD4, BRD4(1) and BRD4(2), were each expressed in *Escherichia coli* as His-tagged proteins and were

purified by nickel-affinity and gel-filtration chromatography as described.<sup>5</sup> After the final gel filtration step on a Superdex-75 column in 10 mM HEPES, pH 7.5, 150 mM NaCl, 0.5 mM TCEP and 5% glycerol, the protein was concentrated to 10 mg/mL, flash-frozen in liquid nitrogen and stored at  $-80^{\circ}\text{C}$ . For setting up co-crystallization trials, aliquots of the purified BRD4(1) domain were mixed with a 50 mM stock solution of TW9, TW12 or TW22 in DMSO to give a final compound concentration 1.5 mM. Crystals were grown at  $4^{\circ}\text{C}$  via the sitting drop vapor diffusion technique using a mosquito crystallization robot (TTP Labtech, Royston UK). For TW9 and TW12, crystals for data collection were grown by mixing 130 nL of protein/ligand solution with 70 nL of reservoir solution containing 24% PEG 3350, 0.1 M sodium formate, 15% ethylene glycol and 0.1 M bis-Tris-propane pH 7.3. BRD4(1) crystals in complex with TW22 were grown by mixing 100 nL of the protein/ligand solution with the same volume of reservoir solution consisting of 24% PEG 3350, 0.2 M sodium formate, 15% ethylene glycol and 0.1 M bis-Tris-propane pH 7.9. Crystals were cryoprotected with mother liquor supplemented with 20% ethylene glycol and flash-frozen in liquid nitrogen. X-ray data sets were collected at 100 K at the ESRF Grenoble, France (beamline ID30B). The diffraction data were integrated with the program XDS<sup>6</sup> and scaled with AIMLESS,<sup>7</sup> which is implemented in the CCP4 package.<sup>8</sup> The structures were solved by difference Fourier analysis in PHENIX<sup>9</sup> using PDB entry 3MXF as a starting model with initial rigid-body refinement. The structural models were then refined using iterative cycles of manual model building with COOT<sup>10</sup> and refinement in PHENIX. Dictionary files for the TW9, TW12 and TW22 ligands were generated using the Grade Web Server (<http://grade.globalphasing.org>). There was excellent electron density for the (+)-JQ1 moiety in all three structures. For TW9 and TW12, there was however not sufficient electron density to unambiguously model the solvent-exposed HDACi moiety. The disordered parts of the ligands were therefore deleted in the final model. In contrast, the HDACi moiety of TW22 was well resolved due to interaction with a symmetry-related molecule. Data collection and refinement statistics are listed in Table S1. Structural figures were prepared using PyMOL ([www.pymol.org](http://www.pymol.org)).

## 2.4 | Isothermal titration calorimetry

ITC measurements were performed using a Nano ITC microcalorimeter (TA Instruments, New Castle, Pennsylvania). All experiments were carried out at  $15^{\circ}\text{C}$  in ITC buffer (10 mM HEPES, pH 7.5, 150 mM NaCl, 0.5 mM TCEP and 5% glycerol). The microsyringe was loaded with the protein solution (50–150  $\mu\text{M}$  protein) and titrated into an 8 to 15  $\mu\text{M}$  compound solution in ITC buffer while stirring at 350 rpm. The titrations were started with an initial injection of 4  $\mu\text{L}$  followed by 24 identical injections of 8  $\mu\text{L}$ , at a rate of 0.5  $\mu\text{L}/\text{sec}$  and a spacing of 200 seconds between injections. The heat of dilution was determined by independent titrations (protein into buffer) and was subtracted from the experimental data. Data were processed using the Nano-Analyze software (Version 3.5.0) supplied with the instrument. A single binding site model was employed.

## 2.5 | XTT cell viability assay

XTT cell viability assays were performed as described,<sup>11</sup> following the XTT kit manufacturer's instructions. Briefly, HEK293T cells were seeded into flat-bottomed 96-well plates 24 hours before the addition of test compound at a density of  $2.5 \times 10^5$  cells/mL (25 000 cells/well). Then, 100  $\mu\text{L}$  of test compound was added at a concentration range from 10  $\mu\text{M}$  to 170 pM as final concentrations and incubated for 24 hours. For XTT measurement, 50  $\mu\text{L}$  of a solution containing XTT (Sigma) and phenazine monosulfate (Sigma) were added to give a final concentration of 300  $\mu\text{g}/\text{mL}$  and 10  $\mu\text{M}$ , respectively, and the reaction was incubated for 30 minutes before measuring absorbance at 475 nm (specific signal) and 660 nm (nonspecific signal). The signal was background-corrected using the following formula: specific absorbance =  $A_{475\text{nm}}(\text{test}) - A_{475\text{nm}}(\text{blank}) - A_{660\text{nm}}(\text{test})$ .

## 2.6 | NanoBRET target engagement intracellular assay

NanoBRET target engagement assays were performed following published protocols.<sup>12,13</sup> Briefly, plasmids for full-length HDAC1 and BRD4 as well as the isolated bromodomains of BRD4 containing either a C-terminal (HDAC1) or an N-terminal (BRD4) placement of NanoLuc were obtained from the manufacturer (Promega, Madison, Wisconsin). To lower intracellular expression levels of the reporter fusion, the NanoLuc/kinase fusion constructs were diluted into transfection carrier DNA (pGEM3ZF-, Promega) at a mass ratio of 1:10 prior to forming FuGENE HD complexes according to the manufacturer's instructions. DNA:FuGENE complexes were formed at a ratio of 1:3 ( $\mu\text{g}$  DNA/ $\mu\text{L}$  FuGENE). One part of transfection complex solution was then mixed with 20 parts (v/v) of HEK293T cells suspended at a density of  $2 \times 10^5/\text{mL}$  in DMEM (Gibco) + 10% FBS (GE Healthcare, Chicago, Illinois), seeded into T75 flasks and allowed to express for 20 hours. For target engagement, the corresponding HDAC1- or BRD4-transfected cells were added and reseeded at a density of  $2 \times 10^5/\text{mL}$  after trypsinization and resuspension in Opti-MEM without phenol red (Life Technologies, Carlsbad, California). Serially diluted test compound and NanoBRET HDAC (Promega cat. N2140) or BRD (Promega cat. N2130) tracer were pipetted (Echo 555 Acoustic Dispenser) into white 384-well plates (Greiner 781 207). The system was allowed to equilibrate for 2 hours at  $37^{\circ}\text{C}/5\%$   $\text{CO}_2$  prior to BRET measurements. To measure BRET, NanoBRET NanoGlo substrate + extracellular NanoLuc inhibitor (Promega) were added according to the manufacturer's protocol, and filtered luminescence was measured on a PHERAstar FSX plate reader (BMG Labtech) equipped with a luminescence filter module (450 nm [donor] and 610 nm [acceptor]).

## 2.7 | Fluorogenic HDAC assay

The fluorogenic HDAC assay was performed according to the manufacturer's instructions (BPS Bioscience, Cat. # 50033). Briefly,

fluorogenic HDAC substrate, test inhibitor and HDAC2 protein were mixed sequentially and incubated at 37°C for 30 minutes. Then, HDAC Assay Developer was added and incubated at room temperature for 15 minutes. The fluorescence values were measured using a Spark Multimode Microplate Reader (Tecan). The wavelengths for excitation and emission were 360 nm (bandwidth 35 nm) and 465 nm (bandwidth 35 nm), respectively.

## 2.8 | CellTiter Glo cell viability assay

The assay was performed according to the manufacturer's instructions (Promega, G7571). Briefly, inhibitors were preprinted in 96-well plates (Corning, Corning, New York). Then, 100 µL of cell suspension was added to the wells and cultured for indicated time periods. Then, 100 µL of diluted CellTiter-Glo Reagent (1:4 with PBS) was added to the wells. Plates were shaken for 2 minutes and incubated for another 10 minutes at room temperature in the dark. Luminescent signals were read by the Tecan Spark Multimode Microplate Reader. The values of luminescent signals were normalized to the DMSO control wells.

## 2.9 | Immunoblot analysis

Cell lysates were prepared in RIPA buffer (9806S, Cell Signaling Technology [CST]) containing protease inhibitor cocktail (Roche). Cell lysates were separated on SDS-polyacrylamide gels, transferred to nitrocellulose membranes with Trans-Blot Turbo Transfer System (Bio-Rad, Hercules, California) and incubated with antibodies dissolved in TBS containing 5% BSA and Tween 20 (0.1%). The following primary antibodies were used: rabbit anti-MYC (9402, CST), rabbit anti-β-actin (ab8227, Abcam, Eugene, Oregon), rabbit anti-cleaved Caspase-3 (Asp175; 5A1E; 9664, CST), rabbit anti-Caspase-3 (9662, CST), rabbit anti-acetyl-histone H3 (Lys9/Lys14; 9677, CST), mouse anti-p21 (F5) (6246, Santa Cruz), mouse anti-involucrin (i9018, Sigma-Aldrich, St. Louis, Missouri), rabbit anti-phospho-CHK1 (Ser345) (2341, CST). Primary antibodies were recognized by a peroxidase-coupled secondary antibody (Jackson, Bar Harbor, Maine) and signals were detected by chemiluminescence (ThermoFisher, Waltham, Massachusetts).

## 2.10 | RNA extraction and quantitative RT-PCR analysis

Total RNA was isolated using Maxwell RSC simplyRNA Cells Kit (Promega) according to the manufacturer's protocol. cDNA was synthesized using PrimeScript Reverse Transcriptase (TaKaRa, Kusatsu, Japan). cDNA was amplified using LightCycler 480 SYBR Green I Master (Roche Diagnostics, Indianapolis, Indiana) and the amplicon was detected by SYBR Green I using LightCycler 480 instrument (Roche). PCR conditions were 5 minutes at 95°C, followed by 45 cycles of

95°C for 10 seconds, 59°C for 10 seconds and 72°C for 20 seconds. The relative gene expression levels were normalized to GUSB or GAPDH and calculated using the  $2^{-\Delta\Delta Ct}$  method. The primer sequences are given in Table S2.

## 2.11 | Crystal violet staining for colony formation assay

Attached cells were rinsed once with PBS and fixed with ice-cold methanol for 10 minutes. Fixed cells were then stained by crystal violet solution (containing 0.1% crystal violet and 25% methanol) for 30 minutes. Cells were rinsed twice with H<sub>2</sub>O and dried overnight.

## 2.12 | Cell proliferation assay

MIA PaCa-2 cells (1200 cells/well) were seeded in 12-well plates (Corning). On the days of measurement, whole-well images were captured and cell confluence was analyzed by NYONE Image Cytometer (Synentec, Elmshorn, Germany).

## 2.13 | Cell-cycle analysis

The attached and floating cells were harvested and fixed in 70% ethanol at 4°C overnight. On the day of measurement, cells were washed once with PBS and incubated in PBS containing 0.5 mg/mL RNase A at 37°C for 30 minutes. Then, 30 µg/mL propidium iodide was added immediately before the measurement. The cellular DNA contents were analyzed by the Guava EasyCyto System.

## 2.14 | Global gene expression profiles

Microarray using HumanHT-12 v4 Expression BeadChip (Illumina, Inc., San Diego, California) was performed by the Genomics & Proteomics Core Facility at the German Cancer Research Center in Heidelberg following the manufacturer's instructions. Raw data were normalized based on the quantile method. Hierarchical clustering of differentially expressed genes was performed using Partek Genomics Suite 7.0.

## 2.15 | Kaplan-Meier survival analysis

The analysis was performed using the human protein atlas data set,<sup>14</sup> which contains a pancreatic cancer patient cohort (n = 176). The FPKMs (number Fragments Per Kilobase of exon per Million reads) were used for quantification of expression of *FOSL1* gene. The cohort was stratified into two expression groups with the FPKM cut-off that yields the lowest P score. The correlation between the expression levels of *FOSL1* and patient survival was examined by Kaplan-Meier survival estimator.

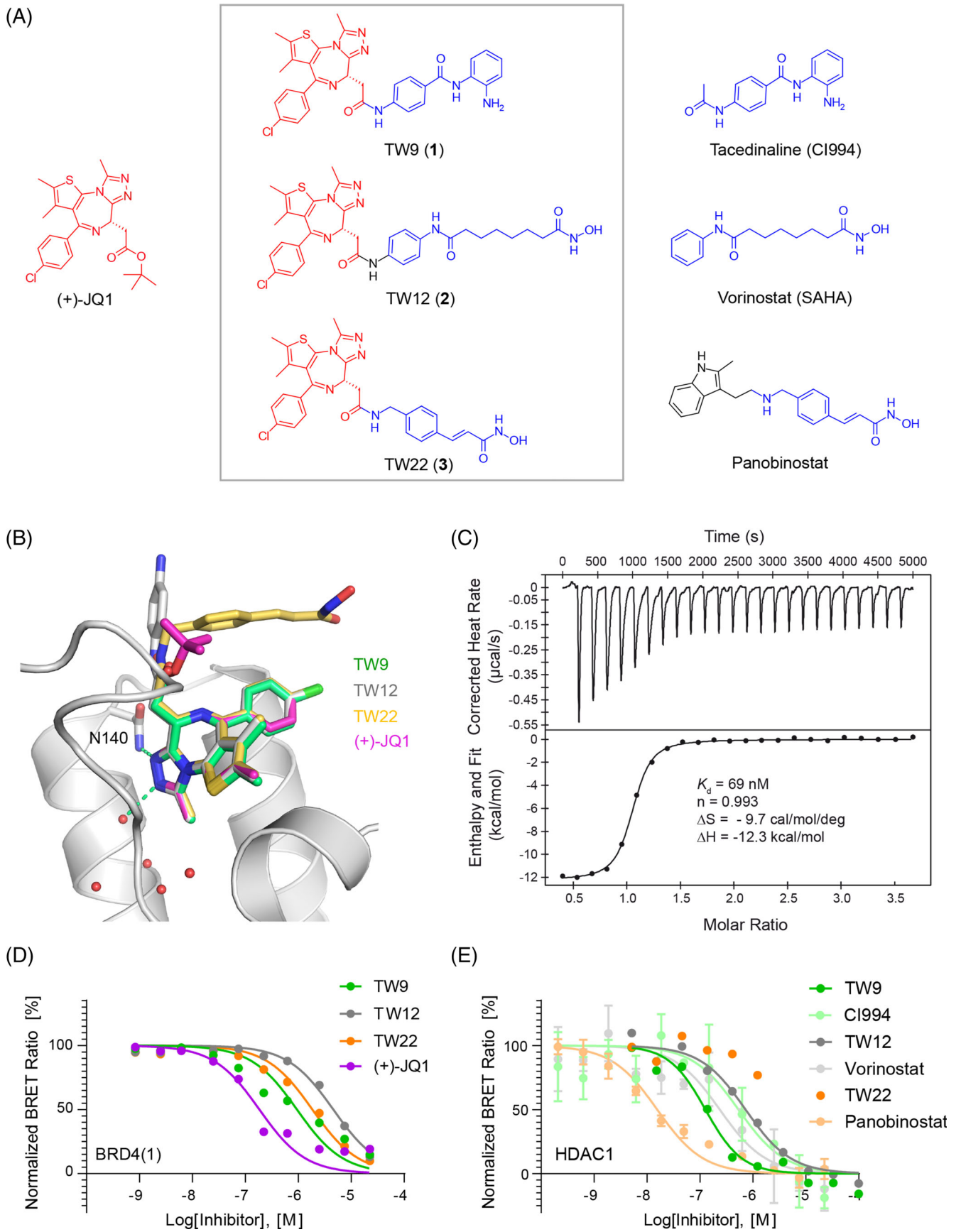


FIGURE 1 Legend on next page.

**TABLE 1** Binding of dual inhibitors to BRD4 bromodomains

Compound	<i>In vitro</i> $K_d$ ( $\mu$ M) ITC		<i>In cellulo</i> $IC_{50}$ ( $\mu$ M) NanoBRET		
	BRD4(1)	BRD4(2)	BRD4(1)	BRD4(2)	FL-BRD4
TW9	0.069 $\pm$ 0.009	0.231 $\pm$ 0.031	0.72 $\pm$ 0.09	0.074 $\pm$ 0.010	0.64 $\pm$ 0.09
TW12	0.052 $\pm$ 0.006	0.088 $\pm$ 0.015	4.53 $\pm$ 0.26	11.0 $\pm$ 3.0	6.85 $\pm$ 1.04
TW22	0.021 $\pm$ 0.004	0.054 $\pm$ 0.016	1.35 $\pm$ 0.15	1.58 $\pm$ 0.54	1.43 $\pm$ 0.07
JQ1	0.051 $\pm$ 0.015	0.089 $\pm$ 0.013	0.231 $\pm$ 0.042	0.039 $\pm$ 0.008	0.104 $\pm$ 0.010

Note: Summary of the dissociation constants  $K_d$  and cellular BRD4 activity of dual inhibitors determined by isothermal titration calorimetry (ITC) and nanoBRET assays, respectively.

**TABLE 2** Binding of dual inhibitors to HDAC1

Compounds	$IC_{50}$ ( $\mu$ M) NanoBRET
TW9	0.29 $\pm$ 0.04
CI944	0.96 $\pm$ 0.17
TW12	1.11 $\pm$ 0.36
Vorinostat	0.52 $\pm$ 0.08
TW22	>20
Panobinostat	0.19 $\pm$ 0.10

Note: Summary of the cellular HDAC1 activity of dual inhibitors determined by nanoBRET assay.

## 2.16 | Bioinformatic analysis

Gene ontology (GO) analysis was performed using Gene Ontology Consortium tool (<http://geneontology.org/>). Gene set enrichment analysis (GSEA) was conducted using default settings on mean expression values from microarray data.<sup>15</sup> Sets included in the analysis ranged from 30 to 2000 genes, and gene set was used as a permutation type. For expression values for the same gene but different isoforms, values for lower expressed isoforms in control samples were disregarded. H3K27ac signal normalized to input was used to identify super-enhancers using the Ranking of Super Enhancer (ROSE) algorithm set at default settings and ignoring regions within 2500 base pairs of transcriptional start sites.<sup>16,17</sup> Genes associated with super-enhancers were identified by Genomic Regions Enrichment of Annotations Tool (GREAT) using default settings.<sup>18</sup> Publicly available datasets were used for PANC-1 [E-MTAB-7034]<sup>19</sup> and healthy pancreas [GSM906397].<sup>20</sup> Mapping to the hg19 genome was performed using BOWTIE/2.2.5.<sup>21</sup> Bam files were generated by SAMTOOLS/1.6<sup>22</sup> and Bigwigs by DEEPTOOLS/2.4.0 with 200 base pair extension and ignoring the duplicates. Occupancy profiles were visualized using the Integrative Genomic Viewer.<sup>23-25</sup>

## 3 | RESULTS

### 3.1 | Generation of selective BET/HDAC dual inhibitors and initial *in vitro* characterization

For the development of dual HDAC/BET inhibitors, we synthesized three adducts that were based on the well-established BET inhibitor (+)-JQ1<sup>5</sup> (Figure 1A). HDAC-inhibitory activity was introduced through substitution of the tertbutyl ester by a class I selective inhibitor moiety (4-acetamido-N-[2-aminophenyl]benzamide) as present in tacedinaline (CI994), yielding the dual inhibitor TW9, as well as inhibitors for panHDAC targeting using hydroxamic acids (vorinostat and panobinostat), yielding the adducts TW12 and TW22. The synthetic routes for these inhibitors and associated analytical data are compiled in the supplemental information. The binding mode of the designed inhibitors was confirmed in crystal structures with the first bromodomain of BRD4, BRD4(1), at a resolution ranging from 1.05 to 1.25 Å (Table S1). As expected, the binding mode of the (+)-JQ1 moiety of all three adducts was essentially the same as that of the parental compound (+)-JQ1 (Figure 1B), and all key interactions with the bromodomain binding pocket were conserved, including the hydrogen bond of the triazole moiety with the highly conserved asparagine (Asn140). All HDAC moieties were solvent-accessible, suggesting that they are free to interact with HDACs even in the BET-bound state. In the case of the TW9 and TW12 complexes, the HDAC inhibitory moieties were disordered. In the structure of the TW22 complex, however, the HDAC inhibitor, which was derived from panobinostat, was visible due to stabilization by crystal contacts (Figures 1B and S1).

For initial functional evaluation, we determined the dissociation constants,  $K_d$ , of binding to the first and second bromodomain of BRD4, BRD4(1) and BRD4(2), by isothermal titration calorimetry (ITC). All three adducts (TW9, TW12 and TW22) bound to the first bromodomain, BRD4(1), with low nM affinity, resulting in  $K_d$  values of

**FIGURE 1** Rational design of BET/HDAC dual inhibitors and initial characterization. A, Chemical structure of (+)-JQ1-HDACi-adducts and their parental molecules. B, Crystal structure of dual inhibitors in complex with BRD4(1). The structure of the BRD4(1)-TW9 complex is shown as a gray cartoon representation, with the TW9 ligand shown as a green stick model. Conserved structural water molecules in the binding pocket are shown as small red spheres. The binding modes of TW12, TW22 and the parental molecule (+)-JQ1 are superimposed, showing that the binding mode of the (+)-JQ1 moiety is essentially the same in all four structures. The solvent-exposed HDACi moieties of TW9 and TW12 were largely disordered, and the corresponding atoms were deleted from the final model, whereas the HDACi moiety of TW22 was stabilized via interaction with a symmetry-related molecule in the crystal. C, Isothermal titration calorimetry experiment of TW9 binding to BRD4(1). The upper panel shows the raw binding heats for each injection, and in the lower panel, normalized binding isotherms are shown. D, Cellular BRD4(1)-targeting activity of dual inhibitors measured by NanoBRET assay. E, Cellular HDAC1-targeting activity of dual inhibitors measured by NanoBRET assay [Color figure can be viewed at [wileyonlinelibrary.com](http://wileyonlinelibrary.com)]

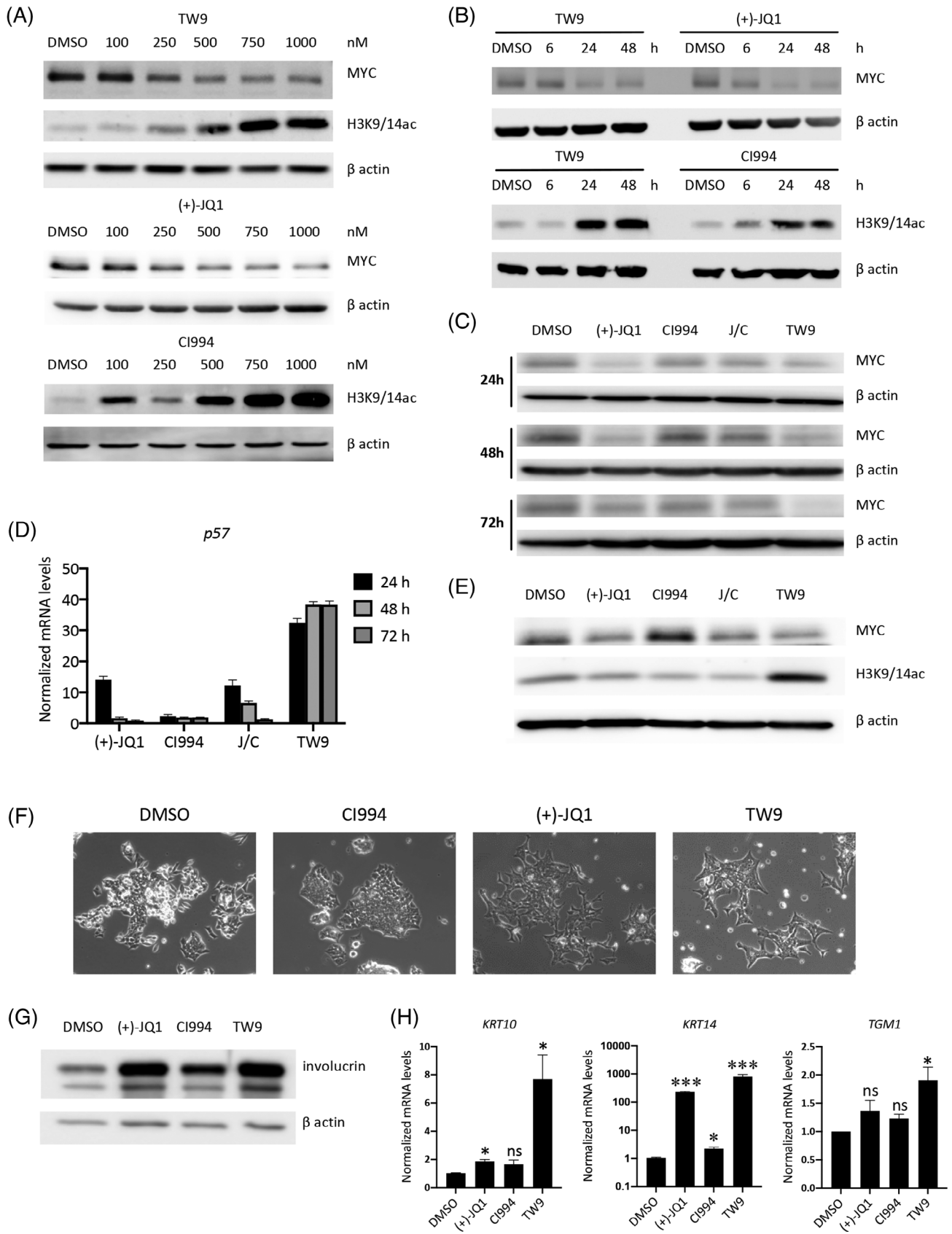


**FIGURE 2** Legend on next page.

69, 52 and 21 nM, respectively, which was in the range of the  $K_d$  value determined for the parental molecule (+)-JQ1 (51 nM; Table 1). A representative ITC experiment for TW9 is shown in Figure 1C.  $K_d$  values for BRD4(1) were all slightly higher, ranging from 230 nM for TW9 to 54 nM for TW22, which again was similar to the  $K_d$  of (+)-JQ1. In summary, the ITC measurements demonstrated excellent BET binding activity of our dual inhibitors, indicating that introduction of the HDAC-inhibitor moiety did not significantly alter affinities for the two bromodomains present in BRD4.

Next, we tested the cellular BRD4 activity of the synthesized adducts using nanoBRET assays (Table 1 and Figure 1D). All nanoBRET experiments were carried out in HEK293T cells under non-toxic conditions (Figure S2). TW9 showed the best BRD4-targeting activity, with an  $IC_{50}$  value of around 700 nM for BRD4(1) (Figure 1D). The affinity of TW12 and TW22 for BRD4(1) in cells was notably weaker, with  $IC_{50}$  values of 5.5 and 12  $\mu$ M, respectively. A similar trend was observed for the cellular affinity of our dual inhibitors to BRD4(2). Notably, TW9 had a 10 times higher affinity for BRD4(2) than for BRD4(1), with an  $IC_{50}$  value of 74 vs 720 nM, and bound BRD4(2) more than 20 times more strongly than did TW12 and TW22 (Table 1). Comparison of the ITC and nanoBRET data suggests that the drastically reduced potency of TW12 and TW22 in cells compared to (+)-JQ1 was most likely due to reduced cellular uptake rather than differences in intrinsic binding affinity. We also measured cellular  $K_d$ s for the full-length BRD4 protein, FL-BRD4. In all cases, the measured apparent binding constants were as expected between the values obtained for the two isolated bromodomains (Table 1).

After confirming the BRD4-targeting activity, we performed further NanoBRET assays to determine the cellular activity of our compounds against HDACs, the second target protein class of our dual inhibitors (Table 2 and Figure 1E). TW9 was a potent inhibitor of HDAC1 with an  $IC_{50}$  value in cells of about 300 nM. As such, it was more potent than the parental HDAC inhibitor CI994, which had an  $IC_{50}$  of around 1  $\mu$ M under the same conditions. TW12 was less potent than TW9 in targeting HDAC1, and TW22 displayed an even lower potency in cells with an  $IC_{50}$  > 20  $\mu$ M, corresponding to a potency more than three orders of magnitude lower compared to its parental compound panobinostat (Table 2). We also performed a cell-free fluorogenic HDAC assay, which showed that TW9 and CI994 inhibited HDAC2 activity to a similar degree, with  $IC_{50}$  values of 2.5 and 1.7  $\mu$ M, respectively (Figure S3). Based on the above results, we chose TW9 as the most potent BET/HDAC dual inhibitor for further characterization in cancer cells.

### 3.2 | TW9 preserves both BETi and HDACi activities in cancer cells

Both *MYC* and *HEXIM1* are often used as readout biomarkers of BET inhibitor activity in cancer cells, while acetylated histone H3 is used as a direct readout for HDAC inhibitor activity. Expression analysis by RT-PCR showed prompt (6 hours) down-regulation of *MYC* and upregulation of *HEXIM1* by TW9 to similar levels as (+)-JQ1 (Figure S4A). Immunoblot analysis showed that *MYC* and histone H3 acetylated at lysines 9 and 14 were regulated in a dose- and time-dependent manner by TW9 (Figure 2A,B), comparable to (+)-JQ1 and CI994, respectively. Consistent with the nanoBRET assays for HDAC-targeting activity of TW9 (Table 2 and Figure 1E), histone H3 acetylation at lysine 9 and 14 was enhanced by TW9 at a much higher level, compared to the parental HDAC inhibitor CI994 (Figures 2B and S4B). Intriguingly, when we treated cells with a higher dose (4  $\mu$ M) of TW9, we observed a more sustained suppression of *MYC* and induction of *p57*, a target previously identified as being regulated by combined BET/HDAC inhibition,<sup>4</sup> indicating more sustained BETi activity of TW9 (Figure 2C,D). In contrast, we did not observe the sustained BETi activity with 1  $\mu$ M TW9 (Figure S2C,D). In addition, we performed washout experiments (1 day on and 2 days off) and still observed enhanced histone H3 acetylation at lysine 9 and 14 in both 1 and 4  $\mu$ M TW9-treated samples on day three (Figures 2E and S2E).

We next implemented immunoblot analysis of *MYC* and histone H3 acetylated at lysines 9 and 14 in cells treated with TW12 and TW22. Both ligands down-regulated *MYC* to the same degree as (+)-JQ1, indicating preserved (+)-JQ1 activity (Figure S4F). However, TW12 and TW22 failed to accumulate acetylated histone H3, indicating decreased activity of the HDAC-inhibitor moiety (Figure S4F).

### 3.3 | TW9 induces squamous differentiation in NUT midline carcinomas

We next assessed the biological activity of TW9. NUT midline carcinoma (NMC) is a poorly differentiated squamous cell carcinoma defined by chromosomal rearrangement of the *NUT* gene, most often fused with *BRD4*. A previous study showed that BRD4-NUT inhibition by (+)-JQ1 was able to induce squamous differentiation.<sup>5</sup> Thus, we tested if TW9 could also induce differentiation in the NMC cell line HCC2429.<sup>26</sup> Like (+)-JQ1, TW9 provoked a differentiation phenotype in HCC2429, featuring cell spreading, flattening, and striking spindle

**FIGURE 2** TW9 preserves both BETi and HDACi activities, and induces squamous differentiation in NMC. A, Dose-dependent manner of *MYC* and H3K9/14 ac protein levels by immunoblot. PaTu 8988t cells were treated with the indicated doses of inhibitors for 48 hours. B, Time-dependent manner of *MYC* and H3K9/14 ac protein levels by immunoblot. PaTu 8988t cells were treated with 1  $\mu$ M indicated inhibitors and harvested at the indicated time points. C and D, Time-course analysis of *MYC* protein levels by immunoblot (C) and *p57* mRNA levels by quantitative RT-PCR (D). PaTu 8988t cells were treated with 4  $\mu$ M indicated inhibitors and harvested at the indicated time points. Mean  $\pm$  SEM from three independent experiments. E, Immunoblot analysis of drug washout experiment in PaTu 8988 t cells treated with 4  $\mu$ M indicated inhibitors (24 hours on and 48 hours off). F, Morphological changes of NMC cell line HCC2429 treated with 500 nM indicated inhibitors for 48 hours. G, Immunoblot analysis of involucrin, a differentiation marker, in HCC2429 cells treated with 500 nM indicated inhibitors for 72 hours. H, Quantitative RT-PCR analysis of canonical squamous tissue genes (*KRT10*, *KRT14* and *TGM1*) in HCC2429 cells treated with 500 nM indicated inhibitors for 72 hours. Mean  $\pm$  SEM from three independent experiments, \*\*\* $P$   $\leq$  .001, \*\* $P$   $\leq$  .01, \* $P$   $\leq$  .05; n.s., not significant

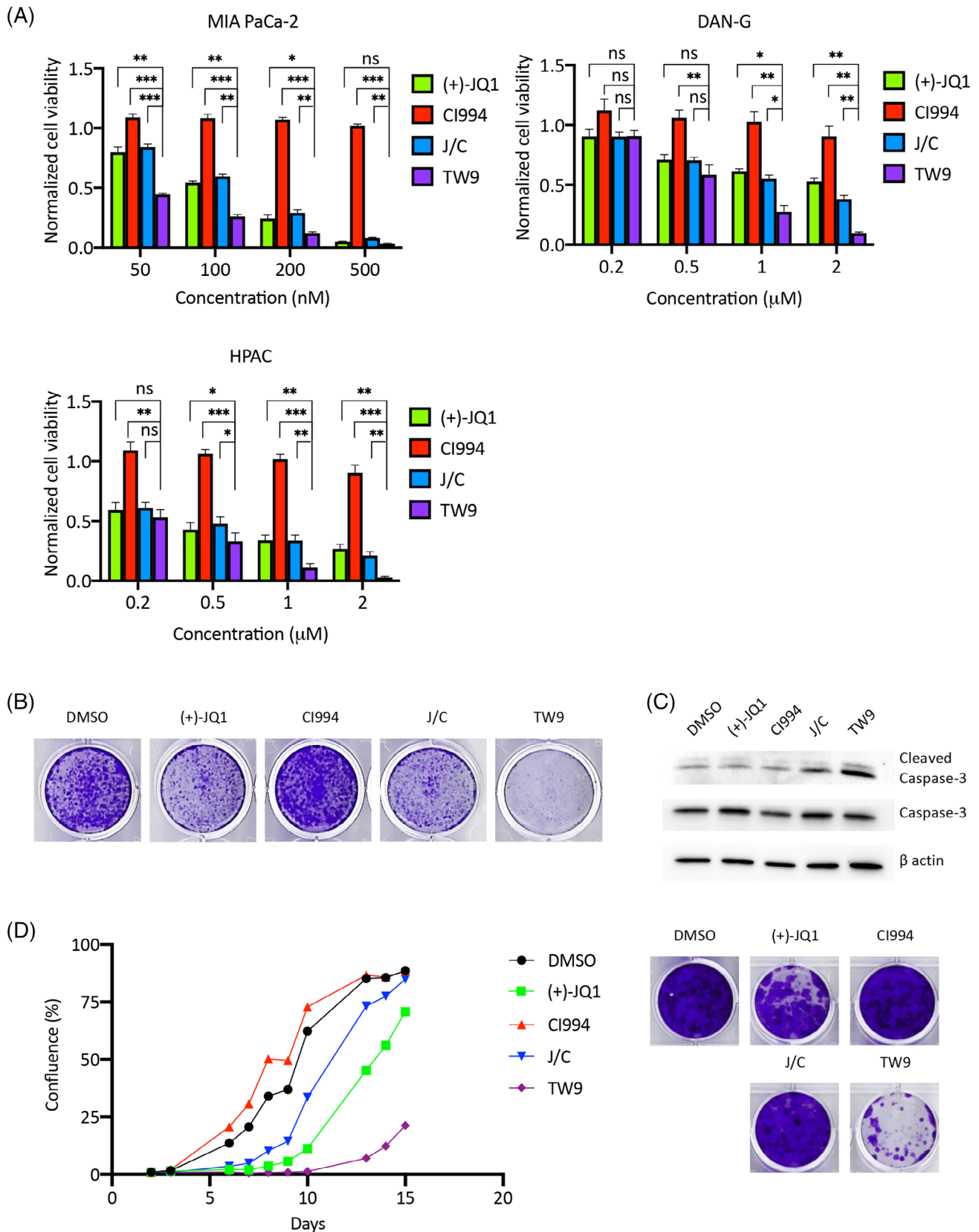


**FIGURE 3** TW9 is a more potent antiproliferation molecule than its parental molecules or combinations thereof. A, CellTiter Glo cell viability assay using four different PDAC cell lines treated with different doses of the indicated inhibitors for 5 days. Mean ± SEM from three independent experiments, \*\*\* $P \leq .001$ , \*\* $P \leq .01$ , \* $P \leq .05$ ; n.s., not significant. B, Colony formation assay of MIA PaCa-2 cells treated with 50 nM indicated inhibitors for 5 days. C, Immunoblot analysis of cleaved caspase-3 in MIA PaCa-2 cells treated with 50 nM indicated inhibitors for 3 days. D, Cell confluence measurement of MIA PaCa-2 cells after treatment of 1 μM indicated inhibitors for 24 hours by NYONE image cytometry (left). At end time point, cells were stained for colony formation assay (right) [Color figure can be viewed at [wileyonlinelibrary.com](http://wileyonlinelibrary.com)]

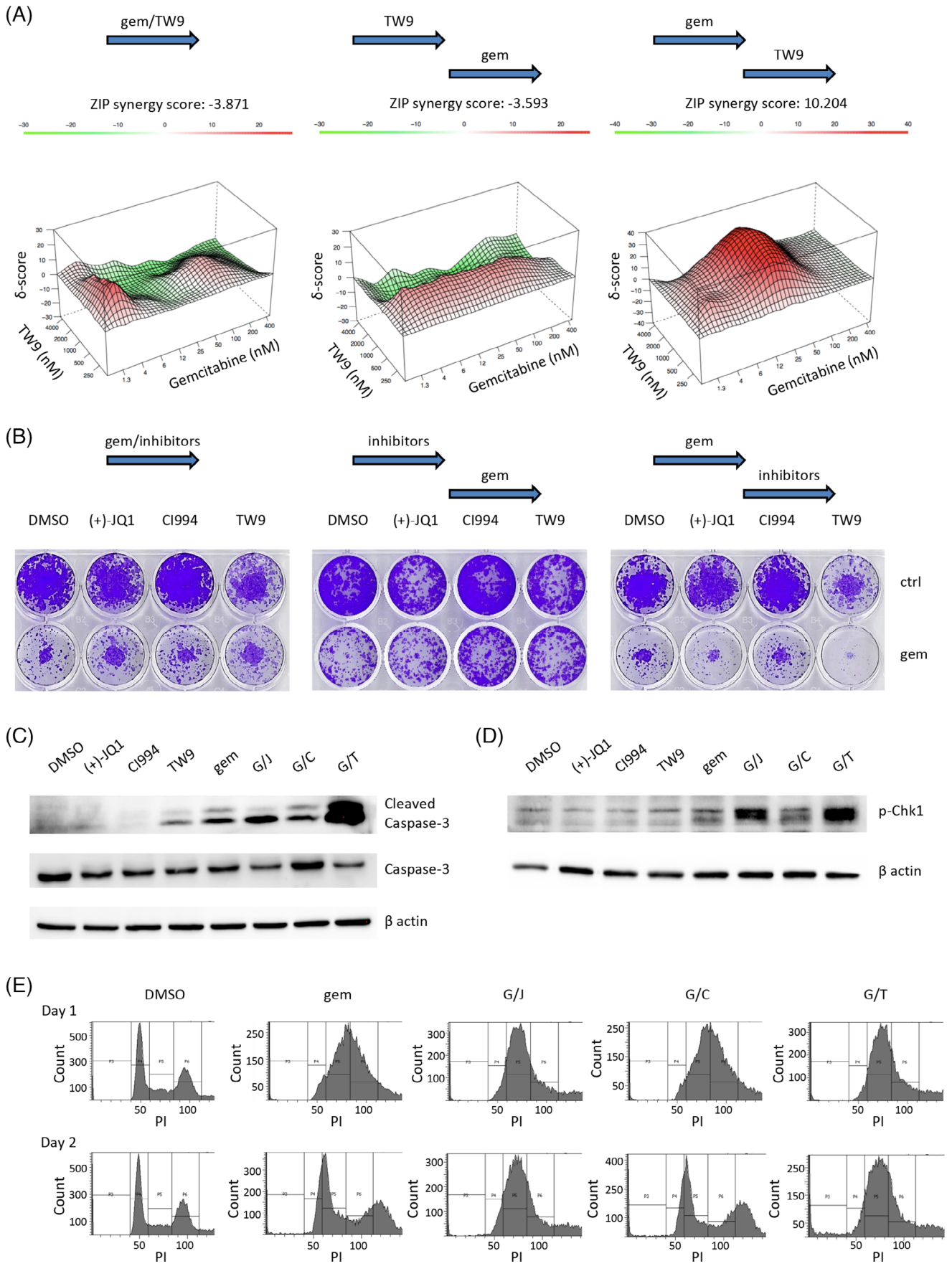


**FIGURE 4** Legend on next page.

morphology (Figure 2F). Furthermore, TW9 induced gene expression of *Involucrin*, a differentiation marker, to a similar level as (+)-JQ1 (Figure 2G). Expression analysis of three canonical squamous tissue genes by RT-PCR showed marked (>700-fold) induction of *KRT14* and modest induction of *KRT10* (6-fold) and *TGM1* (2-fold) by TW9 (Figure 2H). Notably, TW9 was significantly more efficient than (+)-JQ1 in inducing the expression of each of these genes.

### 3.4 | TW9 is more potent in suppressing growth of pancreatic cancer cells than its parental molecules

We next performed cell viability assays in a panel of PDAC cell lines (MIA PaCa-2, DAN-G and HPAC) and observed that TW9 decreased cell survival in a dose-dependent manner (Figure 3A). Furthermore, TW9 showed a more potent effect on cell survival when compared to (+)-JQ1, CI994 alone or the combination of (+)-JQ1 and CI994. Colony formation assay also showed that TW9 was more potent in suppressing cell growth (Figures 3B and S5A,B). Immunoblot analysis clearly showed that TW9 treatment led to increased expression of cleaved caspase 3, consistent with apoptotic cell death (Figure 3C).

In current clinical trials, single-agent BET inhibition is challenged by limited effectiveness, toxicity issues and still largely unknown optimal scheduling strategies.<sup>27</sup> To evaluate alternative scheduling strategies early on, we evaluated the long-term effects on cell survival of TW9 when administered only once for a time period of 24 hours. Compared to single-agent or combination treatment with (+)-JQ1 and CI994, TW9 had more sustained effects on suppressing cell growth, and cells started to grow much later (Day 10; Figure 3D, left panel). Colony formation assay at the end time point also showed much fewer colonies formed by TW9-treated cells (Figure 3D, right panel). Next, we applied a schedule for TW9 (1 day on and 6 days off for 3 cycles), which further prolonged the suppressive effects (Figure S5C). Thus, dosing of TW9 may be reduced with ongoing tumor-suppressive activity.

### 3.5 | Sequential administration of gemcitabine and TW9 shows synergistic effects

Gemcitabine is a standard-of-care chemotherapeutic agent in the treatment of PDAC. Previous combination of gemcitabine with the HDAC inhibitor CI994 resulted in increased toxicity and no beneficial effect of this combination in a phase II clinical trial.<sup>28</sup> Thus, we

evaluated the efficacy of combining TW9 and gemcitabine using different scheduling routes. Gemcitabine and TW9 were administered either at the same time or sequentially. Serial dilutions of each compound were combined, and the effect on the viability of HPAC cells was measured by cell viability assay. A synergistic effect between gemcitabine and TW9 was observed and most prominent when gemcitabine was given 24 hours before TW9 (G1T2 schedule, Figures 4A,B and S6A). Cleaved caspase 3 staining induced by G1T2 schedule supports highly increased apoptosis (Figure 4C). After the same schedule, we also performed synergistic test for JQ1/CI994 when combined with gemcitabine (Figure S6B). The ZIP score (8.96) of JQ1/CI994 is lower than that of TW9 (10.20), proving benefits of TW9 as a dual inhibitor. Strikingly, simultaneous or sequential administration of TW9 first followed by gemcitabine showed no combinatorial benefits or even detrimental effects in colony formation (Figures 4B and S7A), indicating that TW9 may reduce sensitivity to gemcitabine in these schedules. Consistent with previous reports, we found that (+)-JQ1 as well as TW9 induced accumulation of the cell-cycle regulator p21 (Figure S7B), which led to G1 arrest (Figure S7C). We assumed that the attenuated S-phase entry by (+)-JQ1 or TW9 inhibited gemcitabine incorporation into replicating DNA. To support this hypothesis, we found that simultaneous administration of gemcitabine and (+)-JQ1 or TW9 retained more cells in G1 phase compared to gemcitabine treatment alone, which induced early S-phase arrest (Figure S7D).

As known, gemcitabine induces acute replication stress as indicated by the induction of phospho-CHK1, and withdrawal of gemcitabine releases cells from such stress (Figure S7E). Simultaneous treatment of TW9 followed by gemcitabine largely prevented cells from replication stress induced by gemcitabine (Figure S7F). However, G1T2 scheduling enhanced the gemcitabine-induced replication stress (Figure 4D). Withdrawal of gemcitabine relieved replication stress and cells returned to normal cell-cycle distribution (Figure 4E). However, after the G1T2 schedule, cells maintained S-phase arrest after drug withdrawal (Figure 4E). In summary, G1T2 scheduling showed the most prominent synergistic effects by augmenting gemcitabine-induced replication stress and apoptosis.

### 3.6 | TW9 blocks cell-cycle progression through super enhancer-associated transcription factor FOSL1

To explore the molecular mechanisms elicited by TW9, transcriptomic profiling was performed in the established PDAC cell line PANC-1.

**FIGURE 4** Administration of TW9 with chemotherapy. A, Combination response to TW9 and gemcitabine for HPAC cells treated with three administration schedules: (1) simultaneous administration of gemcitabine and TW9 for 24 hours and incubation for another 4 days; (2) Sequential administration of TW9 and gemcitabine (each for 24 hours) and incubation for another 3 days; (3) Sequential administration of gemcitabine and TW9 (each for 24 hours) and incubation for another 3 days. CellTiter Glo cell viability assay was performed to measure cell viabilities for all the indicated dose combinations. Synergy effects were evaluated using SynergyFinder (synergyfinder.fimm.fi).<sup>39</sup> The ZIP synergy score is averaged over all the dose combination cells. B, Colony formation assay for HPAC cells treated with different administration schedules indicated above. Here, 10 nM gemcitabine and 2  $\mu$ M individual inhibitors were used. C and D, HPAC cells were sequentially treated with 10 nM gemcitabine and 2  $\mu$ M individual inhibitors. Then, inhibitors were removed, and cells were cultured for another 1 day for immunoblot analysis of cleaved caspase-3 and phospho-CHK1. E, HPAC cells were treated as above and harvested at 24 and 48 hours after removal of inhibitors for cell-cycle analysis [Color figure can be viewed at [wileyonlinelibrary.com](http://wileyonlinelibrary.com)]

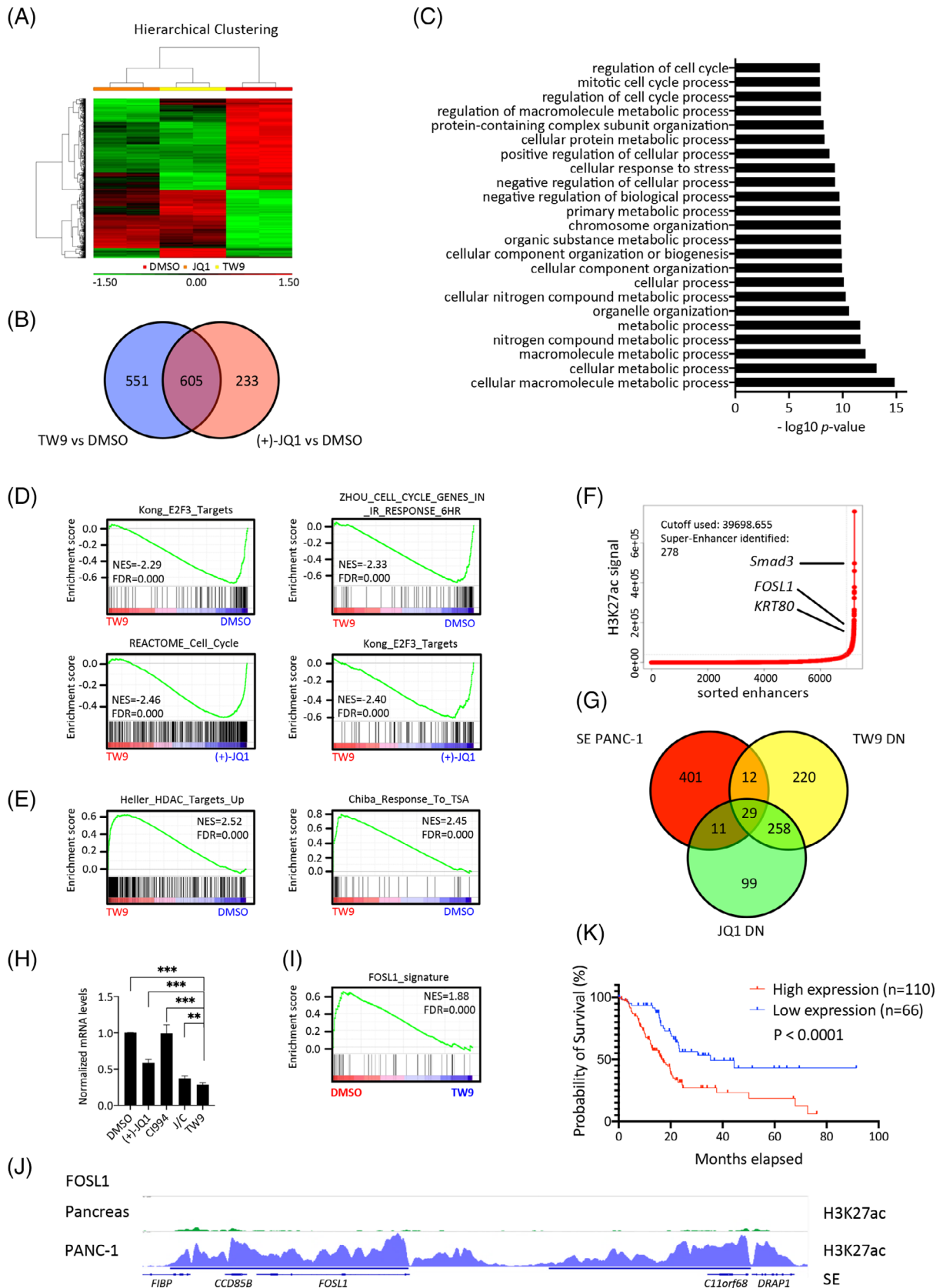


FIGURE 5 Legend on next page.

Hierarchical clustering of the differentially expressed genes by either TW9 or (+)-JQ1 revealed distinct gene expression profiles between TW9 and (+)-JQ1-treated samples (Figure 5A). Around 70% of the differentially expressed genes by (+)-JQ1 were also deregulated by TW9 (Figure 5B), indicating that TW9 largely recapitulates the activity of (+)-JQ1. To obtain a deeper insight into the gene expression patterns altered by TW9, we performed gene ontology (GO) analysis. Interestingly, the genes downregulated by TW9 were mainly associated with metabolic processes, cellular component organization and cell-cycle-related processes (Figure 5C). Gene set enrichment analysis (GSEA) also revealed that the significantly enriched pathways involved in cell cycle progression were downregulated by TW9 in comparison with DMSO or (+)-JQ1 treatment (Figure 5D). Furthermore, HDAC inhibition was among the most significantly enriched pathways in TW9-treated samples (Figure 5E), indicating that TW9 also recapitulates the activity of CI994.

Further, we aimed to identify TW9-regulated master transcriptional regulators (TFs) that control cell-cycle progression. Previous studies suggested that master TFs could be driven by super-enhancers (SEs).<sup>29</sup> We thus performed ChIP-seq using H3K27ac to identify the genomic enhancer landscape. Bioinformatic analysis of the genome-wide occupancy of H3K27ac resulted in the identification of 453 SEs in PANC-1 cells (Figure 5F). We next analyzed SE-associated gene expression of TW9- or (+)-JQ1-treated cells compared to controls. Venn diagram analysis shows that 41 TW9-downregulated genes were associated with SEs (Figure 5G). Compared to (+)-JQ1 treatment, 12 SE-associated genes were identified to be selectively targeted by TW9, including the transcription factor FOSL1. FOSL1 has previously been linked to KRAS-associated mitotic progression.<sup>30</sup> To confirm the downregulation of FOSL1 by TW9, we performed RT-PCR and found that FOSL1 was indeed downregulated by TW9 to a larger extent, compared to (+)-JQ1, CI994 and combined treatment (Figure 5H). Moreover, GSEA analysis revealed that FOSL1 targets<sup>30</sup> were significantly downregulated by TW9 (Figure 5I), implying that TW9 dysregulated the transcriptional program of FOSL1. Consistent with the elevated levels of FOSL1 in PDAC,<sup>30</sup> we found SEs around the FOSL1 gene locus in PANC-1 cells but not in healthy pancreas (Figure 5J), supporting the notion that cancer cells establish super-enhancers at oncogenes during tumor pathogenesis.<sup>29</sup> Statistical analysis of a pancreatic cancer cohort from the Human Protein Atlas data set<sup>14</sup> revealed that FOSL1 is a prognostic marker and that high FOSL1 expression levels are unfavorable for patient survival (Figure 5K). These results suggest that the antiproliferative phenotype observed in

TW9-treated cells may involve targeting of the FOSL1-regulated mitotic machinery.

## 4 | DISCUSSION

Current drug discovery remains widely dominated by the "one gene, one drug, one disease" paradigm. However, this paradigm has been continuously challenged in terms of redundant functions and alternative complex compensatory signaling patterns that are especially common in cancer. Thus, the biological rationale is compelling to consider multitarget approaches over single-target strategies. Conventional multitarget approaches include drug combinations, where it is difficult to achieve equitable pharmacokinetics and bio-distribution. To solve this issue, our study aimed at a single compound that has multiple inhibitory activities. We designed and synthesized ligands by conjugating two distinct pharmacophores (BETi and HDACi).

In our study, the ligand TW9 contains (+)-JQ1 and CI994 moieties showing dual inhibitory activities against BRD4 and HDAC proteins. Here we show that TW9 is a more potent BET/HDAC dual inhibitor than the combination of the parent molecules (+)-JQ1 and CI994, showing promising antiproliferative activities in vitro in PDAC. Similar dual BET/HDAC inhibitors have been reported in previous studies.<sup>31-34</sup> In a recent study,<sup>34</sup> a dual BET/HDAC inhibitor (compound 13a) with a structure very similar to TW9 was reported. The difference is that the *ortho*-aminoanilide in the CI994 moiety is replaced with hydroxamic acid in compound 13a. This modification makes compound 13a a potent pan-HDAC inhibitor, whereas our TW9 is a class I selective HDAC inhibitor. Both probes (TW9 and compound 13a) are valuable and complementary tools in cellular context-dependent studies. However, as a potential limitation, TW9 represents an adduct of two inhibitory moieties, resulting in a dual inhibitor with a relatively large molecular weight. In future studies, we aim to integrate both functionalities in a single inhibitor in a manner that will reduce molecular weight. Such dual inhibitors with BET activity have already been reported for BET-kinase combinations by us and other research groups.<sup>35-38</sup>

Intriguingly, we observed that TW9 had enhanced and more sustained HDAC-inhibiting effects when assessing histone H3 acetylation at lysines 9 and 14 by western blot analysis and in the drug washout experiment, suggesting that the CI994 moiety on TW9 has a longer residence time on its targets. While this needs further

**FIGURE 5** TW9 blocks cell-cycle progression through super-enhancer associated transcription factor FOSL1. A and B, Hierarchical clustering (A) and Venn diagram analysis (B) of the differentially expressed genes in PANC-1 cells treated with 1  $\mu$ M TW9 or (+)-JQ1 for 24 hours compared to DMSO treatment. Each treatment was done in duplicate. C, Gene ontology analysis of TW9-downregulated genes. D and E, GSEA plots comparing the enrichment of cell cycle-related pathways (D) and HDAC inhibition signature (E). F, Enhancers in PANC-1 ranked based on H3K27ac signal intensity using the ROSE algorithm defining 453 super-enhancers. G, Venn diagram analysis identifying TW9-specific super-enhancers. H, Quantitative RT-PCR analysis of FOSL1 gene in PANC-1 cells treated with 1  $\mu$ M indicated inhibitors for 24 hours. Mean  $\pm$  SEM from six independent experiments, \*\*\* $P \leq .001$ , \*\* $P \leq .01$ , \* $P \leq .05$ ; n.s., not significant. I, GSEA plot comparing the enrichment of FOSL1 signature. J, H3K27ac occupancy profiles at the FOSL1 gene in PANC-1 and the healthy counterpart. K, Kaplan-Meier plot showing the survival of pancreatic cancer patients stratified by FOSL1 mRNA expression levels [Color figure can be viewed at [wileyonlinelibrary.com](http://wileyonlinelibrary.com)]

characterization, it may explain why TW9 has more prolonged growth-inhibitory effects in the long-term proliferation assay.

Chemotherapy remains the standard-of-care treatment for PDAC patients with limited long-term effectiveness. In our study, we addressed if TW9 administration could improve the efficacy of gemcitabine, a well-tolerated chemotherapeutic agent with limited single-drug activity in PDAC. Strikingly, different schedules for administration yielded highly different results. We found that the cell-cycle arrest by cotreatment with TW9 interferes with the incorporation of gemcitabine into newly synthesized DNA and suppresses gemcitabine-induced replication stress. In contrast, TW9 treatment after gemcitabine administration sustains gemcitabine-induced S-phase arrest and replication stress. This result may explain why we did not previously observe synergism between (+)-JQ1 and gemcitabine in a PDAC mouse model, in which twice daily treatment of (+)-JQ1 plus a Q3Dx4 schedule (every third day for four cycles) for gemcitabine administration was applied.<sup>4</sup>

Previous studies implied that super-enhancers play key roles in the control of cell identity and disease.<sup>29</sup> In our study, we discovered that PANC-1 tumor cells display super-enhancers at the oncogene FOSL1. This led to the activation of a FOSL1 downstream transcriptional program that supports tumor cell proliferation. The transcriptional addiction of tumor cells to certain regulators of gene expression provides opportunities for therapeutic interventions in cancer. Along this line, we propose a model where TW9, by targeting the super enhancer-associated FOSL1 gene, may counteract the dysregulated transcriptional program and inhibit tumor cell proliferation.

As a proof of concept, our data support future efforts at developing chromatin-acting multitarget drugs harboring potential benefits for clinical application: a linked pharmacokinetic profile, reduced risk of drug-drug interactions and simplified dosing schedules. We are now designing a second generation of BET/HDAC dual inhibitors that integrate the two pharmacophores to achieve a lower molecular weight and more drug-like physicochemical properties.

## ACKNOWLEDGEMENTS

We are grateful to Nicola Bielefeld, Konstantinos Savvatakis, Anna Bazarna and Mihaela Keller for technical assistance. We also thank the staff at ESRF Grenoble beamline ID30B and Deep Chatterjee for assistance during X-ray data collection. J. T. S., S. K., S. J. and S. A. H. are supported by the German Cancer Aid (grant no. 70112505; PIPAC consortium). J. T. S. and S. K. are further supported by the German Cancer Consortium (DKTK). J. T. S. receives also funding from the Deutsche Forschungsgemeinschaft (DFG) through grant SI1549/3-1 (Clinical Research Unit KFO337) and Collaborative Research Center SFB824 (project C4). A. C. J. is funded by the German Research Foundation (DFG) grant JO 1473/1-1. S. K. is grateful for support by the SGC, a registered charity (number 1097737) that receives funds from AbbVie, Bayer Pharma AG, Boehringer Ingelheim, Canada Foundation for Innovation, Eshelman Institute for Innovation, Genome Canada, Innovative Medicines Initiative (EU/EFPIA), Janssen, Merck KGaA Darmstadt Germany, MSD, Novartis Pharma AG, Ontario Ministry of

Economic Development and Innovation, Pfizer, São Paulo Research Foundation-FAPESP, Takeda, and Wellcome [106 169/ZZ14/Z].

## CONFLICT OF INTEREST

No conflicts of interest are disclosed by the authors.

## DATA ACCESSIBILITY

Coordinates and structure factors of the complexes of BRD4(1) with the inhibitors TW9, TW12, and TW22 have been deposited in the Protein Data Bank (PDB). Accession codes: 6YQN, 6YQO, and 6YQP. The Human Protein Atlas data set for Kaplan-Meier survival analysis is available via <https://www.proteinatlas.org>.

## ORCID

Swetlana Ladigan  <https://orcid.org/0000-0003-1923-4096>

Jens T. Siveke  <https://orcid.org/0000-0002-8772-4778>

## REFERENCES

1. Jones PA, Issa JP, Baylin S. Targeting the cancer epigenome for therapy. *Nat Rev Genet.* 2016;17(10):630-641.
2. Li Y, Seto E. HDACs and HDAC inhibitors in cancer development and therapy. *Cold Spring Harb Perspect Med.* 2016;6(10):a026831.
3. Conroy T, Desseigne F, Ychou M, et al. FOLFIRINOX versus gemcitabine for metastatic pancreatic cancer. *N Engl J Med.* 2011;364(19):1817-1825.
4. Mazur PK, Herner A, Mello SS, et al. Combined inhibition of BET family proteins and histone deacetylases as a potential epigenetics-based therapy for pancreatic ductal adenocarcinoma. *Nat Med.* 2015;21(10):1163-1171.
5. Filippakopoulos P, Qi J, Picaud S, et al. Selective inhibition of BET bromodomains. *Nature.* 2010;468(7327):1067-1073.
6. Kabsch W. Xds. *Acta Crystallogr D Biol Crystallogr.* 2010;66(Pt 2):125-132.
7. Evans PR. An introduction to data reduction: space-group determination, scaling and intensity statistics. *Acta Crystallogr D Biol Crystallogr.* 2011;67(Pt 4):282-292.
8. Winn MD, Ballard CC, Cowtan KD, et al. Overview of the CCP4 suite and current developments. *Acta Crystallogr D Biol Crystallogr.* 2011;67(Pt 4):235-242.
9. Adams PD, Afonine PV, Bunkoczi G, et al. PHENIX: a comprehensive python-based system for macromolecular structure solution. *Acta Crystallogr D Biol Crystallogr.* 2010;66(Pt 2):213-221.
10. Emsley P, Lohkamp B, Scott WG, Cowtan K. Features and development of Coot. *Acta Crystallogr D Biol Crystallogr.* 2010;66(Pt 4):486-501.
11. Roehm NW, Rodgers GH, Hatfield SM, Glasebrook AL. An improved colorimetric assay for cell proliferation and viability utilizing the tetrazolium salt XTT. *J Immunol Methods.* 1991;142(2):257-265.
12. Machleidt T, Woodrooffe CC, Schwinn MK, et al. NanoBRET—A novel BRET platform for the analysis of protein-protein interactions. *ACS Chem Biol.* 2015;10(8):1797-1804.
13. Asquith CRM, Berger BT, Wan J, et al. SGC-GAK-1: a chemical probe for Cyclin G associated kinase (GAK). *J Med Chem.* 2019;62(5):2830-2836.
14. Uhlen M, Zhang C, Lee S, et al. A pathology atlas of the human cancer transcriptome. *Science.* 2017;357(6352):eaan2507.
15. Subramanian A, Tamayo P, Mootha VK, et al. Gene set enrichment analysis: a knowledge-based approach for interpreting genome-wide expression profiles. *Proc Natl Acad Sci USA.* 2005;102(43):15545-15550.

16. Loven J, Hoke HA, Lin CY, et al. Selective inhibition of tumor oncogenes by disruption of super-enhancers. *Cell*. 2013;153(2):320-334.
17. Whyte WA, Orlando DA, Hnisz D, et al. Master transcription factors and mediator establish super-enhancers at key cell identity genes. *Cell*. 2013;153(2):307-319.
18. McLean CY, Bristor D, Hiller M, et al. GREAT improves functional interpretation of cis-regulatory regions. *Nat Biotechnol*. 2010;28(5):495-501.
19. Hamdan FH, Johnsen SA. DeltaNp63-dependent super enhancers define molecular identity in pancreatic cancer by an interconnected transcription factor network. *Proc Natl Acad Sci USA*. 2018;115(52):E12343-E12352.
20. Bernstein BE, Stamatoyannopoulos JA, Costello JF, et al. The NIH Roadmap Epigenomics mapping consortium. *Nat Biotechnol*. 2010;28(10):1045-1048.
21. Langmead B, Salzberg SL. Fast gapped-read alignment with Bowtie 2. *Nat Methods*. 2012;9(4):357-359.
22. Li H, Handsaker B, Wysoker A, et al. The sequence alignment/map format and SAMtools. *Bioinformatics (Oxford, England)*. 2009;25(16):2078-2079.
23. Ramirez F, Dundar F, Diehl S, et al. deepTools: a flexible platform for exploring deep-sequencing data. *Nucleic Acids Research*. 2014;42(Web Server Issue):W187-W191.
24. Robinson JT, Thorvaldsdottir H, Winckler W, et al. Integrative genomics viewer. *Nat Biotechnol*. 2011;29(1):24-26.
25. Thorvaldsdottir H, Robinson JT, Mesirov JP. Integrative genomics viewer (IGV): high-performance genomics data visualization and exploration. *Brief Bioinform*. 2013;14(2):178-192.
26. Wang R, Liu W, Helfer CM, et al. Activation of SOX2 expression by BRD4-NUT oncogenic fusion drives neoplastic transformation in NUT midline carcinoma. *Cancer Res*. 2014;74(12):3332-3343.
27. Alqahtani A, Choucair K, Ashraf M, et al. Bromodomain and extra-terminal motif inhibitors: a review of preclinical and clinical advances in cancer therapy. *Future Sci OA*. 2019;5(3):FSO372.
28. Richards DA, Boehm KA, Waterhouse DM, et al. Gemcitabine plus CI-994 offers no advantage over gemcitabine alone in the treatment of patients with advanced pancreatic cancer: results of a phase II randomized, double-blind, placebo-controlled, multicenter study. *Ann Oncol*. 2006;17(7):1096-1102.
29. Hnisz D, Abraham BJ, Lee TI, et al. Super-enhancers in the control of cell identity and disease. *Cell*. 2013;155(4):934-947.
30. Vallejo A, Perurena N, Guruceaga E, et al. An integrative approach unveils FOSL1 as an oncogene vulnerability in KRAS-driven lung and pancreatic cancer. *Nat Commun*. 2017;8:14294.
31. Atkinson SJ, Soden PE, Angell DC, et al. The structure based design of dual HDAC/BET inhibitors as novel epigenetic probes. *Med Chem Commun*. 2014;5(3):342-351.
32. Zhang Z, Hou S, Chen H, et al. Targeting epigenetic reader and eraser: rational design, synthesis and in vitro evaluation of dimethylisoxazoles derivatives as BRD4/HDAC dual inhibitors. *Bioorg Med Chem Lett*. 2016;26(12):2931-2935.
33. Amemiya S, Yamaguchi T, Hashimoto Y, Noguchi-Yachide T. Synthesis and evaluation of novel dual BRD4/HDAC inhibitors. *Bioorg Med Chem*. 2017;25(14):3677-3684.
34. He S, Dong G, Li Y, Wu S, Wang W, Sheng C. Potent dual BET/HDAC inhibitors for efficient treatment of pancreatic cancer. *Angew Chem Int Ed Engl*. 2020;59(8):3028-3032.
35. Ciceri P, Muller S, O'Mahony A, et al. Dual kinase-bromodomain inhibitors for rationally designed polypharmacology. *Nat Chem Biol*. 2014;10(4):305-312.
36. Andrews FH, Singh AR, Joshi S, et al. Dual-activity PI3K-BRD4 inhibitor for the orthogonal inhibition of MYC to block tumor growth and metastasis. *Proc Natl Acad Sci USA*. 2017;114(7):E1072-E1080.
37. Liu S, Yosief HO, Dai L, et al. Structure-guided design and development of potent and selective dual Bromodomain 4 (BRD4)/polo-like kinase 1 (PLK1) inhibitors. *J Med Chem*. 2018;61(17):7785-7795.
38. Watts E, Heidenreich D, Tucker E, et al. Designing dual inhibitors of anaplastic lymphoma kinase (ALK) and Bromodomain-4 (BRD4) by tuning kinase selectivity. *J Med Chem*. 2019;62(5):2618-2637.
39. lanevski A, He L, Aittokallio T, et al. SynergyFinder: a web application for analyzing drug combination dose-response matrix data. *Bioinformatics (Oxford, England)*. 2017;33(15):2413-2415.

## SUPPORTING INFORMATION

Additional supporting information may be found online in the Supporting Information section at the end of this article.

**How to cite this article:** Zhang X, Zegar T, Weiser T, et al. Characterization of a dual BET/HDAC inhibitor for treatment of pancreatic ductal adenocarcinoma. *Int. J. Cancer*. 2020; 1-15. <https://doi.org/10.1002/ijc.33137>

### **3. Therapeutic targeting of p300/CBP HAT domain for the treatment of NUT midline carcinoma**

#### **Summary**

NUT midline carcinoma (NMC), is a rare but highly aggressive and therapy resistant form of undifferentiated squamous cell carcinoma. Its characterized by chromosomal rearrangement of the NUT gene, most commonly to the bromodomain and extraterminal domain (BET) gene BRD4, forming a BRD4-NUT fusion oncogene. Because of the involvement of BRD4, BET inhibitors represent an attractive therapeutic approach. Since toxicity and obtained resistance observed in clinical trials limit the use BET inhibitors, the aim was to identify new selective compounds for the treatment of NMC.

A drug screening approach using a library of different compounds developed by industry and academic collaborators and collected by the Structural Genomics Consortium (SGC) was performed. P300/CBP HAT inhibitor A-485, as well as the known BET inhibitor JQ1, was identified and further characterized. In contrast to JQ1, A-485 was selectively potent in NMC compared to other cell lines tested. Supporting an on-target action of A-485, an inactive analogue A-486 yielded no activity in NMC cells. Immunofluorescence and immunoblot analysis revealed that BRD4-NUT and BRD4 expressed from wild-type allele (BRD4 wt) were co-localized with acetylated H3K27 and decreased and dispersed after treatment with A485. The binding of BRD4-NUT to acetylated histones leads to interaction and recruitment of p300/CBP, which further acetylate histones and recruit even more BRD4-NUT in a feed-forward manner. Large acetylated chromatin regions termed megadomains are created. It was shown, that A485 impairs the formation of hyperacetylated megadomains, induced by binding of BRD4-NUT and recruitment of p300. Further, megadomain-associated genes like MYC, CCAT1 and TP63 were also downregulated. Chromatin immunoprecipitation revealed diminished H3K27ac and BRD4-NUT levels at the MYC promoter and TP63 enhancer regions in A-485-treated cells. Additionally, a loss-of-function experiment was performed and in agreement with A-485 treatment, double knockdown of p300 and CBP also downregulated MYC, CCAT1 and TP63 mRNA levels. It was shown that treatment with A-485 induces a differentiated phenotype and increased levels of pan-cytokeratin in cytoplasm. The three canonical squamous tissue genes KRT10, KRT14 and TGM1 were upregulated as well as C-fos, a transcription factor required for normal epithelial cell differentiation. Further, it was shown, that A-485 induced G1 arrest in NMC cells at early time point (24 h) and apoptosis at later time points (48 h and 72 h). In Addition, strong synergistic anti-proliferative effects between JQ1 and A485 were observed and transcriptomic profiling was performed to explore

the molecular mechanism. Combined treatment differentially regulated significantly more genes than both single treatments together. The most significantly enriched pathways are the p53 pathway, apoptosis and Wnt/ $\beta$  catenin signaling pathway. Additionally, using low dose concentrations, only combined treatment induced squamous differentiation in contrast to single drug treatment.

In summary, p300/CBP HAT domain was identified as a novel potential therapeutic target for the treatment of therapy resistant NMC. The findings indicate that p300/CBP inhibition by A-485 efficiently impairs BRD4-NUT oncogenic functions in NMC megadomains and induces differentiation and apoptosis. Combined p300/CBP and BET inhibition may be a potential approach to overcome obtained resistance to BET inhibitors.

### **Zusammenfassung**

NUT *midline carcinoma* (NMC), ist ein seltenes, aber auch sehr aggressives und therapieresistentes, undifferenziertes Plattenepithelkarzinom. Charakteristisch für NMC ist eine chromosomale Umlagerung des NUT-Gens, zumeist an das *bromodomain and extraterminal domain* (BET)-Gen BRD4, was zur Bildung eines BRD4-NUT-Fusionsonkogens führt. Durch die Beteiligung von BRD4, repräsentieren BET-Inhibitoren einen attraktiven Behandlungsansatz. Da allerdings Toxizität und aufkommende Resistenzen, die in klinischen Studien beobachtet wurden, den Einsatz von BET-Inhibitoren einschränken, war das Ziel dieser Arbeit die Identifizierung neuer selektiver Inhibitoren für die Behandlung von NCM.

Es wurde ein *drug screening* mit einer Sammlung verschiedener compounds, welche sowohl aus der Industrie als auch von akademischen Kooperationspartnern stammen und vom *Structural Genomics Consortium* (SGC) zusammengestellt wurden, durchgeführt. Neben dem bekannten BET-Inhibitor JQ1 wurde der HAT-Inhibitor A485 identifiziert und weiter charakterisiert. Im Gegensatz zu JQ1 war A485 ausschließlich in NMC Zellen aktiv, im direkten Vergleich mit anderen Zelllinien. Gleichzeitig zeigte ein inaktives Kontrollcompound A486 keinerlei Aktivität in NMC Zellen. Immunofluoreszenz- und Immunoblot-Analysen veranschaulichten, dass BRD4-NUT sowie BRD4 Wildtyp co-lokalisiert mit acetyliertem H3K27 waren und nach einer Behandlung mit A485 verschwanden bzw. zerstreut wurden. Das Binden von BRD4-NUT an acetyliertes Histon führt zur Interaktion mit und Rekrutierung von p300/CBP, wodurch umliegende Histone weiter acetyliert werden, was wiederum BRD4-NUT rekrutiert und in einem sich selbst verstärkenden Schleifenmechanismus endet. Riesige acetylierte Megadomänen innerhalb des Chromatins werden auf diese Weise gebildet. Es konnte gezeigt werden, dass eine Behandlung mit A485 die Bildung dieser Megadomänen unterbindet, die durch NUT-BRD4 induziert werden. Des Weiteren wurde beobachtet, dass Gene, welche in

direktem Zusammenhang mit diesen Megadomänen stehen, wie MYC, CCAT1 oder TP63, ebenfalls runterreguliert wurden. Mit Hilfe von Chromatin-Immunoprecipitation wurden zusätzlich verringerte Mengen von acetyliertem Histon und BRD4-NUT am MYC-Promoter bzw. am TP63-*enhancer* in mit A485 behandelten Zellen nachgewiesen. Ein *loss-of-function*-Experiment bestätigte, dass in Zellen mit einem p300/CBP Doppel-*knockdown* ebenfalls MYC, CCAT1 und TP63 runterreguliert wurden. Es konnte gezeigt werden, dass eine A485-Behandlung einen differenzierten Phänotyp auslöste, der erhöhte Mengen pan-Cytokeratin im Cytoplasma aufwies. Die drei Plattenepithelgewebe-Gene KRT10, KRT14 und TGM1 wurden genau wie der Transkriptionsfaktor für epitheliale Zelldifferenzierung c-fos hochreguliert. Darüber hinaus wurde gezeigt, dass A485 zu einem frühen Zeitpunkt (24h) eine Blockade der G1-Phase auslöst und zu einem späteren Zeitpunkt (48h und 72h) Apoptose in NMC Zellen induziert. Zusätzlich wurden synergistische, anti-proliferative Effekte zwischen JQ1 und A485 beobachtet, woraufhin ein Transkriptom-Profil erstellt wurde, um den molekularen Mechanismus genauer zu beleuchten. Es zeigte sich, dass die kombinierte Behandlung mit beiden Inhibitoren deutlich mehr Gene beeinflusste als die Behandlung mit beiden Einzelinhibitoren zusammen. Zu den am stärksten beeinflussten Signalwegen gehörten der P53- als auch Wnt/ $\beta$ -catenin-Signalweg sowie Signalwege, die mit Apoptose in Verbindung gebracht werden. Zusätzlich wurde gezeigt, dass mit geringeren Behandlungskonzentrationen nur die kombinierte Behandlung mit beiden Inhibitoren Zelldifferenzierung auslösen konnte. Zusammenfassend konnte die p300/CBP HAT-Domäne als neue, therapeutische Zielstruktur in NMC identifiziert werden. Die Ergebnisse verdeutlichen, dass der HAT-Inhibitor A485 die Bildung von hyperacetylierten Megadomänen unterbindet und in der Lage ist Differenzierung und Apoptose zu induzieren. Eine Kombinationstherapie mit BET-Inhibitoren könnte ebenfalls eine Möglichkeit bieten, Therapieresistenzen gegen eben diese zu adressieren.

## Cumulative dissertation of Tim Zegar - author contributions

### Therapeutic targeting of p300/CBP HAT domain for the treatment of NUT midline carcinoma

Xin Zhang, Tim Zegar, Anais Lucas, Chevaun Morrison-Smith, Tatiana Knox, Christopher A. French, Stefan Knapp, Susanne Müller and Jens T. Siveke

Xin Zhang and Tim Zegar are co-first authors of this article

**conception** - 0 %: The conception was done by Prof. Dr. Jens T. Siveke and Dr. Xin Zhang.

**experimental work** - 60 %: Tim Zegar was involved in biological and biochemical experiments (immunoblot analysis, RT-qPCR, colony formation assay, immunofluorescence analysis, Hemacolor assay).

**data analysis** - 50 %: Tim Zegar was involved in data analysis from biological and biochemical experiments.

**data collection and statistical analysis** - 30 %: Tim Zegar was collecting and combining results. The final statistical analysis was done by Dr. Xin Zhang.

**writing the manuscript** - 5 %: Tim Zegar was partially writing the experimental part.

**revision process of the manuscript** - 50 %: Tim Zegar was involved in experimental work and revising and editing of figures.

---

Signature PhD student

---

Signature supervisor



# Therapeutic targeting of p300/CBP HAT domain for the treatment of NUT midline carcinoma

Xin Zhang<sup>1,2</sup> · Tim Zegar<sup>1,2</sup> · Anais Lucas<sup>3,4,5</sup> · Chevaun Morrison-Smith<sup>6</sup> · Tatiana Knox<sup>6</sup> · Christopher A. French<sup>6</sup> · Stefan Knapp<sup>3,4,5</sup> · Susanne Müller<sup>3,4</sup> · Jens T. Siveke<sup>1,2</sup>

Received: 8 October 2019 / Revised: 8 April 2020 / Accepted: 9 April 2020  
© The Author(s) 2020. This article is published with open access

## Abstract

Nuclear protein of the testis (NUT) midline carcinoma (NMC), is a rare and highly aggressive form of undifferentiated squamous cell carcinoma. NMC is molecularly characterized by chromosomal rearrangement of the *NUT* gene to another gene, most commonly the bromodomain and extraterminal domain (BET) gene *BRD4*, forming the *BRD4-NUT* fusion oncogene. Therefore, inhibiting BRD4-NUT oncogenic function directly by BET inhibitors represents an attractive therapeutic approach but toxicity may limit the use of pan-BET inhibitors treating this cancer. We thus performed a drug screening approach using a library consisting of epigenetic compounds and ‘Donated Chemical Probes’ collated by the Structural Genomics Consortium (SGC) and identified the p300/CBP HAT inhibitor A-485, in addition to the well-known BET inhibitor JQ1, to be the most active candidate for NMC treatment. In contrast to JQ1, A-485 was selectively potent in NMC compared to other cell lines tested. Mechanistically, A-485 inhibited p300-mediated histone acetylation, leading to disruption of BRD4-NUT binding to hyperacetylated megadomains. Consistently, BRD4-NUT megadomain-associated genes *MYC*, *CCAT1* and *TP63* were downregulated by A-485. A-485 strongly induced squamous differentiation, cell cycle arrest and apoptosis. Combined inhibition of p300/CBP and BET showed synergistic effects. In summary, we identified the p300/CBP HAT domain as a putative therapeutic target in highly therapy-resistant NMC.

These authors contributed equally: Xin Zhang, Tim Zegar

**Supplementary information** The online version of this article (<https://doi.org/10.1038/s41388-020-1301-9>) contains supplementary material, which is available to authorized users.

✉ Jens T. Siveke  
jens.siveke@uk-essen.de

- <sup>1</sup> Institute for Developmental Cancer Therapeutics, West German Cancer Center, University Hospital Essen, Essen, Germany
- <sup>2</sup> Division of Solid Tumor Translational Oncology, German Cancer Consortium (DKTK, Partner Site Essen) and German Cancer Research Center, DKFZ, Heidelberg, Germany
- <sup>3</sup> Structural Genomics Consortium, Buchmann Institute for Life Sciences, Goethe University Frankfurt, 60438 Frankfurt, Germany
- <sup>4</sup> Institute of Pharmaceutical Chemistry, Goethe University Frankfurt, 60438 Frankfurt, Germany
- <sup>5</sup> German Cancer Consortium (DKTK partner site Frankfurt/Mainz) and Frankfurt Cancer Institute (FCI), 60438 Frankfurt, Germany
- <sup>6</sup> Brigham and Women’s Hospital/Harvard Medical School, Boston, MA, USA

## Introduction

Nuclear protein of the testis (NUT) midline carcinoma (NMC) is defined by chromosomal rearrangement of the nuclear protein of the testis (*NUT*) gene on chromosome 15q14 mainly arising in midline structures, such as head, neck and mediastinum. In ~70% of NMCs, most of the coding sequence of *NUT* is fused to *BRD4*, creating a *BRD4-NUT* oncogene [1, 2]. In the *BRD4-NUT* fusion protein, the *BRD4* moiety contains two tandem bromodomains (BD) that bind to acetyl-lysine residues on histones and the *NUT* moiety contains two acidic domains (AD), one of which binds to the histone acetyltransferase p300/CBP stimulating its catalytic activity [3]. Recruitment of p300/CBP leads to regional histone hyperacetylation, which further recruits *BRD4-NUT* in a feed-forward manner [4]. Eventually, massive acetylated chromatin regions termed ‘megadomains’ are created. *BRD4-NUT* megadomains drive transcription of underlying genes (e.g. *MYC* and *TP63*) that prevent differentiation and stimulate growth [4].

NMC is one of the most therapy-resistant tumors. As a major pathogenic driver of transformation, *BRD4-NUT*



◀ **Fig. 1 Chemical probe screening identified a p300/CBP inhibitor that is selectively anti-proliferative in NMC.** **a** Chemical probe screening in three tumor cell lines. HCC2429, NUT midline carcinoma; Patu8988T, pancreatic ductal adenocarcinoma; QGP-1, pancreatic neuroendocrine tumor. Cells were incubated with each of the chemical probes at a concentration of 10  $\mu$ M for 72 h and cell viabilities were measured by CellTiter Glo Cell Viability assay. The values were normalized to dimethyl sulfoxide (DMSO)-treated samples and a heatmap was generated based on the mean values of three independent experiments. The heat map was colored according to normalized cell viability as depicted in the figure capture. The *p*-values of positive hits (JQ1, A-485 and BTOZ-1) were presented in the text. **b** Venn diagram analysis showing NMC-selective and -unselective inhibitors. Probes with cell viability less than 50% in at least one cell line from the screening above were chosen as potent hits. **c** IC<sub>50</sub> of A-485 on three NMC cell lines and six cell lines of other tumor identities. Mean  $\pm$  SEM from three independent experiments, \**P*  $\leq$  0.05. **d** Comparison of the growth effects A-485 (red circles) and the inactive analogue A-486 (black square) on three NMC cell lines. IC<sub>50</sub> of A-485 is shown in the graph. Mean  $\pm$  SD from three technical replicates. In (c) and (d), cells were incubated with inhibitors at a concentration range between 10 nM and 25  $\mu$ M. Cell viability was monitored after 72 h by CellTiter Glo Cell Viability assay. The dose response curve was used to determine the IC50 by Prism.

megadomain-associated genes [4]. Several BETi have entered clinical trials and evidence of clinical activity was observed [6–8]. However, the response rate in NMC to BETi was only 20–30% and patients eventually developed resistance [6, 7]. Another concerning issue is toxicity of pan-BETi, leading most commonly to thrombocytopenia, thus limiting the usage of BETi in NMC [6, 7]. Therefore, alternative regimens or combination therapies need to be developed. In this study, we identified a p300/CBP HAT inhibitor that is selectively potent in NMC. Consistent with the location of p300/CBP in a complex with BRD4-NUT, this inhibitor disrupts BRD4-NUT megadomain and downregulates megadomain-associated genes, leading to squamous differentiation and growth arrest. Additionally, p300/CBP and BET inhibitors confer synergistic anti-tumor effects. These results implicate an alternative regimen in NMC by targeting p300/CBP as a monotherapy or combined with BETi.

## Results

### A-485 is selectively anti-proliferative in NMC

In order to identify potential inhibitors for NMC, we screened two libraries of highly selective and well-characterized inhibitors, so called chemical probes that have been developed by the Structural Genomics Consortium (SGC) chemical probe program (epigenetic library) or have been donated by industry (donated chemical probes, DCP). Each compound of these libraries is accompanied by its inactive structurally highly related analogues. The

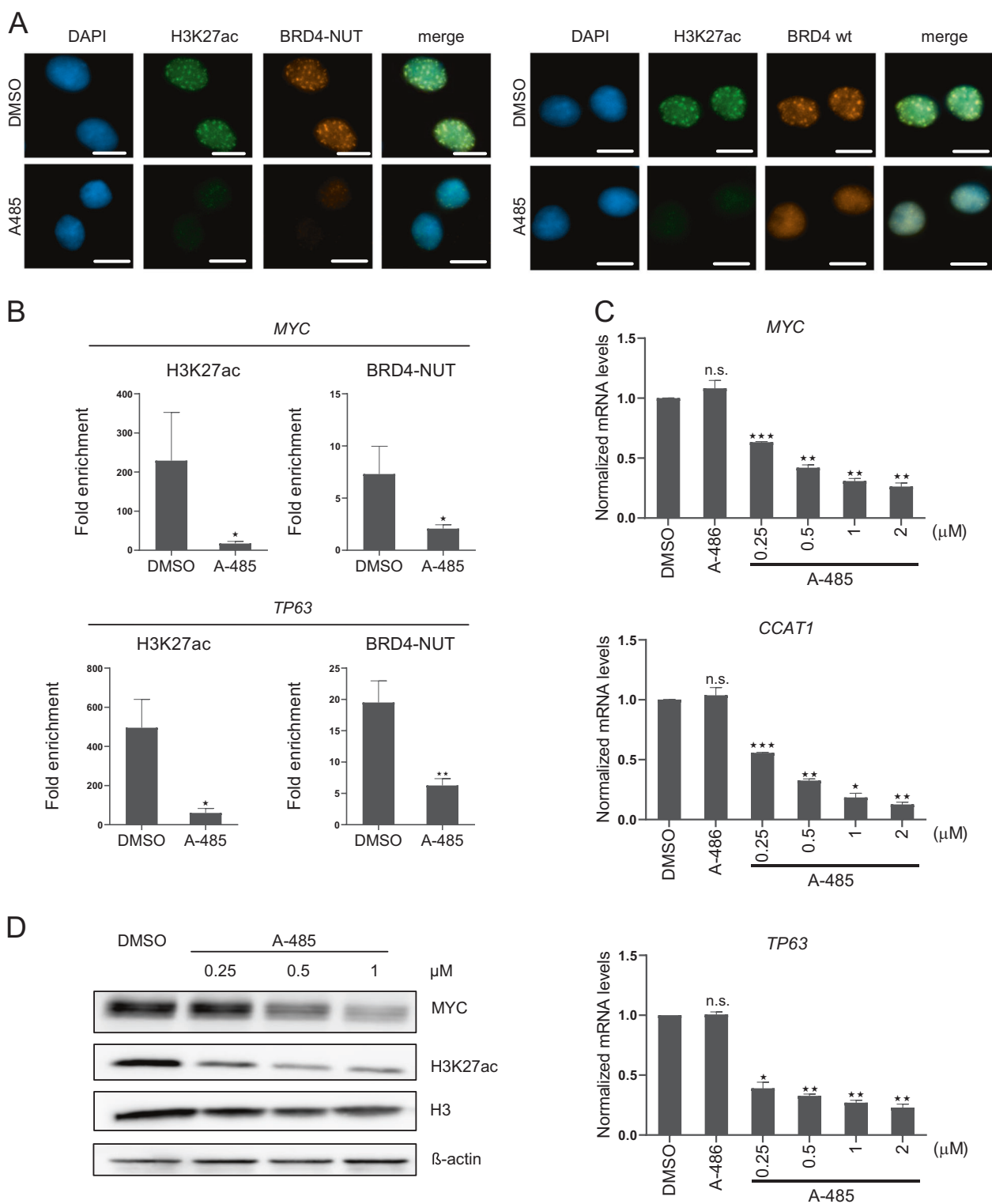
potency, selectivity and cellular activity of all the compounds have been extensively profiled and data are regularly updated in an online database and web resources (<https://www.sgc-ffm.uni-frankfurt.de/> and <https://www.thesgc.org/chemical-probes/epigenetics>). The currently assembled 79 chemical probes cover diverse cellular targets such as epigenetic regulators, receptors and transporters as well as kinases [9–11] (Supplementary Fig. 1).

Next, we analyzed the NMC cell line HCC2429 and two pancreatic tumor cell lines (Patu8988T and QGP-1) to identify NMC-selective inhibitors and distinguish them from compounds of general toxicity (Fig. 1a). Among the chemical probes that showed strong anti-proliferative activity in HCC2429 cells, we identified the BETi JQ1 (*P* < 0.0001; Fig. 1a, b). Consistent with previous studies [12], JQ1 also showed strong activity against non-NMC cells (Fig. 1a, b). In contrast, two compounds, A-485 (*P* = 0.016) and BTZO-1 (*P* = 0.028), only showed activities in HCC2429 cells (Fig. 1a, b). A-485 was developed as a selective catalytic p300/CBP inhibitor, which has demonstrated inhibitory effects in several hematological malignancies and androgen receptor-positive prostate cancer [13]. BTZO-1, a selective inhibitor for macrophage migration inhibitory factor (MIF), was originally discovered as a cardioprotective agent [14]. However, the role of MIF in NMC remains to be established and this strategy was not pursued further in this study.

Considering the important roles of p300/CBP in NMC, we focused on A-485 for further characterization. To validate our findings, we determined the half maximal inhibitory concentration (IC<sub>50</sub>) values of A-485 across three NMC cell lines (HCC2429, 00–143 and Ty-82) and six non-NMC cell lines (Patu8988T, Patu8988S, U2OS, HepG2, M21 and COLO320DM). We found a significantly higher activity in all NMC cell lines compared to non-NMC cells (Fig. 1c). Supporting an on-target action of A-485, the inactive analogue A-486 yielded no activity in NMC cells (Fig. 1d).

### A-485 impairs hyperacetylated chromatin domains and downregulates BRD4-NUT megadomain-associated genes

Because of the critical roles of p300/CBP in creating hyperacetylated chromatin domains associated with BRD4-NUT in NMC [3, 4], we explored the consequences of p300/CBP inhibition by A-485. First, we performed immunofluorescence analysis in HCC2429 cells. In DMSO-treated cells, BRD4-NUT and BRD4 expressed from wild-type allele (BRD4 wt) were co-localized with acetylated H3K27 (H3K27ac) in the distinct chromatin foci (Fig. 2a). A-485 treatment dispersed the hyperacetylated chromatin foci (Fig. 2a). Similar effects were observed in NMC cell



lines TC-797 and PER-403 (Supplementary Fig. 2A). We further observed that BRD4-NUT and BRD4 wt protein levels were decreased by A-485 (Supplementary Fig. 2B).

Previous studies demonstrated that BRD4-NUT megadomains overlap at oncogenic loci and induce abnormal

expression of oncogenes (e.g. *MYC*, *CCAT1* and *TP63*) in NMC [4]. *CCAT1* is an enhancer RNA upstream of *MYC* locus [15], and *CCAT1* and *MYC* share one BRD4-NUT megadomain [4]. We assumed that p30/CBP inhibition could impair BRD4-NUT binding at these oncogenic loci

◀ **Fig. 2 A-485 impairs hyperacetylated chromatin domains and downregulates BRD4-NUT megadomain-associated genes.** **a** Immunofluorescence detection of H3K27ac, BRD4-NUT and BRD4 wt proteins in HCC2429 cells incubated with 1  $\mu$ M A-485 or DMSO for 3 days. Scale bar = 10  $\mu$ m. **b** Chromatin immunoprecipitation (ChIP) analysis of H3K27ac and BRD4-NUT at the *MYC* promoter and *TP63* enhancer regions in HCC2429 cells incubated with 1  $\mu$ M A-485 or DMSO for 3 days. Chromatin was precipitated with normal rabbit IgG (IgG as control), H3K27ac and NUT antibodies. Precipitated chromatin was analyzed using qPCR and presented as fold enrichment to IgG control. Mean  $\pm$  SEM from four independent experiments,  $^{**}P \leq 0.01$ ,  $^{*}P \leq 0.05$ . **c** Quantitative RT-PCR analysis of *MYC*, *CCAT1* and *TP63* genes and **(d)** immunoblot analysis of H3K27ac and MYC proteins in HCC2429 cells incubated with A-485 at indicated concentrations for 48 h. Mean  $\pm$  SEM from three independent experiments,  $^{***}P \leq 0.001$ ,  $^{**}P \leq 0.01$ ,  $^{*}P \leq 0.05$ ; n.s., not significant.

due to the diminished acetylated histone. To confirm this, we performed chromatin immunoprecipitation. Indeed, we observed diminished H3K27ac and BRD4-NUT levels at the *MYC* promoter and *TP63* enhancer regions in A-485-treated HCC2429 cells (Fig. 2b). Consistently, *MYC*, *CCAT1* and *TP63* mRNA levels were significantly repressed by A-485 at a very early time point (6 h, Fig. 2c), suggesting a direct effect of A-485 on the expression of these genes. Similar effects were observed in TC-797 and PER-403 cells (Supplementary Fig. 3A). MYC protein levels were also reduced in A-485-treated HCC2429 cells (Fig. 2d).

To further elucidate the specific role of A-485 on p300/CBP, we performed p300/CBP loss-of-function experiment. The siRNAs showed moderate repression of p300 and CBP mRNA levels respectively (Supplementary Fig. 3B). Since A-485 targets the HAT domain of both p300 and CBP, we combined p300 and CBP siRNAs for the knockdown experiment to maximally phenocopy A-485. In agreement with A-485, double knockdown of p300/CBP also downregulated *MYC*, *CCAT1* and *TP63* mRNA levels supporting target-specific effects of A-485 (Supplementary Fig. 3C). These results indicate that p300/CBP inhibition by A-485 efficiently impairs BRD4-NUT oncogenic functions in NMC.

### A-485 induces squamous differentiation, cell cycle arrest and apoptosis

We reasoned that if competitive inhibition of BRD4-NUT in NMC is sufficient to induce squamous differentiation [5], A-485 might also provoke differentiation by disrupting BRD4-NUT megadomains. Indeed, A-485-treated HCC2429 cells showed a differentiation phenotype, featured by flattening of cells and accumulation of pan-keratin in the cytoplasm (Fig. 3a, b). Expression analysis by quantitative RT-PCR showed induction of three canonical squamous tissue genes (*KRT10*, *KRT14* and *TGM1*) in a

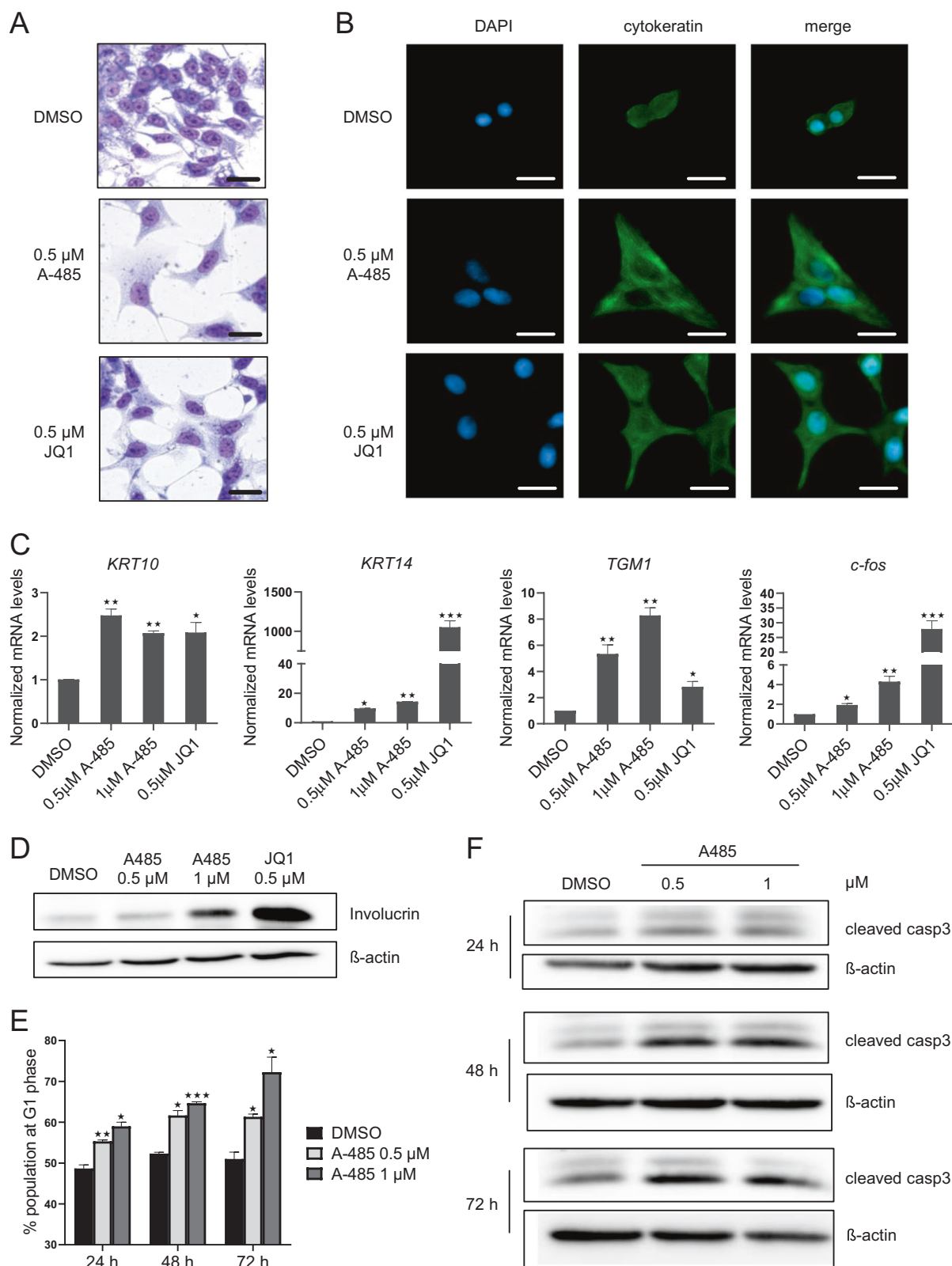
dose-dependent manner (Fig. 3c). *C-fos*, belonging to the Activation Protein-1 (AP-1) family, is an immediate-early inducible transcription factor required for normal epithelial cell differentiation [16]. Here, we also observed the induction of *c-fos* by A-485 (Fig. 3c). Furthermore, A-485 induced the protein levels of Involucrin, a well-known differentiation marker (Fig. 3d). Differentiation phenotype was also observed in TC-797 and PER-403 cells treated with A-485 indicated by morphological changes (Supplementary Fig. 4A). Although TC-797 and PER-403 have different cells of origin and varying degrees of capacity to differentiate, their marker profiles are in most consistent with that of HCC2429 cells (Supplementary Fig. 4B, C). Consistently, p300/CBP double knockdown in HCC2429 cells also induced *c-fos* expression (Supplementary Fig. 4D), although the induction of squamous tissue genes (*KRT10*, *KRT14* and *TGM1*) was not obvious probably due to the moderate downregulation of p300/CBP by siRNAs (Supplementary Fig. 3B). By performing chromatin immunoprecipitation analysis at the *c-fos* promoter region, we also observed diminished H3K27ac and BRD4-NUT enrichment upon A-485 treatment (Supplementary Fig. 5). It would be interesting to further dissect the mechanism of de-repression of differentiation gene by A-485.

In NMC cells, differentiation was shown to be accompanied by cell cycle arrest [5]. Indeed, A-485 induced G1 arrest in HCC2429 cells at early time point (24 h, Fig. 3e). Moreover, elevated levels of cleaved caspase-3 at later time points (48 and 72 h) indicated apoptosis induction by A-485 (Fig. 3f).

### P300/CBP and BET inhibition have synergistic effects in NMC

Because P300/CBP and BRD4-NUT co-localize in hyperacetylated chromatin foci in NMC, we assessed if combination of p300/CBP and BET inhibitors would lead to synergistic anti-proliferative effects. We tested 9 different concentrations of A-485 ranging from 3.91 nM to 1  $\mu$ M in combination with 5 different concentrations of JQ1 ranging from 6.25 to 100 nM for HCC2429 cells. After 72 h incubation, cell viability assays were performed and the synergistic effects were evaluated using SynergyFinder [17]. Combined treatment of A-485 and JQ1 showed strong synergy (ZIP synergy score 13.514, Fig. 4a). We also tested combined treatment in a non-NMC cell line Patu8988S and still observed an albeit smaller synergistic effect (ZIP synergy score 7.531, Supplementary Fig. 6), arguing that combined inhibition of p300/CBP and BET may be synergistic beyond NMC cells.

To further explore this synergistic effect, transcriptomic profiling was performed in HCC2429 cells incubated with A-485 and JQ1 alone or combined at concentrations of 1/3



of cellular  $IC_{50}$  values for 8 h to evaluate the primary transcriptional effect of the inhibitors. Only 149 and 71 genes were affected by A-485 and JQ1 respectively

(Fig. 4b, c), but combined treatment differentially regulated more genes (518 genes, Fig. 4b, c). To obtain insight into the gene expression patterns, we performed gene set

◀ **Fig. 3 A-485 induces squamous differentiation, cell cycle arrest and apoptosis.** **a** Hemacolor staining of HCC2429 cells incubated with 0.5 or 1  $\mu\text{M}$  A-485 for 5 days. **b** Immunofluorescence detection of cytokeratin in HCC2429 cells incubated with 0.5  $\mu\text{M}$  A-485 or JQ1 for 5 days. Scale bar = 20  $\mu\text{m}$ . **c** Quantitative RT-PCR analysis of squamous tissue genes (*KRT10*, *KRT14* and *TGMI*) and *c-fos* in HCC2429 cells incubated with 0.5 or 1  $\mu\text{M}$  A-485 or 0.5  $\mu\text{M}$  JQ1 for 5 days. Mean  $\pm$  SEM from three independent experiments,  $***P \leq 0.001$ ,  $**P \leq 0.01$ ,  $*P \leq 0.05$ . **d** Immunoblot analysis of Involucrin in HCC2429 cells incubated with 0.5 or 1  $\mu\text{M}$  A-485 or 0.5  $\mu\text{M}$  JQ1 for 5 days. **e** Flow cytometry analysis of HCC2429 cells incubated with 0.5 or 1  $\mu\text{M}$  A-485 for 24, 48 and 72 h. Mean  $\pm$  SEM from three independent experiments,  $***P \leq 0.001$ ,  $**P \leq 0.01$ ,  $*P \leq 0.05$ . **f** Immunoblot analysis of cleaved caspase-3 in HCC2429 cells incubated with 0.5 or 1  $\mu\text{M}$  A-485 for 24, 48 and 72 h.

enrichment analysis (GSEA). In combination-treated samples, the p53 pathway and apoptosis were among the most significantly enriched pathways (Fig. 4d), which probably contribute to the observed synergistic effects. Furthermore, gene sets for MYC targets and Wnt/ $\beta$  catenin signaling that support tumor cell growth and inhibit differentiation were significantly downregulated (Fig. 4d). Validating the above findings, immunoblot analysis showed enhanced cleaved caspase-3 by combined treatment (Fig. 4e), indicating induced apoptosis. Consistently, combined treatment, but not single treatment with sub-optimal concentrations, strongly inhibited colony formation (Fig. 4f and Supplementary Fig. 7A). Moreover, at concentrations below the  $\text{IC}_{50}$  values for the single agents, only combined treatment induced squamous differentiation (Fig. 4g and Supplementary Fig. 7B).

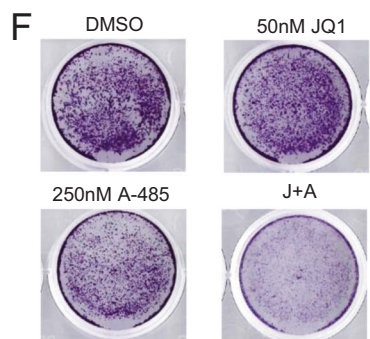
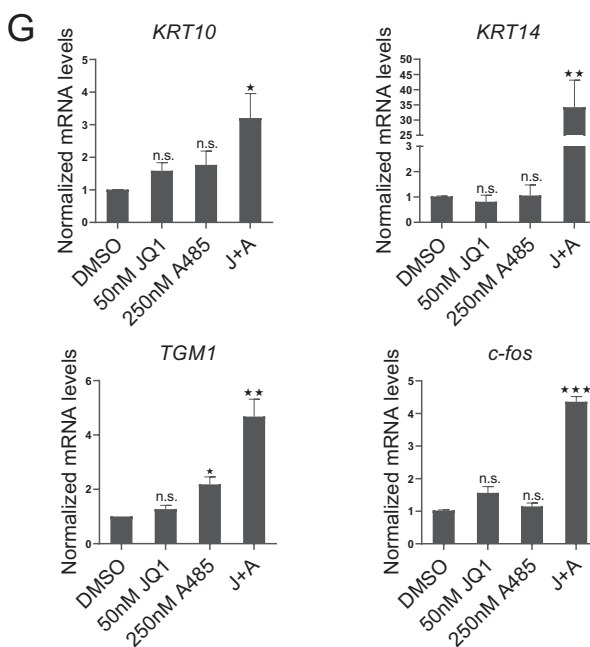
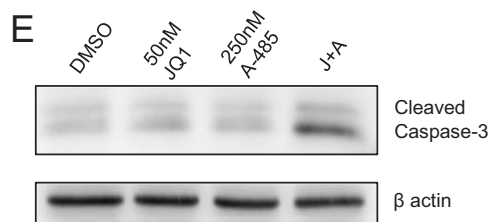
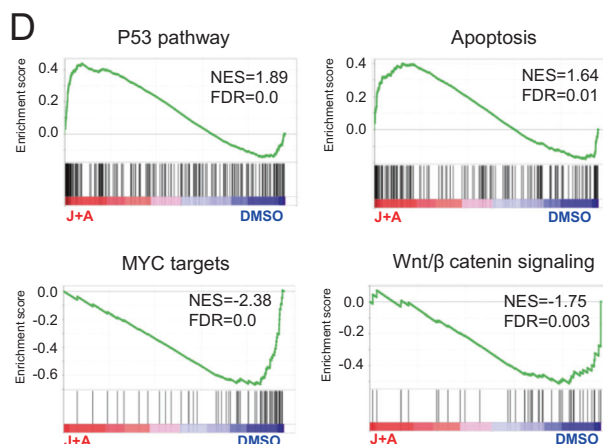
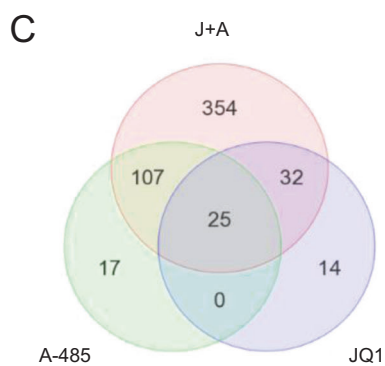
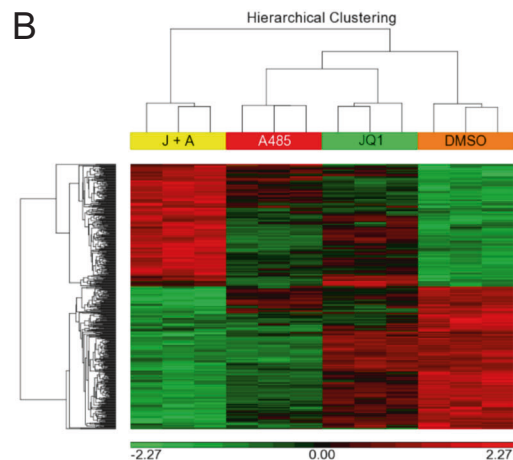
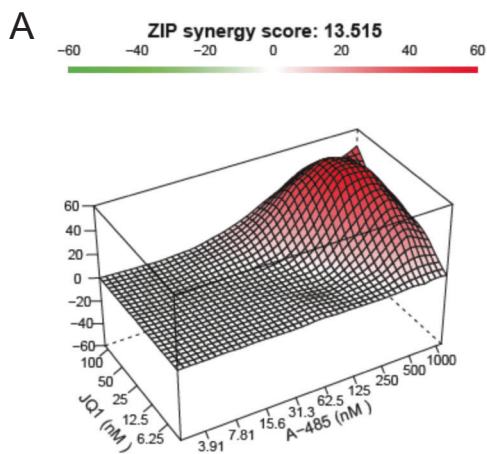
## Discussion

We identified the p300/CBP HAT inhibitor A-485 to be highly potent in NMC but not in tested cell lines derived from other tumor entities. Our chemical probe library also included two p300/CBP bromodomain inhibitors (I-CBP112 and SGC-CBP30) [18, 19]. However, both p300/CBP bromodomain inhibitors showed no or only marginally inhibitory effects on NMC cells raising the question if the bromodomain of p300/CBP is dispensable for its oncogenic function in NMC. In general, the bromodomain is required for p300/CBP to serve as acetyl-lysine binding module tethering the HAT activity to defined chromatin sites to achieve highly specific histone acetylation and transcriptional activation [20, 21]. In NMC, BRD4-NUT binds to acetylated chromatin through its bromodomains and provides a platform for the recruitment of p300/CBP and the stimulation of its HAT activity [3]. Moreover, the bromodomain of p300/CBP is not required for the direct interaction between p300/CBP and BRD4-NUT [3]. Therefore, we reasoned that the bromodomain might be

dispensable for chromatin binding of p300/CBP in NMC. However, whether the bromodomain affects p300/CBP HAT activities in NMC is unknown. Further work will be required to compare the effects of the p300/CBP HAT and bromodomain inhibition to develop the most potent p300/CBP inhibitors.

NMC, one of the most lethal solid tumors, responds poorly to chemo- and radiotherapy. Since the discovery of BET proteins in the tumorigenesis of NMC, current efforts focus on targeting the causative oncoprotein BET. The main targets of the pan-BETi developed so far include BRD2, BRD3 and BRD4, which are ubiquitously expressed in tissues. Given the importance of BET proteins in the basal transcription machinery, BETi inevitably affect normal cell functions. Thrombocytopenia, fatigue, gastrointestinal symptoms, and hyperbilirubinemia are among the dose-limiting side effects reported in patients treated with BETi [7]. Pan-BETi was also reported to have activity for bromodomain testis-specific protein (BRDT), causing testicular atrophy and reversible infertility [22]. Compared to the activity of BETi across broad tumor types, p300/CBP inhibitors selectively target lineage-specific tumors [13]. Moreover, transcriptional profiling of human T cells and one prostate cancer cell line after treatment of p300/CBP inhibitors revealed significantly fewer altered genes than observed with BETi [19, 23]. Thus, p300/CBP inhibition is an alternative therapeutic strategy that potentially leads to fewer adverse events than the broadly acting BETi.

In clinical trials of BEiT, only a small fraction of NMC patients responded and eventually relapsed during treatment [6, 7]. Thus, the development of BETi faces the challenges of how to enhance the sensitivity of patients and how to overcome resistance. Others [18, 23] and our study discovered that combination of p300/CBP and BETi results in a highly synergistic inhibitory effect in several tumor types. Furthermore, BETi-resistant cells continue to respond to the p300/CBP inhibitor [23]. We propose that combination therapy using both p300/CBP and BET inhibitors may be necessary to sensitize patient and overcome BETi resistance. Our efforts in exploring the molecular mechanisms of this synergistic effect in NMC discovered that combined p300/CBP and BET inhibitors significantly downregulate Wnt/ $\beta$  catenin signaling. Interestingly, one study in human and mouse leukemia cells demonstrated that increased Wnt/ $\beta$  catenin signaling contributes to the resistance to BETi and negative regulation of this pathway restores the sensitivity [24]. Recently, a dual inhibitor of both p300/CBP and BET showed promising anti-tumor effect in prostate cancer [25, 26]. Thus, combined p300/CBP and BET inhibition may be a rational and conceivable targeting approach in NMC and other tumor types.



◀ **Fig. 4 P300/CBP and BET inhibition have synergistic effects in NMC.** **a** Combination response to A-485 and JQ1 for HCC2429 cells. CellTiterGlo cell viability assay was performed to measure cell viabilities of all the indicated dose combinations for 72 h. Synergy effects were evaluated using SynergyFinder (<https://synergyfinder.fimm.fi>). The ZIP synergy score is averaged over all the dose combination cells. **b,c** Hierarchical clustering (**b**) and Venn diagram analysis (**c**) of the differentially expressed genes in HCC2429 cells treated with 50 nM JQ1 and 250 nM A-485 alone or combined for 8 h. Each treatment was done in triplicate. **d** Representative GSEA plots showing significantly enriched up- and downregulated pathways (combination-treatment versus DMSO). **e** Immunoblot analysis of cleaved caspase-3 in HCC2429 cells incubated with 50 nM JQ1 and 250 nM A-485 alone or combined for 72 h. **f** Colony formation assay for HCC2429 cells incubated with 50 nM JQ1 and 250 nM A-485 alone or combined for 72 h. **g** Quantitative RT-PCR analysis of squamous tissue genes (*KRT10*, *KRT14* and *TGM1*) and *c-fos* in HCC2429 cells incubated with 50 nM JQ1 and 250 nM A-485 alone or combined for 5 days. Mean  $\pm$  SEM from three independent experiments, \*\*\* $P \leq 0.001$ , \*\* $P \leq 0.01$ , \* $P \leq 0.05$ ; n.s., not significant.

## Materials and Methods

### Cell culture

NMC cell lines HCC2429 [27], Ty-82 [28], 00–143 [29], TC-797 [30], PER-403 [31] and the pancreatic tumor cell line QGP-1 [32] have been described. HCC2429, Ty-82 and 00–143 were kindly provided from Lead Discovery Center GmbH (Dortmund, Germany). The pancreatic tumor cell line Patu8988T was from the American Type Culture Collection. All cell lines were free of mycoplasma contamination and authenticated using short tandem repeat (STR) profiling.

### Data availability

Microarray data are available through ArrayExpress under the accession code E-MTAB-8955.

**Acknowledgements** We are grateful for support by the SGC, a registered charity (no. 1097737) that receives funds from AbbVie, Bayer Pharma AG, Boehringer Ingelheim, Canada Foundation for Innovation, Eshelman Institute for Innovation, Genome Canada through Ontario Genomics Institute [OGI-055], Innovative Medicines Initiative (EU/EFPIA) [ULTRA-DD grant no. 115766], Janssen, Merck KGaA, MSD, Novartis Pharma AG, Ontario Ministry of Research, Innovation and Science (MRIS), Pfizer, São Paulo Research Foundation-FAPESP, Takeda, and the Wellcome Trust. JTS and SK are supported by the German Cancer Aid (grant no. 70112505; PIPAC consortium). JTS is supported by the German Cancer Consortium (DKTK) and the Deutsche Forschungsgemeinschaft (DFG) through grant SI1549/3–1 (Clinical Research Unit KFO337) and Collaborative Research Center SFB824 (project C4). Open access funding provided by Projekt DEAL.

### Compliance with ethical standards

**Conflict of interest** The authors declare that they have no conflict of interest.

**Publisher's note** Springer Nature remains neutral with regard to jurisdictional claims in published maps and institutional affiliations.

**Open Access** This article is licensed under a Creative Commons Attribution 4.0 International License, which permits use, sharing, adaptation, distribution and reproduction in any medium or format, as long as you give appropriate credit to the original author(s) and the source, provide a link to the Creative Commons license, and indicate if changes were made. The images or other third party material in this article are included in the article's Creative Commons license, unless indicated otherwise in a credit line to the material. If material is not included in the article's Creative Commons license and your intended use is not permitted by statutory regulation or exceeds the permitted use, you will need to obtain permission directly from the copyright holder. To view a copy of this license, visit <http://creativecommons.org/licenses/by/4.0/>.

## References

- Bauer DE, Mitchell CM, Strait KM, Lathan CS, Stelow EB, Luer SC, et al. Clinicopathologic features and long-term outcomes of NUT midline carcinoma. *Clin Cancer Res.* 2012;18:5773–9.
- French CA, Miyoshi I, Kubonishi I, Grier HE, Perez-Atayde AR, Fletcher JA. BRD4-NUT fusion oncogene: a novel mechanism in aggressive carcinoma. *Cancer Res.* 2003;63:304–7.
- Reynoird N, Schwartz BE, Delvecchio M, Sadoul K, Meyers D, Mukherjee C, et al. Oncogenesis by sequestration of CBP/p300 in transcriptionally inactive hyperacetylated chromatin domains. *EMBO J.* 2010;29:2943–52.
- Alekseyenko AA, Walsh EM, Wang X, Grayson AR, Hsi PT, Kharchenko PV, et al. The oncogenic BRD4-NUT chromatin regulator drives aberrant transcription within large topological domains. *Genes Dev.* 2015;29:1507–23.
- Filippakopoulos P, Qi J, Picaud S, Shen Y, Smith WB, Fedorov O, et al. Selective inhibition of BET bromodomains. *Nature.* 2010;468:1067–73.
- Stathis A, Zucca E, Bekradda M, Gomez-Roca C, Delord JP, de La Motte Rouge T, et al. Clinical response of carcinomas harboring the brd4-nut oncoprotein to the targeted bromodomain inhibitor OTX015/MK-8628. *Cancer Discov.* 2016;6:492–500.
- O'Dwyer PJ, Piha-Paul SA, French CA, Harward S, Ferron-Brady G, Wu Y, et al. Abstract CT014: GSK525762, a selective bromodomain (BRD) and extra terminal protein (BET) inhibitor: results from part 1 of a phase I/II open-label single-agent study in patients with NUT midline carcinoma (NMC) and other cancers. *Cancer Res.* 2016;76:CT014
- Lewin J, Soria JC, Stathis A, Delord JP, Peters S, Awada A, et al. Phase Ib trial with birabresib, a small-molecule inhibitor of bromodomain and extraterminal proteins, in patients with selected advanced solid tumors. *J Clin Oncol.* 2018;36:3007–14.
- Scheer S, Ackloo S, Medina TS, Schapira M, Li F, Ward JA, et al. A chemical biology toolbox to study protein methyltransferases and epigenetic signaling. *Nat Commun.* 2019;10:19.
- Wu Q, Heidenreich D, Zhou S, Ackloo S, Kramer A, Nakka K, et al. A chemical toolbox for the study of bromodomains and epigenetic signaling. *Nat Commun.* 2019;10:1915.
- Muller S, Ackloo S, Arrowsmith CH, Bauser M, Baryza JL, Blagg J, et al. Donated chemical probes for open science. *eLife.* 2018;7:e34311
- Stathis A, Bertoni F. BET proteins as targets for anticancer treatment. *Cancer Discov.* 2018;8:24–36.
- Lasko LM, Jakob CG, Edalji RP, Qiu W, Montgomery D, Digiammarino EL, et al. Discovery of a selective catalytic p300/CBP inhibitor that targets lineage-specific tumours. *Nature.* 2017;550:128–32.

14. Kimura H, Sato Y, Tajima Y, Suzuki H, Yukitake H, Imaeda T, et al. BTZO-1, a cardioprotective agent, reveals that macrophage migration inhibitory factor regulates ARE-mediated gene expression. *Chem Biol*. 2010;17:1282–94.
15. Xiang JF, Yin QF, Chen T, Zhang Y, Zhang XO, Wu Z, et al. Human colorectal cancer-specific CCAT1-L lncRNA regulates long-range chromatin interactions at the MYC locus. *Cell Res*. 2014;24:513–31.
16. Yan J, Diaz J, Jiao J, Wang R, You J. Perturbation of BRD4 protein function by BRD4-NUT protein abrogates cellular differentiation in NUT midline carcinoma. *J Biol Chem*. 2011;286:27663–75.
17. Ianevski A, He L, Aittokallio T, Tang J. SynergyFinder: a web application for analyzing drug combination dose-response matrix data. *Bioinforma (Oxf, Engl)*. 2017;33:2413–5.
18. Picaud S, Fedorov O, Thanasopoulou A, Leonards K, Jones K, Meier J, et al. Generation of a selective small molecule inhibitor of the CBP/p300 bromodomain for leukemia therapy. *Cancer Res*. 2015;75:5106–19.
19. Hammitzsch A, Tallant C, Fedorov O, O'Mahony A, Brennan PE, Hay DA, et al. CBP30, a selective CBP/p300 bromodomain inhibitor, suppresses human Th17 responses. *Proc Natl Acad Sci USA*. 2015;112:10768–73.
20. Dhalluin C, Carlson JE, Zeng L, He C, Aggarwal AK, Zhou MM. Structure and ligand of a histone acetyltransferase bromodomain. *Nature*. 1999;399:491–6.
21. Syntichaki P, Topalidou I, Thireos G. The Gcn5 bromodomain coordinates nucleosome remodelling. *Nature*. 2000;404:414–7.
22. Matzuk MM, McKeown MR, Filippakopoulos P, Li Q, Ma L, Agno JE, et al. Small-molecule inhibition of BRDT for male contraception. *Cell*. 2012;150:673–84.
23. Brooks N, Prosser A, Young B, Gaughan L, Elvin P, Pegg N. Abstract 3826: CCS1477, a potent and selective p300/CBP bromodomain inhibitor, is targeted & differentiated from BET inhibitors in prostate cancer cell lines in vitro. *Cancer Res*. 2019;79:3826.
24. Fong CY, Gilan O, Lam EY, Rubin AF, Ftouni S, Tyler D, et al. BET inhibitor resistance emerges from leukaemia stem cells. *Nature*. 2015;525:538–42.
25. Giles F, Witcher M, Brown B. NEO2734 - A novel potent oral dual BET and P300/CBP inhibitor. *Ann Oncol*. 2018;29:279–416.
26. Yan Y, Wang D, Ma J, Pang X, Lin D, Giles F, et al. Activity of NEO2734, a novel dual inhibitor of both BET and CBP-P300, in SPOP-mutated prostate cancer. *J Clin Oncol*. 2019;37:62–62.
27. Haruki N, Kawaguchi KS, Eichenberger S, Massion PP, Gonzalez A, Gazdar AF, et al. Cloned fusion product from a rare t(15;19)(q13.2;p13.1) inhibit S phase in vitro. *J Med Genet*. 2005;42:558–64.
28. Kuzume T, Kubonishi I, Takeuchi S, Takeuchi T, Iwata J, Sonobe H, et al. Establishment and characterization of a thymic carcinoma cell line (Ty-82) carrying t(15;19)(q15;p13) chromosome abnormality. *Int J Cancer*. 1992;50:259–64.
29. French CA, Miyoshi I, Aster JC, Kubonishi I, Kroll TG, Dal Cin P, et al. BRD4 bromodomain gene rearrangement in aggressive carcinoma with translocation t(15;19). *Am J Pathol*. 2001;159:1987–92.
30. Toretsky JA, Jenson J, Sun CC, Eskenazi AE, Campbell A, Hunger SP, et al. Translocation (11;15;19): a highly specific chromosome rearrangement associated with poorly differentiated thymic carcinoma in young patients. *Am J Clin Oncol*. 2003;26:300–6.
31. Kees UR, Mulcahy MT, Willoughby ML. Intrathoracic carcinoma in an 11-year-old girl showing a translocation t(15;19). *Am J Pediatr Hematol Oncol*. 1991;13:459–64.
32. Iguchi H, Hayashi I, Kono A. A somatostatin-secreting cell line established from a human pancreatic islet cell carcinoma (somatostatinoma): release experiment and immunohistochemical study. *Cancer Res*. 1990;50:3691–3.

## 4. Discussion

Altered epigenetic states and dysregulated transcription in cancer cells indicated a significant impact of epigenetic therapies. The promising results of dual BET/HDAC inhibitor TW9 in PDAC and HAT inhibitor A485 in NMC underline the important role of targeting epigenetic regulators as essential part of cancer therapy in the future. Exploiting vulnerabilities of transcriptional addiction and a better understanding about the connection between tumor heterogeneity and therapy resistance will be a considerable addition to targeted therapy and improve therapeutic strategies. Thus, this new generation of inhibitors may deliver a powerful tool for treating the most therapy resistant tumors, since their low overall survival (OS) is often linked to relapse of treatment resistant cells. While NMC is a deadly, but also very rare cancer, PDAC is estimated to be the second leading cause of cancer death in the United States by the year 2030<sup>2</sup>, underlining the urgent need for novel therapeutic strategies for pancreatic cancer. Especially the Basal-like subtype is highly involved in therapy resistance and recurrence of tumor cells. Targeting transcriptional regulators could become a promising approach to block or revert the epigenetic driven transition from Classical to Basal-like cells. Since the Classical subtype responds much better to first-line chemotherapy, a combination therapy with chemotherapeutic agents holds great promise for treating PDAC, which is supported by observed synergistic effects between TW9 and gemcitabine. However, a deeper understanding of cellular plasticity, transcriptional dependencies and mechanistic models, how they drive cancer progression, is required to transform these findings into patients benefit. Targeting master TFs and especially oncogenic Myc provides great opportunities, but remains challenging. So far, many BET inhibitors entered clinical evaluation, but no inhibitor reached FDA approval. A focus on epigenetic-based screening platforms and improved assay systems, as well as a new generation of more potent and selective compounds, will hopefully help to develop the field of epigenetic approaches and to yield new therapeutic strategies.

So far, a large body of results points to combination therapies rather than single inhibitor treatment. While advanced diagnostics, identification of oncogenic driver mutations and targeted therapy already revolutionized cancer medicine, transcriptional inhibitors are the most promising approach to complete existing strategies and target the remaining “untreatable” carcinomas as well as emerging therapy resistance.

### 4.1 Combinational and low dose therapies

Recent preclinical studies report synergism for most epigenetic inhibitors in combination with other epigenetic and non-epigenetic therapeutics. The rational design of TW9 was based on previous observation of synergism between the BETi JQ1 and the HDACi SAHA in PDAC

xenograft experiments and TW9 was additionally shown to synergize with gemcitabine, the standard-of-care chemotherapeutic agent in the treatment of PDAC. Further, synergism between HATi A485 and JQ1 was observed in combinational treatment of NMC, indicating that novel therapeutic strategies will consider epigenetic combination therapies rather than single agent treatments. Given the fact, that most cancers are driven by multiple gene alterations and additionally compensatory signaling pathways occur, its rational to focus on multitarget therapies. Like previously reported, HDAC inhibitors were shown to decrease the emergence of resistance and sensitize tumor cells to a specific treatment, thus combinational approaches together with first-line therapeutics is a promising strategy to overcome resistance against targeted or immune therapy. Drug-drug interactions, toxicity or pharmacokinetics are usually limiting the application of combination therapies. If possible, an optimized low dose scheduling is one strategy to solve this issue. Another approach would be the focus on the design of dual active compounds with multiple inhibitory activities. Recent studies about BET/kinase inhibitors underline the importance of dual active compounds in future therapeutic strategies and only a few weeks before publication of TW9, another research group reported about a BET/HDAC inhibitor with nearly similar structure to TW9 for the treatment of pancreatic cancer<sup>100</sup>. After observation of strong synergism between gemcitabine and TW9, the usage of a dual inhibitor allows a potential multitarget treatment, while a therapy containing three different drugs is difficult to implement into clinical applications.

Beside the advantages of the application of a single drug instead of two, dual inhibitor TW9 additionally demonstrated advanced activity in PDAC cells compared to combinational treatment with both single inhibitors. TW9 had a more potent and sustained effect on cell viability, which will increase the therapeutic window and enable more combinational strategies. Especially the HDAC moiety showed enhanced and prolonged activity compared to same levels of CI994. While this observation definitely needs further evaluation, a longer on target residence time or increased molecule stability are possible explanations. However, TW9 was successfully designed as proof of concept compound. Therefore, as adduct of two epigenetic inhibitors, it has a relatively high molecular weight and was not optimized for clinical applications. First in vivo experiments in mouse models also indicate toxicity by TW9. Thus, a second generation of dual BET/HDAC inhibitors with lower molecular weight and improved physicochemical properties has to proof its in vivo application for prospective therapeutic strategies.

Many combinational approaches already demonstrate strong synergy at reduced doses of single inhibitors. Decreased concentrations of A485 and JQ1 were able to induce squamous differentiation in NMC, while single agent treatment was not. A low dose therapy would

additionally lower toxicity and side effects, which are affecting quality of life of most cancer patients, especially in combination with conventional chemotherapy. Working with lower drug concentrations also becomes interesting in the context of therapy resistance. Using the maximum tolerable dose for treatment is not uncommon in clinical anti-cancer applications. As previously mentioned, fluctuating drug tolerant cells are a small subpopulation of cancer cells, becoming the predominant population after treatment and probably the main reason for tumor relapse (Fig. 1). It was also mentioned that therapy resistance comes with a price, since maintenance of alternative pathways requires resources, which must be diverted from proliferation, resulting in slow cycling cells. These findings suggest, that sensitive cells have an increased fitness compared to resistant cells in an environment of limited substrate. In contrast to a conventional high dose therapy, lower concentration treatments may not eliminate all sensitive cells, but in each treatment cycle the tumor remains sensitive, since the sensitive cells will always overgrow the resistant cells after therapeutic withdrawal<sup>2</sup>. This therapeutic strategy would aim for maximizing progression free survival and patient's quality of life. Recent studies underline the potential impact of low dose therapies for treating cancer<sup>101, 102</sup>. However, a well optimized scheduling and dosing as well as a highly flexible and adaptive treatment is required to release the full potential of a low dose combinational therapy. If used properly, these adaptive strategies may prolong therapy response and sustainable increase patient's wellbeing.

#### **4.2 Future directions**

Therapy resistance is one of today's biggest challenges in treating cancer. Even the application of transcriptional inhibitors was shown to be a first successful strategy to target treatment resistance, there are emerging evidences that indicate development of resistance against epigenetic inhibitors by tumor cells<sup>103, 104</sup>. For instance, while most NMC cell lines were shown to be sensitive to treatment with p300/CBP inhibitor A485, two cell lines (TC-797 and PER-403) only demonstrated comparable effects and induced differentiation with high inhibitor concentrations, indicating an emerging escape mechanism. Beside low dose combination therapies, simultaneously targeting of two transcriptional regulators may be a possible approach to avoid resistance against epigenetic inhibitors. I would be interesting to see for example, whether TW9 is able to overcome BET inhibitor resistance in tumor cells.

Studies about BETi resistance report about different mechanisms, which are induced by compensatory signaling and pathways instead of mutations in BET bromodomain genes<sup>91</sup>, suggesting that cellular plasticity is also involved in the development of resistance to BET inhibitors. One of the described escape mechanisms to BETi treatment is an increased WNT

signaling<sup>91</sup>. Wnt/ $\beta$ -catenin signaling in collaboration with TGF- $\beta$ , is highly involved in EMT-induction and cellular plasticity. It has been shown, that they are part of autocrine signaling loops in order to maintain the mesenchymal state and CSC-like properties, including drug resistance<sup>105</sup>. Observations, that chromatin-bound BRD4 levels in BETi-resistant cells are globally reduced, but the expression of target genes like Myc are unchanged, indicate the emerge of compensatory pathways<sup>106</sup>. Wnt/ $\beta$ -catenin inhibition sensitized cells to BET treatment again, demonstrating that a  $\beta$ -catenin-mediated Myc expression is involved in resistance to bromodomain inhibitors<sup>106</sup>. These findings give rise to another combinational approach, targeting transcriptional regulators as well as signaling pathways involved in EMT. Interestingly, gene set enrichment analysis (GSEA) in NMC cells HCC2429 revealed that MYC targets and Wnt/ $\beta$  catenin signaling are significantly downregulated after combinational low dose treatment with HATi A485 together with JQ1. Transcriptomic profiling of treated and untreated NCM cell-lines TC-797 and PER-403, which showed to be more resistant to p300 inhibition, may give more insights into the role of  $\beta$ -catenin and other compensatory pathways. Another interesting aspect which was only minor mentioned before, nevertheless has a significant impact on EMT induction and cell plasticity, is the role of the microenvironment and extracellular matrix (ECM).

The tumor microenvironment is highly involved in tumor progression, but also in response to therapy. Like previously described, especially in pancreatic cancer, an immunosuppressive, dense and considerable hypoxic microenvironment is contributing to low tumor accessibility and treatment resistance. Since cell plasticity represents the ability of cells to change their phenotype in response to environmental signals, the ECM significantly regulates carcinoma cell behaviors. These close interactions between cancer cells, ECM and stroma cells are forming the tumor microenvironment (TME), which is characterized by a chronic inflammatory, pro-angiogenic and immunosuppressive network<sup>107</sup>. Chronic inflammation is linked to genetic instability, enhanced proliferation, resistance to apoptosis and promotes tumor progression by recruiting mitogenic growth factors and cytokines including TGF- $\beta$ <sup>107, 108</sup>. The hypoxic microenvironment, increased expression of programmed death-ligand 1 (PD-L1) by tumor cells and the recruitment of cytokines and regulatory T cells (Treg) are only a few mechanisms of immunosuppression in the TME, that inhibit T-cell activity and allows tumor cells to avoid the immune control<sup>109</sup>. Thus, immune checkpoint blockers (ICBs) against PD-1/PD-L1 or checkpoint protein CTLA-4 got in the center of attention and offered new therapeutic approaches. Interestingly, it was shown, that BETi JQ1 is able to suppress PD-L1 expression and decrease levels of inflammatory mediator interleukin-6 (IL-6) in tumor cells.<sup>99, 110</sup>

Further, the unequal distribution of oxygen and signaling factors in the TME contributes to an already increased heterogeneity within the tumor. It has been shown, that only the variation of oxygen levels in melanoma cells was sufficient to induce a shift between a drug-tolerant slow cycling state and proliferative drug-sensitive state<sup>111</sup>. Specific cytokines, tumor-associated inflammatory cells and macrophages were also linked to activation of the EMT program in cancer cells<sup>42</sup>. This complexity of tumor environment is definitely not captured accurately in current assays system and creates additionally a serious challenge for therapeutic strategies. Advanced methods like patient derived xenografts (PDX) are required to mimic realistic patient's conditions. Even tumor microenvironment is highly contributing to an already increased complexity around cell plasticity, EMT and therapy resistance, it also delivers new opportunities for targeting cancer. A deeper understanding of the interaction between microenvironment and tumor cells and its ability to induce the EMT program could additionally support future investigation.

However, the ability of TME of limiting access to tumor cells has to be considered for all kind of future drug discoveries. Since the tumor microenvironment is much more penetrable and accessible than tumor cells, it also becomes an attractive target for combinational therapies in order to enhance the efficacy of other anti-cancer agents.

## 5. List of literature

1. Lee, Y. T.; Tan, Y. J.; Oon, C. E., Molecular targeted therapy: Treating cancer with specificity. *Eur J Pharmacol* **2018**, *834*, 188-196.
2. Gatenby, R.; Brown, J., The Evolution and Ecology of Resistance in Cancer Therapy. *Cold Spring Harb Perspect Med* **2018**, *8* (3).
3. Yu, Z.; Pestell, T. G.; Lisanti, M. P.; Pestell, R. G., Cancer stem cells. *Int J Biochem Cell Biol* **2012**, *44* (12), 2144-51.
4. Chakraborty, S.; Rahman, T., The difficulties in cancer treatment. *Ecancermedalscience* **2012**, *6*, ed16.
5. Al-Hajj, M.; Wicha, M. S.; Benito-Hernandez, A.; Morrison, S. J.; Clarke, M. F., Prospective identification of tumorigenic breast cancer cells. *Proc Natl Acad Sci U S A* **2003**, *100* (7), 3983-8.
6. Singh, S. K.; Clarke, I. D.; Terasaki, M.; Bonn, V. E.; Hawkins, C.; Squire, J.; Dirks, P. B., Identification of a cancer stem cell in human brain tumors. *Cancer Res* **2003**, *63* (18), 5821-8.
7. Lapidot, T.; Sirard, C.; Vormoor, J.; Murdoch, B.; Hoang, T.; Caceres-Cortes, J.; Minden, M.; Paterson, B.; Caligiuri, M. A.; Dick, J. E., A cell initiating human acute myeloid leukaemia after transplantation into SCID mice. *Nature* **1994**, *367* (6464), 645-8.
8. Raaijmakers, M. H.; de Grouw, E. P.; Heuver, L. H.; van der Reijden, B. A.; Jansen, J. H.; Scheper, R. J.; Scheffer, G. L.; de Witte, T. J.; Raymakers, R. A., Breast cancer resistance protein in drug resistance of primitive CD34+38- cells in acute myeloid leukemia. *Clin Cancer Res* **2005**, *11* (6), 2436-44.
9. Boumahdi, S.; de Sauvage, F. J., The great escape: tumour cell plasticity in resistance to targeted therapy. *Nat Rev Drug Discov* **2020**, *19* (1), 39-56.
10. Roesch, A., Tumor heterogeneity and plasticity as elusive drivers for resistance to MAPK pathway inhibition in melanoma. *Oncogene* **2015**, *34* (23), 2951-7.
11. Hata, A. N.; Niederst, M. J.; Archibald, H. L.; Gomez-Caraballo, M.; Siddiqui, F. M.; Mulvey, H. E.; Maruvka, Y. E.; Ji, F.; Bhang, H. E.; Krishnamurthy Radhakrishna, V.; Siravegna, G.; Hu, H.; Raof, S.; Lockerman, E.; Kalsy, A.; Lee, D.; Keating, C. L.; Ruddy, D. A.; Damon, L. J.; Crystal, A. S.; Costa, C.; Piotrowska, Z.; Bardelli, A.; Iafrate, A. J.; Sadreyev, R. I.; Stegmeier, F.; Getz, G.; Sequist, L. V.; Faber, A. C.; Engelman, J. A., Tumor cells can follow distinct evolutionary paths to become resistant to epidermal growth factor receptor inhibition. *Nat Med* **2016**, *22* (3), 262-9.
12. Sharma, S. V.; Lee, D. Y.; Li, B.; Quinlan, M. P.; Takahashi, F.; Maheswaran, S.; McDermott, U.; Azizian, N.; Zou, L.; Fischbach, M. A.; Wong, K. K.; Brandstetter, K.; Wittner, B.; Ramaswamy, S.; Classon, M.; Settleman, J., A chromatin-mediated reversible drug-tolerant state in cancer cell subpopulations. *Cell* **2010**, *141* (1), 69-80.
13. Biehs, B.; Dijkgraaf, G. J. P.; Piskol, R.; Alicke, B.; Boumahdi, S.; Peale, F.; Gould, S. E.; de Sauvage, F. J., A cell identity switch allows residual BCC to survive Hedgehog pathway inhibition. *Nature* **2018**, *562* (7727), 429-433.
14. Su, Y.; Wei, W.; Robert, L.; Xue, M.; Tsoi, J.; Garcia-Diaz, A.; Homet Moreno, B.; Kim, J.; Ng, R. H.; Lee, J. W.; Koya, R. C.; Comin-Anduix, B.; Graeber, T. G.; Ribas, A.; Heath, J. R., Single-cell analysis resolves the cell state transition and signaling dynamics associated with melanoma drug-induced resistance. *Proc Natl Acad Sci U S A* **2017**, *114* (52), 13679-13684.
15. Shaffer, S. M.; Dunagin, M. C.; Torborg, S. R.; Torre, E. A.; Emert, B.; Krepler, C.; Beqiri, M.; Sproesser, K.; Brafford, P. A.; Xiao, M.; Eggen, E.; Anastopoulos, I. N.; Vargas-Garcia, C. A.; Singh, A.; Nathanson, K. L.; Herlyn, M.; Raj, A., Rare cell variability and drug-induced reprogramming as a mode of cancer drug resistance. *Nature* **2017**, *546* (7658), 431-435.

16. Glasspool, R. M.; Teodoridis, J. M.; Brown, R., Epigenetics as a mechanism driving polygenic clinical drug resistance. *Br J Cancer* **2006**, *94* (8), 1087-92.
17. Tata, P. R.; Rajagopal, J., Cellular plasticity: 1712 to the present day. *Curr Opin Cell Biol* **2016**, *43*, 46-54.
18. Mills, J. C.; Stanger, B. Z.; Sander, M., Nomenclature for cellular plasticity: are the terms as plastic as the cells themselves? *EMBO J* **2019**, *38* (19), e103148.
19. Siegel, R. L.; Miller, K. D.; Jemal, A., Cancer Statistics, 2017. *CA Cancer J Clin* **2017**, *67* (1), 7-30.
20. Rahib, L.; Smith, B. D.; Aizenberg, R.; Rosenzweig, A. B.; Fleshman, J. M.; Matrisian, L. M., Projecting cancer incidence and deaths to 2030: the unexpected burden of thyroid, liver, and pancreas cancers in the United States. *Cancer Res* **2014**, *74* (11), 2913-21.
21. Kleeff, J.; Korc, M.; Apte, M.; La Vecchia, C.; Johnson, C. D.; Biankin, A. V.; Neale, R. E.; Tempero, M.; Tuveson, D. A.; Hruban, R. H.; Neoptolemos, J. P., Pancreatic cancer. *Nat Rev Dis Primers* **2016**, *2*, 16022.
22. Conroy, T.; Desseigne, F.; Ychou, M.; Bouché, O.; Guimbaud, R.; Bécouarn, Y.; Adenis, A.; Raoul, J. L.; Gourgou-Bourgade, S.; de la Fouchardière, C.; Bennouna, J.; Bachet, J. B.; Khemissa-Akouz, F.; Péré-Vergé, D.; Delbaldo, C.; Assenat, E.; Chauffert, B.; Michel, P.; Montoto-Grillot, C.; Ducreux, M.; Unicancer, G. T. D. o.; Intergroup, P., FOLFIRINOX versus gemcitabine for metastatic pancreatic cancer. *N Engl J Med* **2011**, *364* (19), 1817-25.
23. Burris, H. A.; Moore, M. J.; Andersen, J.; Green, M. R.; Rothenberg, M. L.; Modiano, M. R.; Cripps, M. C.; Portenoy, R. K.; Storniolo, A. M.; Tarassoff, P.; Nelson, R.; Dorr, F. A.; Stephens, C. D.; Von Hoff, D. D., Improvements in survival and clinical benefit with gemcitabine as first-line therapy for patients with advanced pancreas cancer: a randomized trial. *J Clin Oncol* **1997**, *15* (6), 2403-13.
24. Von Hoff, D. D.; Ervin, T.; Arena, F. P.; Chiorean, E. G.; Infante, J.; Moore, M.; Seay, T.; Tjulandin, S. A.; Ma, W. W.; Saleh, M. N.; Harris, M.; Reni, M.; Dowden, S.; Laheru, D.; Bahary, N.; Ramanathan, R. K.; Tabernero, J.; Hidalgo, M.; Goldstein, D.; Van Cutsem, E.; Wei, X.; Iglesias, J.; Renschler, M. F., Increased survival in pancreatic cancer with nab-paclitaxel plus gemcitabine. *N Engl J Med* **2013**, *369* (18), 1691-703.
25. Collisson, E. A.; Bailey, P.; Chang, D. K.; Biankin, A. V., Molecular subtypes of pancreatic cancer. *Nat Rev Gastroenterol Hepatol* **2019**, *16* (4), 207-220.
26. Chan-Seng-Yue, M.; Kim, J. C.; Wilson, G. W.; Ng, K.; Figueroa, E. F.; O'Kane, G. M. et al., Transcription phenotypes of pancreatic cancer are driven by genomic events during tumor evolution. *Nat Genet* **2020**, *52* (2), 231-240.
27. Aung, K. L.; Fischer, S. E.; Denroche, R. E.; Jang, G. H.; Dodd, A.; Creighton, S.; Southwood, B.; Liang, S. B.; Chadwick, D.; Zhang, A.; O'Kane, G. M.; Albaba, H.; Moura, S.; Grant, R. C.; Miller, J. K.; Mbabaali, F.; Pasternack, D.; Lungu, I. M.; Bartlett, J. M. S.; Ghai, S.; Lemire, M.; Holter, S.; Connor, A. A.; Moffitt, R. A.; Yeh, J. J.; Timms, L.; Krzyzanowski, P. M.; Dhani, N.; Hedley, D.; Notta, F.; Wilson, J. M.; Moore, M. J.; Gallinger, S.; Knox, J. J., Genomics-Driven Precision Medicine for Advanced Pancreatic Cancer: Early Results from the COMPASS Trial. *Clin Cancer Res* **2018**, *24* (6), 1344-1354.
28. French, C. A.; Miyoshi, I.; Kubonishi, I.; Grier, H. E.; Perez-Atayde, A. R.; Fletcher, J. A., BRD4-NUT fusion oncogene: a novel mechanism in aggressive carcinoma. *Cancer Res* **2003**, *63* (2), 304-7.
29. Napolitano, M.; Venturelli, M.; Molinaro, E.; Toss, A., NUT midline carcinoma of the head and neck: current perspectives. *Onco Targets Ther* **2019**, *12*, 3235-3244.
30. Lewin, J.; Soria, J. C.; Stathis, A.; Delord, J. P.; Peters, S.; Awada, A.; Aftimos, P. G.; Bekradda, M.; Rezai, K.; Zeng, Z.; Hussain, A.; Perez, S.; Siu, L. L.; Massard, C., Phase Ib Trial With Birabresib, a Small-Molecule Inhibitor of Bromodomain and Extraterminal Proteins, in Patients With Selected Advanced Solid Tumors. *J Clin Oncol* **2018**, *36* (30), 3007-3014.

31. Piha-Paul, S. A.; Sachdev, J. C.; Barve, M.; LoRusso, P.; Szmulewitz, R.; Patel, S. P.; Lara, P. N.; Chen, X.; Hu, B.; Freise, K. J.; Modi, D.; Sood, A.; Hutt, J. E.; Wolff, J.; O'Neil, B. H., First-in-Human Study of Mivebresib (ABBV-075), an Oral Pan-Inhibitor of Bromodomain and Extra Terminal Proteins, in Patients with Relapsed/Refractory Solid Tumors. *Clin Cancer Res* **2019**, *25* (21), 6309-6319.
32. Flavahan, W. A.; Gaskell, E.; Bernstein, B. E., Epigenetic plasticity and the hallmarks of cancer. *Science* **2017**, *357* (6348).
33. Paksa, A.; Rajagopal, J., The epigenetic basis of cellular plasticity. *Curr Opin Cell Biol* **2017**, *49*, 116-122.
34. Waddington, C. H., The Strategy of the Genes: A Discussion of Some Aspects of Theoretical Biology. George Allen and Unwin, London: 1957.
35. Zaret, K. S.; Mango, S. E., Pioneer transcription factors, chromatin dynamics, and cell fate control. *Curr Opin Genet Dev* **2016**, *37*, 76-81.
36. Rajagopal, J.; Stanger, B. Z., Plasticity in the Adult: How Should the Waddington Diagram Be Applied to Regenerating Tissues? *Dev Cell* **2016**, *36* (2), 133-7.
37. Ito, M.; Liu, Y.; Yang, Z.; Nguyen, J.; Liang, F.; Morris, R. J.; Cotsarelis, G., Stem cells in the hair follicle bulge contribute to wound repair but not to homeostasis of the epidermis. *Nat Med* **2005**, *11* (12), 1351-4.
38. Manohar, R.; Lagasse, E., Transdetermination: a new trend in cellular reprogramming. *Mol Ther* **2009**, *17* (6), 936-8.
39. Rao, M. S.; Dwivedi, R. S.; Subbarao, V.; Usman, M. I.; Scarpelli, D. G.; Nemali, M. R.; Yeldandi, A.; Thangada, S.; Kumar, S.; Reddy, J. K., Almost total conversion of pancreas to liver in the adult rat: a reliable model to study transdifferentiation. *Biochem Biophys Res Commun* **1988**, *156* (1), 131-6.
40. Yano, S.; Nakataki, E.; Ohtsuka, S.; Inayama, M.; Tomimoto, H.; Edakuni, N.; Kakiuchi, S.; Nishikubo, N.; Muguruma, H.; Sone, S., Retreatment of lung adenocarcinoma patients with gefitinib who had experienced favorable results from their initial treatment with this selective epidermal growth factor receptor inhibitor: a report of three cases. *Oncol Res* **2005**, *15* (2), 107-11.
41. Kurata, T.; Tamura, K.; Kaneda, H.; Nogami, T.; Uejima, H.; Asai Go, G.; Nakagawa, K.; Fukuoka, M., Effect of re-treatment with gefitinib ('Iressa', ZD1839) after acquisition of resistance. *Ann Oncol* **2004**, *15* (1), 173-4.
42. Shibue, T.; Weinberg, R. A., EMT, CSCs, and drug resistance: the mechanistic link and clinical implications. *Nat Rev Clin Oncol* **2017**, *14* (10), 611-629.
43. Yilmaz, M.; Christofori, G., EMT, the cytoskeleton, and cancer cell invasion. *Cancer Metastasis Rev* **2009**, *28* (1-2), 15-33.
44. Shook, D.; Keller, R., Mechanisms, mechanics and function of epithelial-mesenchymal transitions in early development. *Mech Dev* **2003**, *120* (11), 1351-83.
45. Kalluri, R.; Weinberg, R. A., The basics of epithelial-mesenchymal transition. *J Clin Invest* **2009**, *119* (6), 1420-8.
46. Hay, E. D., The mesenchymal cell, its role in the embryo, and the remarkable signaling mechanisms that create it. *Dev Dyn* **2005**, *233* (3), 706-20.
47. De Craene, B.; Berx, G., Regulatory networks defining EMT during cancer initiation and progression. *Nat Rev Cancer* **2013**, *13* (2), 97-110.

48. Akamatsu, S.; Wyatt, A. W.; Lin, D.; Lysakowski, S.; Zhang, F.; Kim, S.; Tse, C.; Wang, K.; Mo, F.; Haegert, A.; Brahmhatt, S.; Bell, R.; Adomat, H.; Kawai, Y.; Xue, H.; Dong, X.; Fazli, L.; Tsai, H.; Lotan, T. L.; Kossai, M.; Mosquera, J. M.; Rubin, M. A.; Beltran, H.; Zoubeydi, A.; Wang, Y.; Gleave, M. E.; Collins, C. C., The Placental Gene PEG10 Promotes Progression of Neuroendocrine Prostate Cancer. *Cell Rep* **2015**, *12* (6), 922-36.
49. Sequist, L. V.; Waltman, B. A.; Dias-Santagata, D.; Digumarthy, S.; Turke, A. B.; Fidias, P.; Bergethon, K.; Shaw, A. T.; Gettinger, S.; Cospes, A. K.; Akhavanfard, S.; Heist, R. S.; Temel, J.; Christensen, J. G.; Wain, J. C.; Lynch, T. J.; Vernovsky, K.; Mark, E. J.; Lanuti, M.; Iafrate, A. J.; Mino-Kenudson, M.; Engelman, J. A., Genotypic and histological evolution of lung cancers acquiring resistance to EGFR inhibitors. *Sci Transl Med* **2011**, *3* (75), 75ra26.
50. Mareel, M.; Vleminckx, K.; Vermeulen, S.; Bracke, M.; Van Roy, F., E-cadherin expression: a counterbalance for cancer cell invasion. *Bull Cancer* **1992**, *79* (4), 347-55.
51. Winter, J. M.; Ting, A. H.; Vilardeell, F.; Gallmeier, E.; Baylin, S. B.; Hruban, R. H.; Kern, S. E.; Iacobuzio-Donahue, C. A., Absence of E-cadherin expression distinguishes noncohesive from cohesive pancreatic cancer. *Clin Cancer Res* **2008**, *14* (2), 412-8.
52. Cano, A.; Pérez-Moreno, M. A.; Rodrigo, I.; Locascio, A.; Blanco, M. J.; del Barrio, M. G.; Portillo, F.; Nieto, M. A., The transcription factor snail controls epithelial-mesenchymal transitions by repressing E-cadherin expression. *Nat Cell Biol* **2000**, *2* (2), 76-83.
53. Yang, J.; Mani, S. A.; Donaher, J. L.; Ramaswamy, S.; Itzykson, R. A.; Come, C.; Savagner, P.; Gitelman, I.; Richardson, A.; Weinberg, R. A., Twist, a master regulator of morphogenesis, plays an essential role in tumor metastasis. *Cell* **2004**, *117* (7), 927-39.
54. Bieri, B.; Pierce, S. E.; Kroeger, C.; Stover, D. G.; Pattabiraman, D. R.; Thiru, P.; Liu Donaher, J.; Reinhardt, F.; Chaffer, C. L.; Keckesova, Z.; Weinberg, R. A., Integrin- $\beta$ 4 identifies cancer stem cell-enriched populations of partially mesenchymal carcinoma cells. *Proc Natl Acad Sci U S A* **2017**, *114* (12), E2337-E2346.
55. Tsai, J. H.; Donaher, J. L.; Murphy, D. A.; Chau, S.; Yang, J., Spatiotemporal regulation of epithelial-mesenchymal transition is essential for squamous cell carcinoma metastasis. *Cancer Cell* **2012**, *22* (6), 725-36.
56. Ocaña, O. H.; Córcoles, R.; Fabra, A.; Moreno-Bueno, G.; Acloque, H.; Vega, S.; Barrallo-Gimeno, A.; Cano, A.; Nieto, M. A., Metastatic colonization requires the repression of the epithelial-mesenchymal transition inducer Prrx1. *Cancer Cell* **2012**, *22* (6), 709-24.
57. Hüsemann, Y.; Geigl, J. B.; Schubert, F.; Musiani, P.; Meyer, M.; Burghart, E.; Forni, G.; Eils, R.; Fehm, T.; Riethmüller, G.; Klein, C. A., Systemic spread is an early step in breast cancer. *Cancer Cell* **2008**, *13* (1), 58-68.
58. Ye, X.; Tam, W. L.; Shibue, T.; Kaygusuz, Y.; Reinhardt, F.; Ng Eaton, E.; Weinberg, R. A., Distinct EMT programs control normal mammary stem cells and tumour-initiating cells. *Nature* **2015**, *525* (7568), 256-60.
59. Rhim, A. D.; Mirek, E. T.; Aiello, N. M.; Maitra, A.; Bailey, J. M.; McAllister, F.; Reichert, M.; Beatty, G. L.; Rustgi, A. K.; Vonderheide, R. H.; Leach, S. D.; Stanger, B. Z., EMT and dissemination precede pancreatic tumor formation. *Cell* **2012**, *148* (1-2), 349-61.
60. Scheel, C.; Weinberg, R. A., Cancer stem cells and epithelial-mesenchymal transition: concepts and molecular links. *Semin Cancer Biol* **2012**, *22* (5-6), 396-403.
61. Liao, B. B.; Sievers, C.; Donohue, L. K.; Gillespie, S. M.; Flavahan, W. A.; Miller, T. E.; Venteicher, A. S.; Hebert, C. H.; Carey, C. D.; Rodig, S. J.; Shareef, S. J.; Najm, F. J.; van Galen, P.; Wakimoto, H.; Cahill, D. P.; Rich, J. N.; Aster, J. C.; Suvà, M. L.; Patel, A. P.; Bernstein, B. E., Adaptive Chromatin Remodeling Drives Glioblastoma Stem Cell Plasticity and Drug Tolerance. *Cell Stem Cell* **2017**, *20* (2), 233-246.e7.

62. Touil, Y.; Igoudjil, W.; Corvaisier, M.; Dessen, A. F.; Vandomme, J.; Monté, D.; Stechly, L.; Skrypek, N.; Langlois, C.; Grard, G.; Millet, G.; Leteurtre, E.; Dumont, P.; Truant, S.; Pruvot, F. R.; Hebbar, M.; Fan, F.; Ellis, L. M.; Formstecher, P.; Van Seuning, I.; Gespach, C.; Polakowska, R.; Huet, G., Colon cancer cells escape 5FU chemotherapy-induced cell death by entering stemness and quiescence associated with the c-Yes/YAP axis. *Clin Cancer Res* **2014**, *20* (4), 837-46.
63. Sánchez-Danés, A.; Larsimont, J. C.; Liagre, M.; Muñoz-Couselo, E.; Lapouge, G.; Brisebarre, A.; Dubois, C.; Suppa, M.; Sukumaran, V.; Del Marmol, V.; Tabernero, J.; Blanpain, C., A slow-cycling LGR5 tumour population mediates basal cell carcinoma relapse after therapy. *Nature* **2018**, *562* (7727), 434-438.
64. Bradner, J. E.; Hnisz, D.; Young, R. A., Transcriptional Addiction in Cancer. *Cell* **2017**, *168* (4), 629-643.
65. Vaquerizas, J. M.; Kummerfeld, S. K.; Teichmann, S. A.; Luscombe, N. M., A census of human transcription factors: function, expression and evolution. *Nat Rev Genet* **2009**, *10* (4), 252-63.
66. Graf, T.; Enver, T., Forcing cells to change lineages. *Nature* **2009**, *462* (7273), 587-94.
67. Lee, T. I.; Young, R. A., Transcriptional regulation and its misregulation in disease. *Cell* **2013**, *152* (6), 1237-51.
68. Lelli, K. M.; Slattery, M.; Mann, R. S., Disentangling the many layers of eukaryotic transcriptional regulation. *Annu Rev Genet* **2012**, *46*, 43-68.
69. Lai, F.; Orom, U. A.; Cesaroni, M.; Beringer, M.; Taatjes, D. J.; Blobel, G. A.; Shiekhattar, R., Activating RNAs associate with Mediator to enhance chromatin architecture and transcription. *Nature* **2013**, *494* (7438), 497-501.
70. Chapuy, B.; McKeown, M. R.; Lin, C. Y.; Monti, S.; Roemer, M. G.; Qi, J.; Rahl, P. B.; Sun, H. H.; Yeda, K. T.; Doench, J. G.; Reichert, E.; Kung, A. L.; Rodig, S. J.; Young, R. A.; Shipp, M. A.; Bradner, J. E., Discovery and characterization of super-enhancer-associated dependencies in diffuse large B cell lymphoma. *Cancer Cell* **2013**, *24* (6), 777-90.
71. Hnisz, D.; Day, D. S.; Young, R. A., Insulated Neighborhoods: Structural and Functional Units of Mammalian Gene Control. *Cell* **2016**, *167* (5), 1188-1200.
72. Hnisz, D.; Schuijers, J.; Lin, C. Y.; Weintraub, A. S.; Abraham, B. J.; Lee, T. I.; Bradner, J. E.; Young, R. A., Convergence of developmental and oncogenic signaling pathways at transcriptional super-enhancers. *Mol Cell* **2015**, *58* (2), 362-70.
73. Nie, Z.; Hu, G.; Wei, G.; Cui, K.; Yamane, A.; Resch, W.; Wang, R.; Green, D. R.; Tessarollo, L.; Casellas, R.; Zhao, K.; Levens, D., c-Myc is a universal amplifier of expressed genes in lymphocytes and embryonic stem cells. *Cell* **2012**, *151* (1), 68-79.
74. Brown, J. D.; Lin, C. Y.; Duan, Q.; Griffin, G.; Federation, A.; Paranal, R. M.; Bair, S.; Newton, G.; Lichtman, A.; Kung, A.; Yang, T.; Wang, H.; Luscinskas, F. W.; Croce, K.; Bradner, J. E.; Plutzky, J., NF- $\kappa$ B directs dynamic super enhancer formation in inflammation and atherogenesis. *Mol Cell* **2014**, *56* (2), 219-231.
75. Allen, B. L.; Taatjes, D. J., The Mediator complex: a central integrator of transcription. *Nat Rev Mol Cell Biol* **2015**, *16* (3), 155-66.
76. Barbieri, C. E.; Baca, S. C.; Lawrence, M. S.; Demichelis, F.; Blattner, M.; Theurillat, J. P.; White, T. A.; Stojanov, P.; Van Allen, E.; Stransky, N.; Nickerson, E. et al., Exome sequencing identifies recurrent SPOP, FOXA1 and MED12 mutations in prostate cancer. *Nat Genet* **2012**, *44* (6), 685-9.
77. Jones, P. A.; Issa, J. P.; Baylin, S., Targeting the cancer epigenome for therapy. *Nat Rev Genet* **2016**, *17* (10), 630-41.
78. Hnisz, D.; Abraham, B. J.; Lee, T. I.; Lau, A.; Saint-André, V.; Sigova, A. A.; Hoke, H. A.; Young, R. A., Super-enhancers in the control of cell identity and disease. *Cell* **2013**, *155* (4), 934-47.

79. Hnisz, D.; Weintraub, A. S.; Day, D. S.; Valton, A. L.; Bak, R. O.; Li, C. H.; Goldmann, J.; Lajoie, B. R.; Fan, Z. P.; Sigova, A. A.; Reddy, J.; Borges-Rivera, D.; Lee, T. I.; Jaenisch, R.; Porteus, M. H.; Dekker, J.; Young, R. A., Activation of proto-oncogenes by disruption of chromosome neighborhoods. *Science* **2016**, *351* (6280), 1454-1458.
80. Flavahan, W. A.; Drier, Y.; Liau, B. B.; Gillespie, S. M.; Venteicher, A. S.; Stemmer-Rachamimov, A. O.; Suvà, M. L.; Bernstein, B. E., Insulator dysfunction and oncogene activation in IDH mutant gliomas. *Nature* **2016**, *529* (7584), 110-4.
81. Bailey, P.; Chang, D. K.; Nones, K.; Johns, A. L.; Patch, A. M.; Gingras, M. C.; Miller, D. K.; Christ, A. N.; Bruxner, T. J.; Quinn, M. C.; Nourse, C.; Murtaugh, L. C.; Harliwong, I.; Idrisoglu, S.; Manning, S.; Nourbakhsh, E.; Wani, S.; Fink, L.; Holmes, O.; Chin, V.; Anderson, M. J.; Kazakoff, S.; Leonard, C.; Newell, F.; Waddell, N.; Wood, S.; Xu, Q.; Wilson, P. J.; Cloonan, N.; Kassahn, K. S.; Taylor, D.; Quek, K.; Robertson, A.; Pantano, L.; Mincarelli, L. et al., Genomic analyses identify molecular subtypes of pancreatic cancer. *Nature* **2016**, *531* (7592), 47-52.
82. Byers, L. A.; Diao, L.; Wang, J.; Saintigny, P.; Girard, L.; Peyton, M.; Shen, L.; Fan, Y.; Giri, U.; Tumula, P. K.; Nilsson, M. B.; Gudikote, J.; Tran, H.; Cardnell, R. J.; Bearss, D. J.; Warner, S. L.; Foulks, J. M.; Kanner, S. B.; Gandhi, V.; Krett, N.; Rosen, S. T.; Kim, E. S.; Herbst, R. S.; Blumenschein, G. R.; Lee, J. J.; Lippman, S. M.; Ang, K. K.; Mills, G. B.; Hong, W. K.; Weinstein, J. N.; Wistuba, I. I.; Coombes, K. R.; Minna, J. D.; Heymach, J. V., An epithelial-mesenchymal transition gene signature predicts resistance to EGFR and PI3K inhibitors and identifies Axl as a therapeutic target for overcoming EGFR inhibitor resistance. *Clin Cancer Res* **2013**, *19* (1), 279-90.
83. Soucek, L.; Whitfield, J.; Martins, C. P.; Finch, A. J.; Murphy, D. J.; Sodik, N. M.; Karnezis, A. N.; Swigart, L. B.; Nasi, S.; Evan, G. I., Modelling Myc inhibition as a cancer therapy. *Nature* **2008**, *455* (7213), 679-83.
84. Felsher, D. W.; Bishop, J. M., Reversible tumorigenesis by MYC in hematopoietic lineages. *Mol Cell* **1999**, *4* (2), 199-207.
85. Carabet, L. A.; Rennie, P. S.; Cherkasov, A., Therapeutic Inhibition of Myc in Cancer. Structural Bases and Computer-Aided Drug Discovery Approaches. *Int J Mol Sci* **2018**, *20* (1).
86. Lo-Coco, F.; Avvisati, G.; Vignetti, M.; Thiede, C.; Orlando, S. M.; Iacobelli, S.; Ferrara, F.; Fazi, P.; Cicconi, L.; Di Bona, E.; Specchia, G.; Sica, S.; Divona, M.; Levis, A.; Fiedler, W.; Cerqui, E.; Breccia, M.; Fioritoni, G.; Salih, H. R.; Cazzola, M.; Melillo, L.; Carella, A. M.; Brandts, C. H.; Morra, E.; von Lilienfeld-Toal, M.; Hertenstein, B.; Wattad, M.; Lübbert, M.; Hänel, M.; Schmitz, N.; Link, H.; Kropp, M. G.; Rambaldi, A.; La Nasa, G.; Luppi, M.; Ciceri, F.; Finizio, O.; Venditti, A.; Fabbiano, F.; Döhner, K.; Sauer, M.; Ganser, A.; Amadori, S.; Mandelli, F.; Döhner, H.; Ehninger, G.; Schlenk, R. F.; Platzbecker, U.; dell'Adulto, G. I. M. E.; Group, G.-A. A. M. L. S.; Leukemia, S. A., Retinoic acid and arsenic trioxide for acute promyelocytic leukemia. *N Engl J Med* **2013**, *369* (2), 111-21.
87. Filippakopoulos, P.; Qi, J.; Picaud, S.; Shen, Y.; Smith, W. B.; Fedorov, O.; Morse, E. M.; Keates, T.; Hickman, T. T.; Felletar, I.; Philpott, M.; Munro, S.; McKeown, M. R.; Wang, Y.; Christie, A. L.; West, N.; Cameron, M. J.; Schwartz, B.; Heightman, T. D.; La Thangue, N.; French, C. A.; Wiest, O.; Kung, A. L.; Knapp, S.; Bradner, J. E., Selective inhibition of BET bromodomains. *Nature* **2010**, *468* (7327), 1067-73.
88. Suraweera, A.; O'Byrne, K. J.; Richard, D. J., Combination Therapy With Histone Deacetylase Inhibitors (HDACi) for the Treatment of Cancer: Achieving the Full Therapeutic Potential of HDACi. *Front Oncol* **2018**, *8*, 92.
89. Prachayasittikul, V.; Prathipati, P.; Pratiwi, R.; Phanus-Umporn, C.; Malik, A. A.; Schaduengrat, N.; Seenprachawong, K.; Wongchitrat, P.; Supokawej, A.; Wikberg, J. E.; Nantasenamat, C., Exploring the epigenetic drug discovery landscape. *Expert Opin Drug Discov* **2017**, *12* (4), 345-362.
90. Eckschlagner, T.; Plch, J.; Stiborova, M.; Hrabeta, J., Histone Deacetylase Inhibitors as Anticancer Drugs. *Int J Mol Sci* **2017**, *18* (7).

91. Stathis, A.; Bertoni, F., BET Proteins as Targets for Anticancer Treatment. *Cancer Discov* **2018**, *8* (1), 24-36.
92. Wapenaar, H.; Dekker, F. J., Histone acetyltransferases: challenges in targeting bi-substrate enzymes. *Clin Epigenetics* **2016**, *8*, 59.
93. Ganesan, A.; Arimondo, P. B.; Rots, M. G.; Jeronimo, C.; Berdasco, M., The timeline of epigenetic drug discovery: from reality to dreams. *Clin Epigenetics* **2019**, *11* (1), 174.
94. Cabaye, A.; Nguyen, K. T.; Liu, L.; Pande, V.; Schapira, M., Structural diversity of the epigenetics pocketome. *Proteins* **2015**, *83* (7), 1316-26.
95. SGC Frankfurt, <https://www.sgc-frankfurt.de/>.
96. Pervaiz, M.; Mishra, P.; Günther, S., Bromodomain Drug Discovery - the Past, the Present, and the Future. *Chem Rec* **2018**, *18* (12), 1808-1817.
97. Gilan, O.; Rioja, I.; Knezevic, K.; Bell, M. J.; Yeung, M. M.; Harker, N. R.; Lam, E. Y. N.; Chung, C. W.; Bamborough, P.; Petretich, M.; Urh, M.; Atkinson, S. J.; Bassil, A. K.; Roberts, E. J.; Vassiliadis, D.; Burr, M. L.; Preston, A. G. S.; Wellaway, C.; Werner, T.; Gray, J. R.; Michon, A. M.; Gobetti, T.; Kumar, V.; Soden, P. E.; Haynes, A.; Vappiani, J.; Tough, D. F.; Taylor, S.; Dawson, S. J.; Bantscheff, M.; Lindon, M.; Drewes, G.; Demont, E. H.; Daniels, D. L.; Grandi, P.; Prinjha, R. K.; Dawson, M. A., Selective targeting of BD1 and BD2 of the BET proteins in cancer and immunoinflammation. *Science* **2020**, *368* (6489), 387-394.
98. Stratikopoulos, E. E.; Dendy, M.; Szabolcs, M.; Khaykin, A. J.; Lefebvre, C.; Zhou, M. M.; Parsons, R., Kinase and BET Inhibitors Together Clamp Inhibition of PI3K Signaling and Overcome Resistance to Therapy. *Cancer Cell* **2015**, *27* (6), 837-51.
99. Mazur, P. K.; Herner, A.; Mello, S. S.; Wirth, M.; Hausmann, S.; Sánchez-Rivera, F. J.; Lofgren, S. M.; Kuschma, T.; Hahn, S. A.; Vangala, D.; Trajkovic-Arsic, M.; Gupta, A.; Heid, I.; Noël, P. B.; Braren, R.; Erkan, M.; Kleeff, J.; Sipos, B.; Sayles, L. C.; Heikenwalder, M.; Heßmann, E.; Ellenrieder, V.; Esposito, I.; Jacks, T.; Bradner, J. E.; Khatri, P.; Sweet-Cordero, E. A.; Attardi, L. D.; Schmid, R. M.; Schneider, G.; Sage, J.; Siveke, J. T., Combined inhibition of BET family proteins and histone deacetylases as a potential epigenetics-based therapy for pancreatic ductal adenocarcinoma. *Nat Med* **2015**, *21* (10), 1163-71.
100. He, S.; Dong, G.; Li, Y.; Wu, S.; Wang, W.; Sheng, C., Potent Dual BET/HDAC Inhibitors for Efficient Treatment of Pancreatic Cancer. *Angew Chem Int Ed Engl* **2020**, *59* (8), 3028-3032.
101. Fernandes Neto, J. M.; Nadal, E.; Bosdriesz, E.; Ooft, S. N.; Farre, L.; McLean, C.; Klarenbeek, S.; Jurgens, A.; Hagen, H.; Wang, L.; Felip, E.; Martinez-Marti, A.; Vidal, A.; Voest, E.; Wessels, L. F. A.; van Tellingen, O.; Villanueva, A.; Bernards, R., Multiple low dose therapy as an effective strategy to treat EGFR inhibitor-resistant NSCLC tumours. *Nat Commun* **2020**, *11* (1), 3157.
102. Xie, X.; Wu, Y.; Luo, S.; Yang, H.; Li, L.; Zhou, S.; Shen, R.; Lin, H., Efficacy and Toxicity of Low-Dose versus Conventional-Dose Chemotherapy for Malignant Tumors: a Meta-Analysis of 6 Randomized Controlled Trials. *Asian Pac J Cancer Prev* **2017**, *18* (2), 479-484.
103. Rathert, P.; Roth, M.; Neumann, T.; Muerdter, F.; Roe, J. S.; Muhar, M.; Deswal, S.; Cerny-Reiterer, S.; Peter, B.; Jude, J.; Hoffmann, T.; Boryń, Ł.; Axelsson, E.; Schweifer, N.; Tontsch-Grunt, U.; Dow, L. E.; Gianni, D.; Pearson, M.; Valent, P.; Stark, A.; Kraut, N.; Vakoc, C. R.; Zuber, J., Transcriptional plasticity promotes primary and acquired resistance to BET inhibition. *Nature* **2015**, *525* (7570), 543-547.
104. Fantin, V. R.; Richon, V. M., Mechanisms of resistance to histone deacetylase inhibitors and their therapeutic implications. *Clin Cancer Res* **2007**, *13* (24), 7237-42.
105. Scheel, C.; Eaton, E. N.; Li, S. H.; Chaffer, C. L.; Reinhardt, F.; Kah, K. J.; Bell, G.; Guo, W.; Rubin, J.; Richardson, A. L.; Weinberg, R. A., Paracrine and autocrine signals induce and maintain mesenchymal and stem cell states in the breast. *Cell* **2011**, *145* (6), 926-40.

106. Fong, C. Y.; Gilan, O.; Lam, E. Y.; Rubin, A. F.; Ftouni, S.; Tyler, D.; Stanley, K.; Sinha, D.; Yeh, P.; Morison, J.; Giotopoulos, G.; Lugo, D.; Jeffrey, P.; Lee, S. C.; Carpenter, C.; Gregory, R.; Ramsay, R. G.; Lane, S. W.; Abdel-Wahab, O.; Kouzarides, T.; Johnstone, R. W.; Dawson, S. J.; Huntly, B. J.; Prinjha, R. K.; Papenfuss, A. T.; Dawson, M. A., BET inhibitor resistance emerges from leukaemia stem cells. *Nature* **2015**, *525* (7570), 538-42.
107. Pitt, J. M.; Marabelle, A.; Eggermont, A.; Soria, J. C.; Kroemer, G.; Zitvogel, L., Targeting the tumor microenvironment: removing obstruction to anticancer immune responses and immunotherapy. *Ann Oncol* **2016**, *27* (8), 1482-92.
108. Kundu, J. K.; Surh, Y. J., Inflammation: gearing the journey to cancer. *Mutat Res* **2008**, *659* (1-2), 15-30.
109. Tormoen, G. W.; Crittenden, M. R.; Gough, M. J., Role of the immunosuppressive microenvironment in immunotherapy. *Adv Radiat Oncol* **2018**, *3* (4), 520-526.
110. Zhu, H.; Bengsch, F.; Svoronos, N.; Rutkowski, M. R.; Bitler, B. G.; Allegranza, M. J.; Yokoyama, Y.; Kossenkov, A. V.; Bradner, J. E.; Conejo-Garcia, J. R.; Zhang, R., BET Bromodomain Inhibition Promotes Anti-tumor Immunity by Suppressing PD-L1 Expression. *Cell Rep* **2016**, *16* (11), 2829-2837.
111. Roesch, A.; Vultur, A.; Bogeski, I.; Wang, H.; Zimmermann, K. M.; Speicher, D.; Körbel, C.; Laschke, M. W.; Gimotty, P. A.; Philipp, S. E.; Krause, E.; Pätzold, S.; Villanueva, J.; Krepler, C.; Fukunaga-Kalabis, M.; Hoth, M.; Bastian, B. C.; Vogt, T.; Herlyn, M., Overcoming intrinsic multidrug resistance in melanoma by blocking the mitochondrial respiratory chain of slow-cycling JARID1B(high) cells. *Cancer Cell* **2013**, *23* (6), 811-25.

Images are used and edited from <https://smart.servier.com> for Fig. 1, 2, 4 and 5 under the Creative Commons Attribution 3.0 Unported License

## 6. Acknowledgements

I am very grateful to Prof. Dr. Jens Siveke and the DKFZ for providing me the opportunity to join the research team at University Hospital Essen and for the precious support and the encouragement during my study.

I would also like to pay my special regards and express my thanks to Dr. Xin Zhang for guiding me through all steps of my graduation, for sharing his knowledge, the successful teamwork and the sleepless nights before deadlines.

In Addition, I want to thank my fellow labmates, who became friends quickly. I appreciate the invaluable assistance they provided me during my study and the great working atmosphere in last three years.

I also wish to show my gratitude to the research group of Prof. Dr. Stefan Knapp for the close and successful cooperation. Without their precious contribution, it would not be possible to work on these projects.

My thanks also go to Prof. Dr. Andrea Vortkamp and Dr. Marc Remke, who joined the Thesis Advisory Committee (TAC) for scientific mentoring and provided further support during my graduation.

Last but not least I would like to thank my family and close friends for always supporting me in many different ways, since the beginning of my study until the writing of my thesis.

## 7. Statutory declaration

Hiermit erkläre ich, gem. § 7 Abs. 2, d und f der Promotionsordnung der Fakultät für Biologie zur Erlangung des Dr. rer. nat., dass ich die vorliegende Dissertation selbständig verfasst und mich keiner anderen als der angegebenen Hilfsmittel bedient habe und alle wörtlich oder inhaltlich übernommenen Stellen als solche gekennzeichnet habe.

Essen, den \_\_\_\_\_

Unterschrift des Doktoranden

Hiermit erkläre ich, gem. § 7 Abs. 2, e und g der Promotionsordnung der Fakultät für Biologie zur Erlangung des Dr. rer. nat., dass ich keine anderen Promotionen bzw. Promotionsversuche in der Vergangenheit durchgeführt habe, dass diese Arbeit von keiner anderen Fakultät abgelehnt worden ist, und dass ich die Dissertation nur in diesem Verfahren einreiche.

Essen, den \_\_\_\_\_

Unterschrift des Doktoranden

Hiermit erkläre ich, gem. § 6 Abs. 2, g der Promotionsordnung der Fakultät für Biologie zur Erlangung der Dr. rer. nat., dass ich das Arbeitsgebiet, dem das Thema „*Targeting transcriptional regulators for the treatment of therapy resistant carcinomas*“ zuzuordnen ist, in Forschung und Lehre vertrete und den Antrag von Tim Zegar befürworte.

Essen, den \_\_\_\_\_

Prof. Dr. Jens T. Siveke

Name des wissenschaftl.  
Betreuers/ Mitglieds der  
Universität Duisburg-Essen

\_\_\_\_\_

Unterschrift des wissenschaftl.  
Betreuers/ Mitglieds der Universität  
Duisburg-Essen